VOLUME 1
ISSUE 1

NATURAL SCIENCES

A multi-disciplinary research journal

The University for Innovation

NATURAL SCIENCES

A multi-disciplinary research journal

The journal of Natural Sciences is a multi-disciplinary research journal, published by the Institute of Advanced Research, *The University for Innovation*, Gandhinagar, Gujarat, India.

The purpose of the journal is to provide a platform for disseminating novel and innovative research and development to help address the global grand challenges that we confront.

The journal publishes peer reviewed scientific and technical articles in all disciplines encompassing natural sciences and those at the interfaces of natural sciences and other disciplines.

The journal is available free on line at

https://www.iar.ac.in/naturalsciences

Information for Authors

https://www.iar.ac.in/journal/authorinformation

Editorial Office

The Journal of Natural Sciences
Institute of Advanced Research
Koba Institutional Area
Gandhinagar – 382 426
India

NATURAL SCIENCES

A multi-disciplinary research journal

Foreword

Research in universities and research institutions has traditionally been discipline based. Therefore, research in institutions is organized to promote research in respective disciplines. Challenges we face today, whether climate change, life long health, ever frequent infectious diseases, demand cross fertilization of ideas from different disciplines ranging from sciences, engineering, social sciences and humanities in order to confront them..

Multidisciplinary approach is traditionally directed at problem solving, for example in engineering. However, knowledge enhancement at the interfaces of disciplines is critically important in order to find novel solutions to increasingly comple problems. Multidisciplinary research is very much in vogue. Multidisciplinary research requires inputs from a variety of individual disciplines operating in a culture of collaborative exploration across the discipline boundaries. More and more institutions recognize the need for facilitating multi-disciplinary research and development and promoting multidisciplinary teams and research.

Recent decades have seen exciting multidisciplinary research and novel solutions being found based on new knowledge.

I am pleased to introduce this new journal of Natural Sciencesthe first issue of Natural Sciences, which is intended to provide a venue for dissemination of multidisciplinary research and development. While there are several other platform for multidisciplinary and interdisciplinary research, this publication is intended for research with direct impact on emerging challenges.

Professor Rao Bhamidimarri
Editor-in-Chief

NATURAL SCIENCES

A multi-disciplinary research journal

ON- DUTY AFTER DEATH: PROGRAMMED CELL DEATH DURING XYLEM DEVELOPMENT IN HIGHER PLANTS

Rohi Bhatt and Budhi Sagar Tiwari*

Department of Biological Sciences & Biotechnology, Institute of Advanced Research

Gandhinagar 382007 Gujrat, India

*Corresponding Author: E-mail: bstiwari@iar.ac.in

Programmed cell death (PCD) is an intrinsically instituted phenomenon operated in multicellular organisms. In this process, targeted cells die off themselves to maintain homeostasis of natality and mortality thus maintaining cell number, removing unwanted or damaged cells for uninterrupted development of an organism. *In-planta*, the process is developmentally regulated and reported during abiotic and biotic stress conditions. There are number of spots in the plant that show PCD at different junctures of the development in a growing plant. Some of them include development of unisexual flowers, root cap formation, shaping different types of leaves, suspensor cell death during embryo development. Among all notches of plants showing PCD, development of the xylem is unique as xylem comes into the function of supplying water and minerals to the whole plant body only once when cells die off through PCD. In this article, we attempt to elaborate on xylem development that involves the cell death process.

Key words: Xylogenesis, PCD, developmentally regulated, Abiotic stress

Introduction

Programmed cell death is the process in which the cell itself goes under-regulated killing process within the control of genetic and molecular signals. In both plants and animals, PCD is an utmost essential process. Based on molecular and morphological features two types of PCD are observed i). Developmentally regulated PCD and ii) Environmental induced PCD (Huysmans et al. 2016).

The PCD process is essential for appropriate plant development and for providing a strong defence mechanism against environmental stress stimuli. PCD regulates reproductive development to the whole plant until the senescence including vegetative and reproductive

developmental stages. It is also involved in plant defence mechanism activated against stress stimuli such as pathogens and /or fluctuations in an abiotic environment where the plant is growing. Different type of developmental PCD has distinguished on the context of their development (Beers 1997). Based on the differentiation processes, developmental PCD occurs at particular cell types leading to the final differentiation step some of examples include root cap cells, xylem differentiation (Escamez&Tuominen 2014, kumpf & Nowack 2015). During the initiation of developmental PCD in a facultative fashion, some cell types work in the manner of cell-to-cell signalling during self-incompatibility response (Wilkins et al., 2014). These types of events constitute a specific ability of plants such as elimination of the negative genetic features in the progeny by ending inbreeding problems and promote outbreeding and avoiding self-pollination in bisexual flowers activation of PCD in the pollen tube (Bosch et al., 2008). Plant activates PCD in senescent tissues to recycle nutrients before the elimination of the tissues that they do not need further during age and/or stress leading to degradation of organisms, tissues, or organs (Wingler et al., 2015).

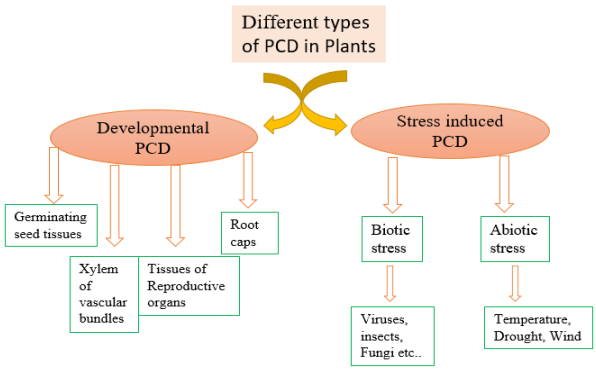

Fig.1: Different types of PCD found in plant

Figure 1:- Cell death in Plants

Cell death might also cause the formation of leaf lobes, perforation, and many kinds of trichomes that is essential for the formation of specialized cells (Mittler and Lam, 1995).

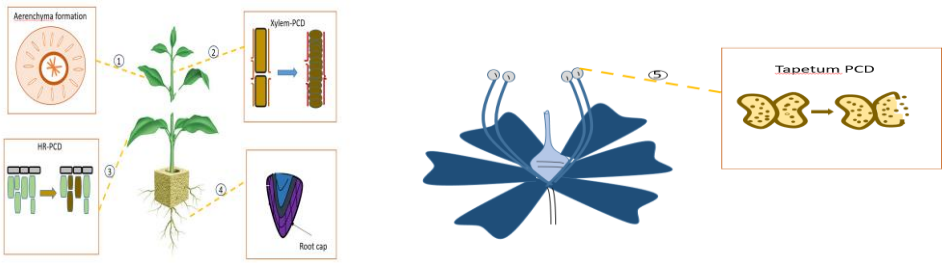

Figure: 2:- Categories of PCD in plants based on fate and function of cell (1) Aerenchyma formation including in the aerenchyma formation, complete hydrolysis of the cell results in gas spaces. (2) Xylogenesis is the only plant part that starts work after death. (3) Hypersensitive Response in plants host-pathogen interaction makes HR that kills the pathogen-infected area as well as kill the cell that is nearby the infection for preventing further infection. (4) Root cap cell formation is the example of plant cells that activate all the time in their life. (5) Tapetum PCD important for the reproduction of plants is important for maturation and release of pollen grains.

During plant development, different cells are destined to play a different role in the life of a plant. Based on their destined functions/fate and involvement of the PCD in the plant, cell death has been categorized into five categories (Krishnamurthy et al., 2000) and illustrated in the figure:-2.

Stress-triggered PCD includes biotic and abiotic attacks. When the plant cell face pathogen attack, it will activate hypersensitive response (HR), against biotrophic pathogen and plants activate PCD. HR is the defence strategy of plants it limits pathogens from spreading in the whole plant. Because of its ability to recognize the effecter, molecules, and then HR prevent further spreading. Interestingly HR contributing to the autophagic events in the surrounding cells, for removal of the death signals that prevent PCD at the site of attack (Moeder et al., 2008, Liu et al., 2005). Abiotic stress such as flooding, temperature, and drought affects the normal metabolism of plants by protein synthesis and protein turnover reduction, restraining photosynthesis and disturb the electron flow in the respiratory chain in mitochondria as well as in chloroplast and ultimately results in the increasing production of ROS and RNS in the cell. Overproduction of the reactive oxygen species and reactive nitrogen species activates PCD pathways to remove redundant and damaged cells for preventing further damage in the plant. In normal physiological conditions, RNS and ROS work as signaling molecules (Locato et al., 2016).

In the plant and animal, kingdom PCD can identify with its unique signature that includes DNA fragmentation, cytochrome c release from the mitochondria, cell shrinkage, generation of reactive oxygenic and reactive nitrogen species, exposure of phosphatidylserine, etc. In PCD of plants, unrecognized caspase-like protease activation observed and observed that these proteases hydrolyse various substrates of caspases (Bonneau et al., 2008).

Plants PCD employs different mechanisms for the tissue and organ expression and functions, as well as for well-organized reproduction and nutrition. PCD in plants ensues in HR during plant-

pathogen interaction, responsible for seizes the pathogen infection in a particular plant part. Reproductive organs such as Tapetum PCD in plants tapetum layer found within the anther, it's a nutritive layer of pollen sac, it is necessary for normal pollen development ominously functional pollen development totally depends on the death of the tapetum tissues and ultimately anther rupture and results in the dispersal of pollen grains (Liu et al, 2018).

On the other side in root cap cells it is necessary for maintaining the organ size and shape and as root cells have to deal with harsh conditions root cap cells continuously produce new cells, root cap only covers the meristematic region and root cap avoid the extension of the root cap cells beyond the meristematic region (Tsukaya, 2003). In all these organs, PCD occurs, and after that, functions of these organs seize (Pennell and Lamb., 1997). Despite that, Xylem PCD are including in developmentally regulated PCD but the xylem is the only organ that is functionally activated when xylem tissues undergo the PCD process before that xylem tissue are not able to transport water and minerals from the root to areal organs of the plant (Menard & Pesquet 2015). Cell differentiation and cell death in cells make a way for functional xylem tissue formation. This unique characteristic of xylem tissues not found elsewhere and make this organ unique in functionality. Xylem differentiation and PCD are well-organized cascades.

Xylem differentiation

Plant root absorbs water and minerals from the soil which are needed to be transported to the different plant tissues i.e. stem, leaves, flowers, fruits, etc. this transportation process is carried out with the help of the very specialized tissues called Xylem. It is present in all types of plants whether they are herbs, shrubs, or trees; in taller trees, the water and mineral transported from the roots to the topmost leaf distance measuring more than 100 meters. For the distribution of nutrients all over the plant for photosynthesis and transpiration, the movement of water is required. Water is important for plant growth and development that involves its signature process of photosynthesis and removal of excess water molecules during the transpiration process from stomata. Xylem tissue comprises main three types of cells: a) xylem tracheary (vessel) elements, b) xylary fibres, and c) xylem parenchyma cells. These three types of cells formed by the differentiation of xylem precursor cells, which derived from pro-cambial and cambial cells. Among all the cells mentioned, only tracheary elements and fibres lignified and form secondary cell wall through a process known as xylogenesis. Xylem parenchyma is involved in many biological functions, including lignification of the secondary cell of the tracheary elements and fibres.

The development of secondary xylem cells can be divided into the following phases: cambial cell division, cell expansion or elongation, cell wall thickening, cell wall sculpturing (formation of modified structure), lignification, and cell death (autocytolysis) (Funada, 2000, 2008). The cambial cell has two types of cells that are mainly responsible for the cellular arrangement of the xylem and phloem in the vascular system of angiosperm & gymnosperms. While angiosperms represent an axial vascular system, the radial vascular system is the signature of gymnosperms that lacks xylem vessel elements and fibres. The formation of the axial and the radial vascular system takes place from the two types of cambium cells:
fusiform initials form axial (vessel elements, fibres, and parenchyma of the xylem) elements of the secondary vascular system whose cells are elongated and narrowed but flattened on the tangential face, whereas ray initials form radial elements of the secondary vascular system consist of shorter cells which are somewhat elongated along their radial axis (Kitin et al.,1999). The cell elongation process takes place as protoplast of the cell forces (Turgor pressure) against the cell wall, which initiated from the vacuole. It is the volume of vacuole whose increment forms water gradient between cytoplasm, vacuole and, apoplast via turgor pressure. This turgor pressure acts as a dynamic force, which plays a major role in the enlargement of cells in plants. At certain point turgor, pressure in the cell becomes unable to increase expansion and elongation in the cell as the cell wall becomes rigid. In the process of cell enlargement, the formation of primary cell wall characterized by very thin and rigid loose bulks of cellulose microfibrils for the cell to elongate and expand (Abe and funuda, 2005). Cellulose microfibrils are important for the skeleton of the cell wall whereas other important main constituent cellulose is crystalline and has high tensile strength.

Cellulose microfibrils are the innermost layer of the cell wall and mostly aligned longitudinally in the normal cell wall for cell differentiation but in tracheids, they confine the longitudinal elongation due to turgor pressure in the early phase of cell elongation. Therefore, lateral expansion was seen in the primary wall containing fusiform cambial cells whose cellulose microfibrils longitudinally aligned. The alignment of cellulose microfibrils changes to transverse from longitudinal as the cell expansion takes place (Abe et al., 1995). All the cellulose microfibrils aligned transversely when cell expansion reaches its final stage. The cell wall, which forms in tracheid cells, consists of different alignments of cellulose microfibrils wherein the outer and inner layer shows incompatibility to the multi net growth hypothesis. When cell expansion is about to complete in the tracheid, the alignment of cellulose microfibrils becomes well organized on the innermost layer of the cell wall, this sets up for the deposition

secondary wall. As the formation of the secondary cell wall begins no more cell elongation or expansion of tracheid takes place. The continuous formation of cell walls leads to cell wall thickening. The cell wall thickness differs for different cells, which depend on cell function, cambial age, and season of cell formation, for example, earlywood and latewood. Cells that are required for maintaining the skeleton of the tree (tracheids and wood fibre) contain a thick secondary wall. Hence, the structure of tracheids and wood fibre is important for the mechanical properties of wood. Woody plant's structures containing woody fibres, tracheids and, vessel elements have highly organized skeleton. After the formation of the secondary cell wall, it plays an important function in supporting heavyweight of the tree, transportation of water from roots to leaves, which can reach the distance of more than 100 meters in height; it also protects the cell from microbial and insect attacks (Kimura et al., 1999).

The formation of semi-helicoidal structure takes place during the formation of secondary wall, as the alignment of microfibrils changes to steep Z-helix (S_1 layer) from the flat helix (S_2 layer) when observed from the lumen side of cell it rotates clockwise. After the rotation it gets align at about 5–30° with respect to the cell axis. During the formation of S_2 layer, cellulose microfibrils with S-helix alignment not seen. The S_2 layer of the cellulose microfibrils aligned with high degree of parallelism. The formation of the thick wall results as the rotational change in the alignment of cellulose microfibrils arrested. The thickness of the S_2 layer (thickness of the secondary wall.) is determined from the number of times the orientation of microfibrils arrested. Specific gravity is one of the important characteristics of wood, which correlated to the thickness of the secondary wall (Gidding and Staehelin., 1991). When the formation of the secondary wall is in the last phase, the alignment of lastly deposited cellulose microfibril changes from the steep Z-helix to the flat helix and rotates in an anticlockwise direction when observed from the lumen side of the cell. Directional switch from clockwise to anticlockwise when observed from the lumen side of the cell leads to the formation of the S_3 layer with flat helix alignment of cellulose microfibril and the deposition of this layer occurs in bundles. The texture of S_3 layer differs from the high degree of parallelism seen in the cellulose microfibril of S_2 layer. When the alignment changes in the layers of the cellulose microfibril, a change in angle seen which is different in S_2 to S_3 layer switch and is more sudden than that of in S_1 to S_2 layer switch. The structure of the cell wall layer decided by the rate of transitions in the alignment of the cellulose microfibril (Chaffey et al., 1997, Abe et al., 1997). Cellulose and hemicellulose along with heterogeneous phenolic polymer lignin deposited in secondary cell walls. In the polymerization of lignin secondary xylem, the formation role of 4-coumarate-CoA

ligase encoded by At1g51680 gene is very important; Apart from 4-coumarate-CoA ligase, other enzymes such as ferulate-5-hydroxylase genes (At4g36220), cinnamyl alcohol dehydrogenase (At2g21890), and Putative laccase (At2g40370) are also involved in polymerization process (Dharmawardhana et al., 1992). S-adenosyl methionine synthetase (SAMS) and CCoAOAMT enzymes are responsible for methylation of lignin precursors. SAMS are responsible for transferring adenosyl group from ATP to the sulphur atom of methionine, which synthesize SAM, a methyl donor group (Vender et al., 2000). Lignification starts at the intercellular layer, and eventually progresses from the primary cell wall to the secondary cell wall.

Cell death

After the lignifications in tracheary elements, it is destined to undergo the cell death process (Funada et al., 2000, 2008). In-vessel elements and wood fibres, the collapse of vacuoles and disappearance of tonoplast initiates cell death event (Arend and fromm, 2003). In the cascade of the events of degradation of TEs cell organelles earliest sign is vacuole collapse (Fukuda., 1997; Groover et al., 1997). After the collapse of vacuoles, a single membrane containing organelles, endoplasmic reticulum (ER), and Golgi bodies' swell first and at the end entire length, convert into the balloon-like structure and ultimately disappear, usually, Chloroplast and mitochondrial degradation occurs first in their matrix and later in their membrane. *In vitro* study in Arabidopsis and zinnia has shown that secondary cell wall formation and PCD regulation by the common transcription factors and transcripts accumulation in the similar time during an advanced and prior stage of TE development (Fukuda,2004,2016; Ohashi-Ito et al.,2010; Demura et al.,2002; Milioni et al.,2002). PCD and secondary cell wall formation work in a coordinated manner, it hypothesized that directly or indirectly VND6 and VND7 regulates the gene that contains the tracheary element-regulating cis-element (TERE) sequence (Ohashiito et al., 2010).

As observed in the *Zinnia elegance* cell suspension, xylem PCD might be induced by calcium influx, in response to extracellular proteolysis. Initiation of PCD might be induced by ROS and execute the cell death processes, Differentiation and PCD together are cooperative process in the xylogenesis. PCD undergoes two successive phases: Execution of cell death and autolysis followed by protoplast elimination (Groover and jones 1999; Jones 2001; Kozela and Regan 2003). After TE cell dies, autolysis starts the clearance of the organelles remnants to form dead mature hollow TEs through **cellular post-mortem** that includes the sequence of events that are a part of programmed cell death after the vacuole collapse (Escamez and Tuominen, 2014). The

Sequence of Cell death event follows rapid hydrolytic vacuole collapse, mixing of contents of cytoplasm and vacuoles, sudden cessation of cytoplasmic streaming. Not all these processes in the cell cease normal metabolism, but it creates an environment for downstream events such as autolysis. Hydrolytic enzymes that are responsible for vacuole collapse are caspases found in animals, As Caspases works, in the same way, caspase-like protein regulates the xylem PCD in the plant. The homologue of caspases are not found in the plants but caspase-like activity detected in the xylem differentiation however it has not been directly linked with xylem PCD yet (Twumasi et al.,2010). Hydrolytic enzymes such as cysteine/serine proteases encoded by the gene XCP1 and XCP2 are responsible for the autolysis of xylem TEs. Plant have Metacaspases that have different substrate specificity but it is a structural analogue of caspases, xylem PCD shows highly expressed serine dependent proteases (Groover and Jones,1999) This lytic enzyme leads to the formation of the hollow dead conduits by complete degradation of cellular contents (Fukuda,2001; Groover et al.,1997; Obara et al.,2001; Obara and Fukuda,2004). During the late stage of TE differentiation in Arabidopsis and xylem maturation in Populus microarray analysis revealed upregulation of a homologue of Arabidopsis metacaspase 9 (AtMC9) (Turner et al.,2007; Courtois Moreau et al.,2009; Bollho``ner et al.,2013). In a manner similar to AtMC9, two papain-like cysteine proteases (PLCPs) named xylem cysteine peptides 1 (XCP1) and XCP2 were upregulated. These proteases were associated in micro-autolysis of cellular structures before tonoplast rupture and in mega-autolysis of the whole protoplast following tonoplast breakage in differentiation TEs in Arabidopsis cell culture (Zhao et al., 2000; Avci et al., 2008; Funk et al., 2002). AtMC9 may regulate XCP1 and XCP2 but in an elegant study, experiments with atmc9-2 and double xcp1/xcp2 mutants showed that these metacaspases and the studied PLCPs independently related to autolysis. The author suggested that AtMc9 might potentially affect other papain-like proteases participating in post-mortem protoplast clearance. This presumption sustained by observations of participation of a cysteine protease (Tr-cp14) in post-mortem protoplast clearance. Cysteine proteases Tr-cp14) closely related with XCP1 and XCP2 accumulated in the endoplasmic reticulum and Golgi bodies and may extend throughout the cell during vacuole collapse in the planta differentiating TEs of Trifoliumrepen (Mulisch et al., 2013).

Conclusion

Programmed Cell death in its definition is the process that ends up the life of a living and functional cell under certain circumstances that include whether it has completed its life and role, the cell damaged or diseased that is no longer required for plants or plants in its non-living

state require it. In the same line of definition xylem cells of plant present a unique platform where a developing cell is destined to come into function after it passes through cell death, in one way it indicates extreme preciseness of cells machinery to target a cell and secondly, keep the cells in dead form until the life of a plant. These features indicate the importance of the process in plants and its possible applications. Several reports have been discussed that describe regulatory mechanisms underlying xylogenesis but still a length of work is required to know the stepwise molecular events mainly related to the cell death process to look for translational part of the process.

Acknowledgement: This work is supported by the facilities made available from Institute of Advanced Research Gandhinagar, Gujarat, India.

Reference

Abe, H., &Funada, R. (2005). The orientation of cellulose microfibrils in the cell walls of tracheids in conifers. *Iawa Journal*, *26*(2), 161-174.

Abe, H., Funada, R., Imaizumi, H., Ohtani, J., & Fukazawa, K. (1995). Dynamic changes in the arrangement of cortical microtubules in conifer tracheids during differentiation. *Planta*, *197*(2), 418-421.

Abe, H., Funada, R., Ohtani, J., & Fukazawa, K. (1997). Changes in the arrangement of cellulose microfibrils associated with the cessation of cell expansion in tracheids. *Trees*, *11*(6), 328-332.

Arend, M., & Fromm, J. (2007). Seasonal change in the drought response of wood cell development in poplar. *Tree physiology*, *27*(7), 985-992.

Avci, U., Earl Petzold, H., Ismail, I. O., Beers, E. P., &Haigler, C. H. (2008). Cysteine proteases XCP1 and XCP2 aid micro-autolysis within the intact central vacuole during xylogenesis in Arabidopsis roots. *The Plant Journal*, *56*(2), 303-315.

Baskin, T. I. (2001). On the alignment of cellulose microfibrils by cortical microtubules: a review and a model. *Protoplasma*, *215*(1-4), 150-171.

Beemster, G. T., Fiorani, F., Inzé, D., Kozela, C., Regan, S., Casimiro, I., ... &Casero, P. (2003). 154 Cell cycle: the key to plant growth control? *Plant Science*, *8*(4), 143-194.

Beers, E. P. (1997). Programmed cell death during plant growth and development. *Cell Death & Differentiation*, *4*(8), 649-661.

Bonneau, L., Ge, Y., Drury, G. E., & Gallois, P. (2008). What happened to plant caspases?. *Journal of Experimental Botany*, *59*(3), 491-499.

Chaffey, N. J., Barnett, J. R., & Barlow, P. W. (1997). Visualization of the cytoskeleton within the secondary vascular system of hardwood species. *Journal of Microscopy*, *187*(2), 77-84.

Chaffey, N., Cholewa, E., Regan, S., &Sundberg, B. (2002). Secondary xylem development in Arabidopsis: a model for wood formation. *Physiologia plantarum*, *114*(4), 594-600.

Courtois-Moreau, C. L., Pesquet, E., Sjödin, A., Muñiz, L., Bollhöner, B., Kaneda, M., ... &Tuominen, H. (2009). A unique program for cell death in xylem fibers of Populus stem. *The Plant Journal*, *58*(2), 260-274.

De Pinto, M. C., Locato, V., & De Gara, L. (2012). Redox regulation in plant programmed cell death. *Plant, Cell & Environment*, *35*(2), 234-244.

Demura, T., Tashiro, G., Horiguchi, G., Kishimoto, N., Kubo, M., Matsuoka, N., ... &Sassa, N. (2002). Visualization by comprehensive microarray analysis of gene expression programs during transdifferentiation of mesophyll cells into xylem cells. *Proceedings of the National Academy of Sciences* USA *99*(24), 15794-15799.

Dharmawardhana, D. P., Ellis, B. E., & Carlson, J. E. (1992). Characterization of vascular lignification in Arabidopsis thaliana. *Canadian Journal of Botany*, *70*(11), 2238-2244.

Escamez, S., &Tuominen, H. (2014). Programmes of cell death and autolysis in tracheary elements: when a suicidal cell arranges its own corpse removal. *Journal of Experimental Botany*, *65*(5), 1313-1321.

Escamez, S., André, D., Zhang, B., Bollhöner, B., Pesquet, E., &Tuominen, H. (2016). METACASPASE9 modulates autophagy to confine cell death to the target cells during Arabidopsis vascular xylem differentiation. *Biology Open*, *5*(2), 122-129.

Fukuda, H. (1997). Tracheary element differentiation. *The Plant Cell*, *9*(7), 1147.

Fukuda, H. (2004). Signals that control plant vascular cell differentiation. *Nature reviews Molecular Cell Biology*, *5*(5), 379-391.

Funada, R. (2008). Microtubules and the control of wood formation. In *Plant Microtubules* (pp. 83-119). Springer, Berlin, Heidelberg.

Funada, R., Kubo, T., Sugiyama, T., &Fushitani, M. (2002). Changes in levels of endogenous plant hormones in cambial regions of stems ofLarixkaempferi at the onset of cambial activity in springtime. *Journal of Wood Science*, *48*(1), 75-80.

Funada, R., Yamagishi, Y., Begum, S., Kudo, K., Nabeshima, E., Nugroho, W. D., ... &Nakaba, S. (2016). Xylogenesis in trees: from cambial cell division to cell death. In *Secondary Xylem Biology* (pp. 25-43). Academic Press.

Funk, V., Kositsup, B., Zhao, C., & Beers, E. P. (2002). The Arabidopsis xylem peptidase XCP1 is a tracheary element vacuolar protein that may be a papain ortholog. *Plant Physiology*, *128*(1), 84-94.

Giddings, T. H., and L. A. Staehelin.(1991)."The cytoskeletal basis of plant growth and form." (pp. 85-99) Academic Press, San Diego.

Groover, A., & Jones, A. M. (1999). Tracheary element differentiation uses a novel mechanism coordinating programmed cell death and secondary cell wall synthesis. *Plant Physiology*, *119*(2), 375-384.

Groover, A., DeWitt, N., Heidel, A., & Jones, A. (1997). Programmed cell death of plant tracheary elements differentiating in vitro. *Protoplasma*, *196*(3-4), 197-211.

Hatfield, J. L., &Prueger, J. H. (2015). Temperature extremes: Effect on plant growth and development. *Weather and Climate Extremes*, *10*, 4-10.

Hernández, I., &Munné-Bosch, S. (2015). Linking phosphorus availability with photo-oxidative stress in plants. *Journal of Experimental Botany*, *66*(10), 2889-2900.

Huang, G. H., Tian, H. H., Liu, H. Y., Fan, X. W., Liang, Y., & Li, Y. Z. (2013). Characterization of plant-growth-promoting effects and concurrent promotion of heavy metal accumulation in the tissues of the plants grown in the polluted soil by Burkholderia strain LD-11. *International Journal of Phytoremediation*, *15*(10), 991-1009.

Huysmans, M., Coll, N. S., &Nowack, M. K. (2017). Dying two deaths—programmed cell death regulation in development and disease. *Current opinion in plant biology*, *35*, 37-44.

Kawamura, Y., Satow, J., Fukuda, K., Oya, E., Itoh, K., Kita, H., ... & Ishikawa, K. (1996). *U.S. Patent No. 5,518,994*. Washington, DC: U.S. Patent and Trademark Office.

Kimura, S., Laosinchai, W., Itoh, T., Cui, X., Linder, C. R., & Brown, R. M. (1999). Immunogoldlabeling of rosette terminal cellulose-synthesizing complexes in the vascular plant Vignaangularis. *The Plant Cell*, *11*(11), 2075-2085.

Kitin, P., Funada, R., Sano, Y., Beeckman, H., & Ohtani, J. (1999). Variations in the lengths of fusiform cambial cells and vessel elements in Kalopanax pictus. *Annals of Botany*, *84*(5), 621-632.

Krishnamurthy, K. V., Krishnaraj, R., Chozhavendan, R., & Christopher, F. S. (2000). The programme of cell death in plants and animals–a comparison. *Current Science*, 1169-1181.

Kumpf, R. P., &Nowack, M. K. (2015). The root cap: a short story of life and death. *Journal of Experimental Botany*, *66*(19), 5651-5662.

Liu, J. H., Kitashiba, H., Wang, J., Ban, Y., &Moriguchi, T. (2007). Polyamines and their ability to provide environmental stress tolerance to plants. *Plant Biotechnology*, *24*(1), 117-126.

Liu, Y., Schiff, M., Czymmek, K., Tallóczy, Z., Levine, B., & Dinesh-Kumar, S. P. (2005). Autophagy regulates programmed cell death during the plant innate immune response. *Cell*, *121*(4), 567-577.

Liu, Z., Shi, X., Li, S., Hu, G., Zhang, L., & Song, X. (2018). Tapetal-delayed programmed cell death (PCD) and oxidative stress-induced male sterility of Aegilops uniaristata cytoplasm in wheat. *International Journal of Molecular Sciences*, *19*(6), 1708.

Locato, V., Paradiso, A., Sabetta, W., De Gara, L., & de Pinto, M. C. (2016). Nitric oxide and reactive oxygen species in PCD signaling. In *Advances in Botanical Research* (Vol. 77, pp. 165-192). Academic Press.

Matsuoka, K., Demura, T., Galis, I., Horiguchi, T., Sasaki, M., Tashiro, G., & Fukuda, H. (2004). A comprehensive gene expression analysis toward the understanding of growth and differentiation of tobacco BY-2 cells. *Plant and Cell Physiology*, *45*(9), 1280-1289.

Ménard, D., & Pesquet, E. (2015). Cellular interactions during tracheary elements formation and function. *Current Opinion in Plant Biology*, *23*, 109-115.

Milioni, D., Sado, P. E., Stacey, N. J., Roberts, K., & McCann, M. C. (2002). Early gene expression associated with the commitment and differentiation of a plant tracheary element is revealed by cDNA–amplified fragment length polymorphism analysis. *The Plant Cell*, *14*(11), 2813-2824.

Mittler, R., & Lam, E. (1995). In situ detection of nDNA fragmentation during the differentiation of tracheary elements in higher plants. *Plant Physiology*, *108*(2), 489-493.

Moeder, W., & Yoshioka, K. (2008). Lesion mimic mutants: a classical, yet still fundamental approach to study programmed cell death. *Plant Signaling & Behavior*, *3*(10), 764-767.

Mulisch, M., &Krupinska, K. (2013). Ultrastructural analyses of senescence associated dismantling of chloroplasts revisited. In *Plastid development in leaves during growth and senescence* (pp. 307-335). Springer, Dordrecht.

Obara, K., Kuriyama, H., & Fukuda, H. (2001). Direct evidence of active and rapid nuclear degradation triggered by vacuole rupture during programmed cell death in Zinnia. *Plant Physiology*, *125*(2), 615-626.

Ohashi-Ito, K., Oda, Y., & Fukuda, H. (2010). Arabidopsis VASCULAR-RELATED NAC-DOMAIN6 directly regulates the genes that govern programmed cell death and secondary wall formation during xylem differentiation. *The Plant Cell*, *22*(10), 3461-3473.

Ohashi-Ito, K., Oda, Y., &FukudTuominen, H. (2016). METACASPASE9 modulates autophagy to confine cell death to the target cells during Arabidopsis vascular xylem differentiation.a, H. (2010). Arabidopsis VASCULAR-RELATED NAC-DOMAIN6 directly regulates the genes that govern programmed cell death and secondary wall formation during xylem differentiation. *The Plant Cell*, *22*(10), 3461-3473.

Pesquet, E., Zhang, B., Gorzsás, A., Puhakainen, T., Serk, H., Escamez, S., ... & Paulin, L. (2013). Non-cell-autonomous postmortem lignification of tracheary elements in Zinnia elegans. *The Plant Cell*, *25*(4), 1314-1328.

Reape, T. J., & McCabe, P. F. (2010). Apoptotic-like regulation of programmed cell death in plants. *Apoptosis*, *15*(3), 249-256.

Tounekti, T., Vadel, A. M., Oñate, M., Khemira, H., &Munné-Bosch, S. (2011). Salt-induced oxidative stress in rosemary plants: Damage or protection?. *Environmental and Experimental Botany*, *71*(2), 298-305.

Tsukaya, H. (2003). Organ shape and size: a lesson from studies of leaf morphogenesis. *Current Opinion in Plant Biology*, *6*(1), 57-62.

Turner, S., Gallois, P., & Brown, D. (2007). Tracheary element differentiation. *Annu. Rev. Plant Biol.*, *58*, 407-433.

Twumasi, P., Iakimova, E. T., Qian, T., van Ieperen, W., Schel, J. H., Emons, A. M., ... & Woltering, E. J. (2010). Caspase inhibitors affect the kinetics and dimensions of tracheary elements in xylogenic Zinnia (Zinnia elegans) cell cultures. *BMC Plant Biology*, *10*(1), 162.

Uzair, M., Xu, D., Schreiber, L., Shi, J., Liang, W., Jung, K. H., ... & Zhang, D. (2020). PERSISTENT TAPETAL CELL2 Is Required for Normal Tapetal Programmed Cell Death and Pollen Wall Patterning. *Plant Physiology*, *182*(2), 962-976.

Vander Mijnsbrugge, K., Meyermans, H., Van Montagu, M., Bauw, G., & Boerjan, W. (2000). Wood formation in poplar: identification, characterization, and seasonal variation of xylem proteins. *Planta*, *210*(4), 589-598.

Wilkins, K. A., Poulter, N. S., & Franklin-Tong, V. E. (2014). Taking one for the team: self-recognition and cell suicide in pollen. *Journal of Experimental Botany*, *65*(5), 1331-1342.

Wingler, A., Juvany, M., Cuthbert, C., & Munné-Bosch, S. (2015). Adaptation to altitude affects the senescence response to chilling in the perennial plant Arabis alpina. *Journal of Experimental Botany*, *66*(1), 355-367.

Yamagishi, Y., Uchiyama, H., Sato, T., Kitamura, K., Yoshimoto, J., Nakaba, S., ... &Funada, R. (2015). In vitro induction of the formation of tracheary elements from suspension-cultured cells of the conifer Cryptomeria japonica. *Trees*, *29*(4), 1283-1289.

Zhao, Y. (2010). Auxin biosynthesis and its role in plant development. *Annual Review of Plant Biology*, *61*, 49-64.

MEDIATOR OF DNA DAMAGE CHECKPOINT 1 – INTERACTIONS AND FUNCTIONS

Neeru Singh

Department of Biological Sciences and Biotechnology, Institute of Advanced Research, Gandhinagar-382426

*Corresponding Author: E-mail: neeru.singh@iar.ac.in

Abstract

Mediator of DNA damage checkpoint 1 (MDC1) is a master regulator of Ataxia telangiectasia mutated (ATM) kinase pathway for DNA double strand (DSB) break repair as well as intra S phase and G2/M cell cycle checkpoint. Apart from this, MDC1 has few other although significant yet lesser known roles. The phosphorylation and ubiquitination cycle govern the threshold level of MDC1, its interaction with multiple effector proteins, and later its activity. This review aims to summarize the various findings till date on the functional aspects of the protein and its importance in maintaining the genomic integrity.

***Keywords*:** MDC1, ATM, cell cycle checkpoint, DSB, phosphorylation, ubiquitination, genomic integrity

Abbreviations

IR- ionizing radiation; MDC1-Mediator of Checkpoint 1; DDR-DNA damage response; DSB-double stranded break; ATM-Ataxia telangiectasia mutated like kinase; Chk2- checkpoint kinase2; FHA-fork head associated; BRCT-BRCA like C terminal domain; HR-homologous recombination; NHEJ-non homologous end joining; WSTF-Williams-Beuren syndrome transcription factor; WICH complex-WSTF-ISWI ATP-dependent chromatin-remodelling complex; DNA-PKcs- DNA dependent protein kinase C; XRCC4-ray cross-complementation group 4 and APC/C-Anaphase promoting complex/cyclosome.

Introduction

DNA Damage Repair

The genetic information encoded by chromosome must be transferred accurately to the daughter cells to maintain genome stability and prevent tumour development. However, numerous assaults to the genome by factors such as ionizing radiation (IR), ultraviolet radiation (UVR),

pathogens, reactive oxygen species, or chemotherapeutic drugs can frequently induce DNA damage. If not repaired arrantly, these can lead to gene mutations and loss of genomic integrity. Therefore, DNA damage induces cellular responses involving checkpoint arrest leading to delay or arrest of cell cycle progression, damage repair, and if irreparable, activation of apoptosis. The pathways involved in repairing damaged DNA and hence ensuring the faithful transmission of chromosomes to the daughter cells have intensive signalling network and are collectively referred to as the DNA damage repair (DDR) pathways (Jackson & Bartek, 2009). DDR involves a sensor protein which detects the damage like MRN, RAD9-RAD1-HUS1, and RAD17-RFC complex that activates the transducer kinases as Ataxia telangiectasia mutated (ATM), Ataxia-telangiectasia and RAD3 related (ATR) and DNA dependent protein kinase (DNA-PKc) respectively.The transducer protein through multiple phosphorylation activates several other proteins participating in the pathway including the mediator proteins that contain essentially BRCA1 C-terminus repeat (BRCT) domains serving as protein–phosphoprotein interaction modules. Finally, isactivation and recruitment of effector proteins like p53, Wee1 and Cdc25, determine the fate of the cell. Hence, proteins in the DDR are classified broadly as sensors, transducers, mediators, and effectors (Niida & Nakanishi, 2006). This accumulation of proteins spreads along the entire length of the damaged chromatin is visible microscopically in the form of foci. The importance of this foci formation lies in the fact that they amplify the DNA damage signal so that there is efficient recruitment and activation of machinery involving the repair (Soutoglou & Misteli, 2008).

MDC1- A Multi Domain Protein

MDC1, also known as NFBD1 (Nuclear Factor with BRCT Domains 1) is an important mediator protein in the DDR which arrives early during the event of DNA damage and plays a significant role in the recruitment and retention of other DDR proteins at the site of damage. MDC1 was cloned during random sequencing of cDNAs obtained from the human myeloid cell line KG-1 and was called KIAA0170 (Nagase *et al*., 1996). It was identified as 2089 amino acid long protein with three main domains- N-Terminal fork head associated (FHA) domain, Central proline/ serine/ threonine (PST) rich domain, and tandem C terminal BRCT domain (t-BRCT) (Goldberg *et al*., 2003). MDC1 also contains a large S/TQ cluster domain encompassing its N-terminal half (Stewart *et al*., 2003). The central PST region is a unique domain with an imperfect repetitive motif of ~41 residues. Human MDC1 is highly conserved in the central region and contains 13 full PST repeats with a few partial repeats flanking both sides of these central repeats (Figure 1). Importantly, MDC1 has more than 20 potential ATM/ATR consensus target phosphorylation motifs (Ser/Thr-Gln) scattered throughout the N-terminal half and

additional Ser/Thr-Gln sites are present in the PST region. MDC1 is oligomerized following DNA damage and ATM mediated phosphorylation of Threonine 98 at FHA domain is required for MDC1 oligomerization. Mutation of Thr-98 abolishes MDC1 oligomerization and compromises the accumulation of MDC1 and downstream DDR factors at the sites of DNA damage resulting in defective checkpoint activation (Luo *et al*., 2011). All domains of MDC1 act as a protein binding module mediating protein-protein interaction necessary for DDR. It is important for the recruitment of BRCA1, 53BP1, and the Mre11/Rad50/NBS1 (MRN) complex (Goldberg *et al*., 2003; Lou *et al*., 2003; Mochan *et al*., 2003**;** Stewart *et al*., 2003). MDC1 depletion has been linked to radio-sensitive phenotype, improper activation of the G2 /M, and the intra-S-phase checkpoints and aberrant activation of DNA damage induced apoptosis (Stewart *et al*., 2003). Hence, MDC1 is at the core of the DDR apart from which it has other important roles beyond DDR (Coster & Goldberg, 2010).

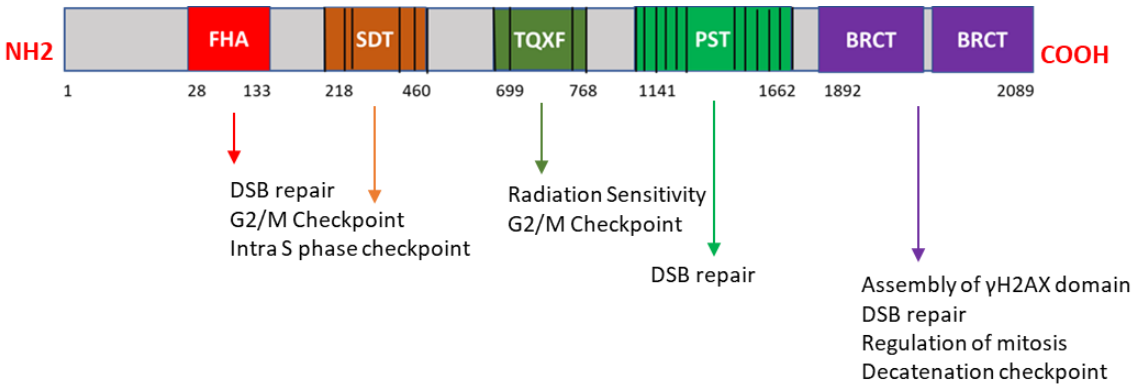

Figure 1: A schematic representation of human MDC1

Five domains have been recognized based on the ability to bind the interacting proteins - N terminal FHA domain, SDT and TQXF repeats, Central PST domain, and two repeats of BRCT domain at the C terminal.

MDC1 and its Interacting Partners in ATM Pathway

The two important players in cellular response to DSBs are ATM and MDC1. ATM is a 350 KDa oligomeric protein belonging to phosphatidylinositol-3 kinase-like kinase (PIKK) family which is activated and recruited to DSBs immediately following DSB induction. ATM undergoes many post-translational modifications including autophosphorylation of Ser-1981 during the process which is necessary for its activation through dissociation of the inactive ATM dimer. However, it has been reported that mutations in several such sites in mice including Ser-1981, do not affect ATM activity (Daniel *et al*., 2008; Pellegrini *et al*., 2006).

Also, MDC1 does not affect the activation of ATM but its recruitment to sites of damage and its chromatin retention are impaired in the absence of MDC1 (Lou *et al*., 2006). Importantly, the FHA domain of MDC1 deviates from the typical specificity of FHA domains for phospho-Thr motives as it binds a phospho-Ser motif in ATM (Durocher *et al*., 2002).

The intricate DDR signalling network is initiated by the primary sensor MRE11-RAD50-NBS1 (MRN) complex which senses and binds to DSB regions and mediates the recruitment of ATM kinase. The MRN complex is a heterodimer of Mre11, NBS1, and Rad50 which is capable of tethering DNA ends. NBS1 is the regulatory sub-unit of the complex with an important role in recruiting the entire MRN complex to sites of damage. More recently, NBS1 was found to contain a conserved C-terminal motif that binds ATM thus revealing the molecular mechanism for the role of the MRN complex in ATM recruitment (Uziel *et al*., 2003; D'Amours *et al*., 2002). After its recruitment, ATM phosphorylates Ser-139 of histone H2AX in the chromatin surrounding the DSB site, creates a docking site for the tandem BRCT domain of MDC1. One of the many substrates of ATM is MDC1 which is activated and phosphorylated by it and recruited to DSBs through direct interaction with γH2AX as well as other DDR members. The post translational modifications including phosphorylation, dephosphorylation, methylation, and ubiquitination play a significant role in the entire cellular process of managing DNA damage (Figure 2).

After induction of DSB, (A) the MRN sensor complex is the first to localize at the break site. It recruits ATM through an interaction with a C-terminal motif in NBS1; (B) ATM phosphorylates histone H2AX molecules at Ser 139; (C) MDC1 binds γ-H2AX through its BRCT domain and recruits more ATM molecules both directly via its FHA domain and indirectly via an interaction with NBS1; (D) More histone H2AX molecules are phosphorylated by ATM thus, spreading the initial signal and amplifying it and MDC1 also recruits the E3 Ub ligase RNF8 which attaches Ub molecules onto histones H2A and H2AX; (E) RNF168 binds ubiquitinated histones H2A/X and it results in the formation of poly-UB chains on these histones; and (F) These interactions favour the subsequent arrival of important DDR proteins such as 53BP1 and the BRCA1.

The interaction and methylation of MDC1 at lysine 45 by histone-lysine *N*-methyltransferase 1 (EHMT1) and EHMT2 promotes the interaction between MDC1 and ATM. This regulatory mechanism also supports the amplification of ATM signalling along the entire length of the damaged chromatin (Wantanabe *et al*., 2018). MDC1 also interacts with NBS1 and facilitates its

retention at DSBs and this interaction is mediated through phosphorylated SDT repeat motifs at the N terminal of MDC1 and FHA, tBRCT domain of NBS1. MDC1 has multiple such SDT

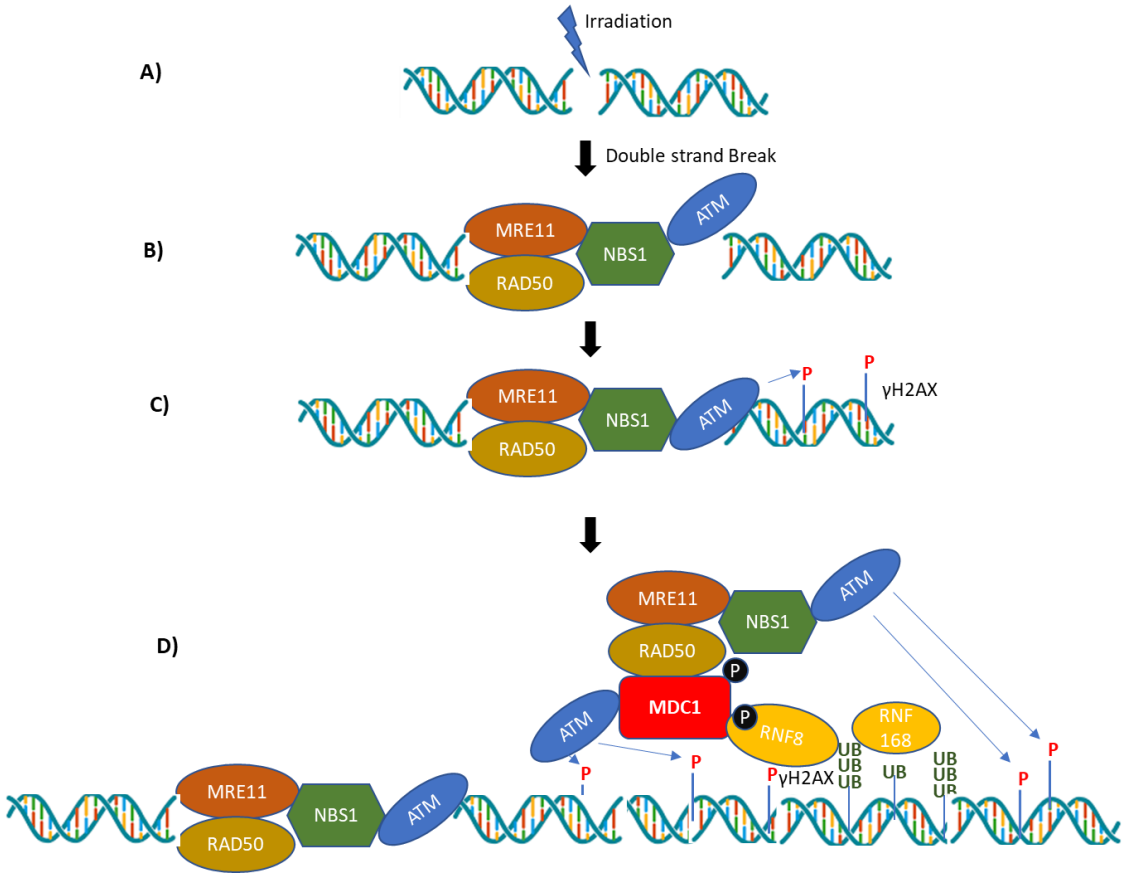

Figure 2: Representation of foci formation at a double-strand break

repeats whereas for interaction with NBS1 only one repeat should be enough. However, various studies have shown that presence of multiple repeat is necessary for higher affinity of MDC1 for NBS1. Interestingly, the two proteins exhibit bipartite mode of binding wherein both the FHA and tBRCT domians of NBS1 bind two different phosphorylated SDT repeats spaced at least 22 amino acids and both the NBS1 domains seem to fuse resulting in a structure which could be bound by only one molecule (Loyd *et al.*, 2009; William *et al.*, 2009). The phosphorylation of MDC1 on its SDT repeats is mediated by casein kinase 2 (CK2) and inhibition of CK2 activity or mutations in either of SDT repeats of MDC1 prevents binding to NBS1 and localization of NBS1 to DSBs (Chapman and Jackson, 2008; Melander *et al.*, 2008). It is noteworthy to say that MDC1 can recruit ATM directly through interaction with its FHA domain and also indirectly via interaction with NBS1. The recruitment of MDC1 itself to damaged chromatin depends on its interaction with helix-loop-helix protein known as inhibitor of DNA binding-3 (ID3). ID3 can interact and recruit MDC1 only when it is phosphorylated by ATM on serine 65 residue following DNA damage. It has been reported that ID3 is essential for

γH2AX and MDC1 interaction and its downregulation can impair DSB repair and lead to hypersensitivity to IR and genomic instability (Lee *et al*., 2017).

The interaction between MDC1 and γH2AX is influenced by the presence of specific motif on H2AX. MDC1 recognizes phosphoserine residue with Tyr or Phe at +3 positions and a free carboxyl terminus in H2AX phosphorylated by ATM and interacts with it through its C-terminal tBRCT domain (Stucki *et al*., 2005). It binds C-terminus of histone H2AX only in its phosphorylated form that is upon DNA damage when it is has been phosphorylated by ATM. The binding of MDC1 to γH2AX has been proposed to protect it from dephosphorylation by the phosphatases, PP2A and PP4, thus maintaining and promoting downstream γ-H2AX signals (Xiao *et al*., 2009). Another recently reported regulatory mechanism influencing this interaction involves a novel tyrosine kinase WSTF (Williams-Beuren syndrome transcription factor, also known as BAZ1B), a component of the WICH complex (WSTF-ISWI ATP-dependent chromatin-remodelling complex). WSTF phosphorylates γH2AX at tyrosine 142 residue at C terminal BRCT domain blocks the binding of MDC1 to γH2AX and only when a tyrosine phosphatase EYA brings about the dephosphorylation of γH2AX that MDC1 could interact with it. Themechanism is important to prevent the spread of γH2AX signalling in the absence of DNA damage (Cook *et al*., 2009; Xiao *et al*., 2009). Hence, it can be concluded that MDC1 and γH2AX interaction is crucial to DNA damage repair and it is through interaction with γH2AX that MDC1 is recruited to damaged chromatin. In lieu of this, recently, an interesting finding reports that MDC1 can bind to chromatin independent of γH2AX through its PST domain (Salguero *et al*., 2019). Infact, several key DDR proteins including NBS1, BRCA1, and 53BP1 can be recruited to DSBs in the absence of histone H2AX. The plausible explanation to the scenario is that for the less severe DSBs that are repaired quickly, H2AX might not be necessary whereas severe DSBs need H2AX for sustained accumulation of the DDR factors if not for their initial recruitment. Also, it has been reported that histone H2AX null cells fail to properly activate cell cycle checkpoints in response to physiological doses of IR whereas non-physiological doses of IR can lead to activation of these checkpoints even in the absence of histone H2AX (Fernandez-Capetillo *et al*., 2002).

Another MDC1 interacting protein identified recently is RNF8, a ubiquitin ligase with FHA domain and catalytic, RING finger domain. Recruitment of RNF8 to DSBs depends on both γH2AX and MDC1 and is mediated through interaction with its FHA domain. While RING domain is essential to the recruitment of downstream factors including BRCA1 and 53BP, the

phospho-specific binding of RNF8 via its FHA domain to MDC1 depends on the presence of phosphorylated TQXF repeats and the Phosphorylation of these repeats occurs in response to DNA damage in an ATM-dependent manner. Also, this binding is redundant in manner as a single phospho TQXF peptide could bind RNF8 but mutations of at least three of the four TQXF repeats were needed to prevent RNF8 binding (Huen *et al*., 2007; Kolas *et al*., 2007; Mailand *et al*., 2007). As mentioned before, RNF8 is important for the recruitment of both BRCA1 and 53 BP1 and this is manifested through ubiquitination of H2A and H2AX at DSBs by RNF8 in coordination with the E2 Ub activating enzyme UBC13. It is suggested but not very well established that MDC1 and RNF8 mediated poly ubiquitination events at DSBs relaxes chromatin and exposes several histone modifications at the histone core essential to the recruitment of various DDR proteins including p53 Binding Protein 1 (53BP1) which is a large mediator protein like MDC1 containing a C-terminal tBRCT domain. 53BP1 also contains a tandem Tudor (tTudor) domain that is essential for its localization to DSBs through binding the methylated lysine 79 of histone H3 and demethylated lysine 20 of histone H4 (Eliezer *et al*., 2009; Zgheib *et al*., 2009) (see Table 1).

Table 1: A tabular representation of all the MDC1 interacting proteins namely, the MDC1 participant domain as well as the necessary post translational modifications.

Interacting protein	Protein type	MDC1 interacting domain	Posttranslational modification involved
ATM	Transducer kinase	FHA	Autophosphorylation on Ser 1981
γ-H2AX	Histone variant	BRCT	phosphorylation on Ser139
NBS1	Part of MRN complex	SDT repeats	phosphorylation of MDC1-SDT
RNF8	E3 Ub ligase	TQXF repeats	phosphorylation of MDC1-TQXF
RAD51	Involved in HR pathway	FHA	Phosphorylation independent

53BP1	Mediator protein	BRCT	Phosphorylation of CDK of 53BP1
DNA-PK	Transducer kinase- NHEJ pathway	PST	Not known
ChK2	Effector protein-Checkpoint kinase	FHA	Phosphorylation of Thr68 on ChK2
p53	Effector protein-transcription factor	BRCT	Inhibited by Ser 15 phosphorylation of p53
MDM2	E3 Ub ligase	BRCT	Not known
APC/C	E3 Ub ligase- cell cycle	FHA, PST, BRCT	Not known
Cdc27	APC/C subunit	BRCT	Phosphorylation of Ser 821 of Cdc27
TOPO Iiα	Topoisomerase	BRCT	Phosphorylation of Ser 1524 of TOPOIIα

To summarize, the DSB-repair pathway is a complex signalling mechanism. The first step involves recruitment of MRN complex to DSBs which in turn recruit and activate the ATM protein kinase (Sun *et al*., 2010). Auto phosphorylated and activated ATM has been shown to phosphorylate hundreds of proteins, including proteins involved in checkpoint activation and DNA repair proteins (Ciccia & Elledge, 2010; Jackson & Bartek, 2009). An important target protein for ATM phosphorylation is the C terminus of the histone variant H2AX which creates a binding site for the BRCT domains of the MDC1. MDC1 recruitment at the DSB creates a docking site for additional DSB repair proteins including the MRN-ATM complex. The MDC1 protein also recruits other effector proteins including the RNF8 and RNF168 ubiquitin ligases which ubiquitinate the chromatin and lead to mobilisation of brca1 and 53BP1 proteins. It is this way that the chromatinubiquitination can spread for tens of kilobases from the DSB (Xu *et al*., 2010). The two E3 ligases, TRIP12 and UBR5 promote the ubiquitin-dependent degradation of RNF168 (Gudjonsson *et al*., 2012).

MDC1 in Non-Homologous End Joining (NHEJ) and Homologous Recombination (HR)

The DSBs can be repaired by either of the two commonly known pathways that are HR and NHEJ. Since HR requires sister chromatid as template, it is restricted to S and G2 phase while NHEJ can take place at any point in cell cycle. The overall process of NHEJ mediated DNA repair involves binding of broken DNA ends by Ku70/Ku80 heterodimer, followed by recruitment of catalytic subunit of DNA dependent protein kinase (DNA-PKcs). The broken DNA ends are made compatible by a nuclease activity of Artemis or filling of end by DNA polymerases and sealed by the ligation complex consisting of DNA ligase IV, X-ray cross-complementation group 4 (XRCC4), and Xrcc4 like factor (XLF)/Cernuous (Meek et al., 2004; Chan *et al*., 2002). The recruitment of DNA-PK requires its activation by auto- phosphorylation on Thr-2609 following DSB induction and requires interaction with MDC1 through its unique PST repeat domain (Lou *et al*., 2004).The NHEJ repair is pathway of choice for the G0 and G1 phases (Heyer *et al*., 2010) and is more error-prone than HR. NHEJ is predominantly utilized because our cells spend maximum time in the G0 and G1 phases. Importantly, ubiquitination of histones adjacent to DSB sites promotes NHEJ over HR (Kolas *et al*., 2007; Mailand *et al*., 2007). In this regard, ASF1 (anti-silencing factor 1) is a histone chaperone which plays an important role in NHEJ as it interacts with newly synthesized H3-H4 heterodimers and mediates interaction of histones to the histone chaperone CAF-1 for nucleosome assembly after replication or repair (Mello *et al.*, 2002). ASF1a promotes H3 acetylation at lys56 by theCBP/p300 acetyltransferase which is required for nucleosomere assembly after DNA repair (Das *et al*., 2009). Recently, ASF1a has been reported to interact with MDC1and is recruited to sites of DSBs to facilitate theinteraction of phospho ATM with MDC1 and promote the recruitment of RNF8/RNF168 histone ubiquitin ligases. Thus, ASF1a is crucial to histone ubiquitination at DSBs and its depletion results in decline in the recruitment of 53BP1 and decreases NHEJ rendering cells that are more sensitive to DSBs (Lee *et al*., 2017).

MDC1 is also necessary for HR pathway as its knock down has been reported to impair the repair process (Zhang *et al*., 2005). The first step in the HR pathway is the resection of the broken DNA ends to generate 3’ single stranded DNA (ssDNA) which is executed by the MRN-complex together (Stracker & Pertini, 2011; Heyer & Ehmsen, 2010) with CtBP-interacting protein (CtIP) and other exonucleases (Limbo *et al*., 2007; Sartori *et al*., 2007). The replication protein A (RPA) first coats the ssDNA to remove secondary structure (Sugiyama *et al*., 1997) and thereafter, it is replaced by RAD51 by BRCA2 to form a nucleoprotein filament that searches for the homologous sequence on the sister chromatid. RAD 51 plays a crucial role in DNA repair and it has been reported that MDC1 is necessary for maintaining RAD 51 foci following ionization radiation (IR) exposure and its depletion leads to lower nuclear levels of

RAD51 (Goldberg *et al*., 2003). It has been suggested that the main mechanism of action of MDC1 in HR is mediated by the regulation of Rad51 stability which affects its recruitment to DSBs and subsequent repair. However, the initial recruitment of RAD51 to DSBs is not impacted by the presence of MDC1. The interaction between the two proteins is most likely through the FHA domain of MDC1 but surprisingly, it is not a phospho-specific interaction and is not necessarily just FHA domain dependent as MDC1 depleted for the domain has been reported to partially rescue the HR defect. Therefore, while MDC1 is required to stabilize the RAD51, it is not just FHA domain but also other protein domains that could also be important in contributing to the effect (Zhang *et al*., 2005).

To conclude, MDC1 is necessary for foci formation in response to DSBs and this is achieved by it primarily through interaction with the key players in the DNA repair, their recruitment to the site of DNA damage, and their stabilization. After foci formation, depending on the severity of damage, the cells either undergo repair via HR or NHEJ pathway and MDC1 plays a significant role in both. If the damage is irreparable, it participates in cell cycle checkpoint arrest and apoptosis.

MDC1 as Mediator of DNA Damage Checkpoint and Apoptosis

The cells inbuilt mechanisms called checkpoints are a regulatory network to sense DNA damage and coordinate DNA replication, cell-cycle arrest, and DNA repair. The effector proteins regulate cell cycle checkpoint arrest and bring about apoptosis in response to DSB and ChK2, an important effector protein which is phosphorylated at Thr 68 by ATM and is not present in the DSB foci rather is scattered in nucleoplasm to carry out its effector functions. MDC1 interacts with phospho Chk2 through its FHA domain (Lou *et al*., 2003). It has been reported that as compared to normal cells which exhibit apoptosis on exposure to ionizing radiations (IR), cells depleted of MDC1 fail to activate intra-S-phase and G2/M checkpoint and or IR-induced apoptosis due to lack of accumulation of p53 and its phosphorylation on Ser-20. Same is true for cells lacking activated Chk2. Both ATM and Chk2, bind MDC1 through FHA domain which leads to the possibility that MDC1 plays essential role in phosphorylation of Chk2 by ATM by bringing the proteins to the proximity. The G2/M checkpoint arrest is a result of p53 independent pathway involving a phosphorylation cascade leading to the activation of Chk1 kinase.

MDC1 has been considered as antiapoptotic in nature as it inhibits p53 activation andhence apoptosis through direct interaction with p53 itself as well as with mdm2 (Inoue *et al.,* 2008; Nakanishi *et al*., 2007). Nakanishi and co-workers reported the direct interaction of MDC1 with

p53 via it NH2- terminal transactivation domain. The DNA damage-induced phosphoryation at Ser-392 and acetylation at Lys-382 of p53 has been shown to enhance the complex formation between p53 and MDC1 (Shahr *et al.,* 2013). Decline in MDC1 accumulation with DSB induction is concomitant with accumulation of p53 thus, indicating an inverse relation between the two and emphasizes on the fact that MDC1 inhibits p53 accumulation and apoptotic activity. There are many reports which show increase in apoptosis in response to MDC1 downregulation following DNA damage whereas apoptosis is inhibited in cells overexpressing MDC1. During the early phase of DDR, MDC1 inhibits ATM-dependent phosphorylation of p53 at Ser-15 thereby, allowing cells to repair damaged DNA while in the late DDR, the expression level of MDC1 sharply reduced and p53 dissociated from MDC1/p53 complex to exert its pro-apoptotic activity (Ozaki *et al*., 2015) (Figure 3).

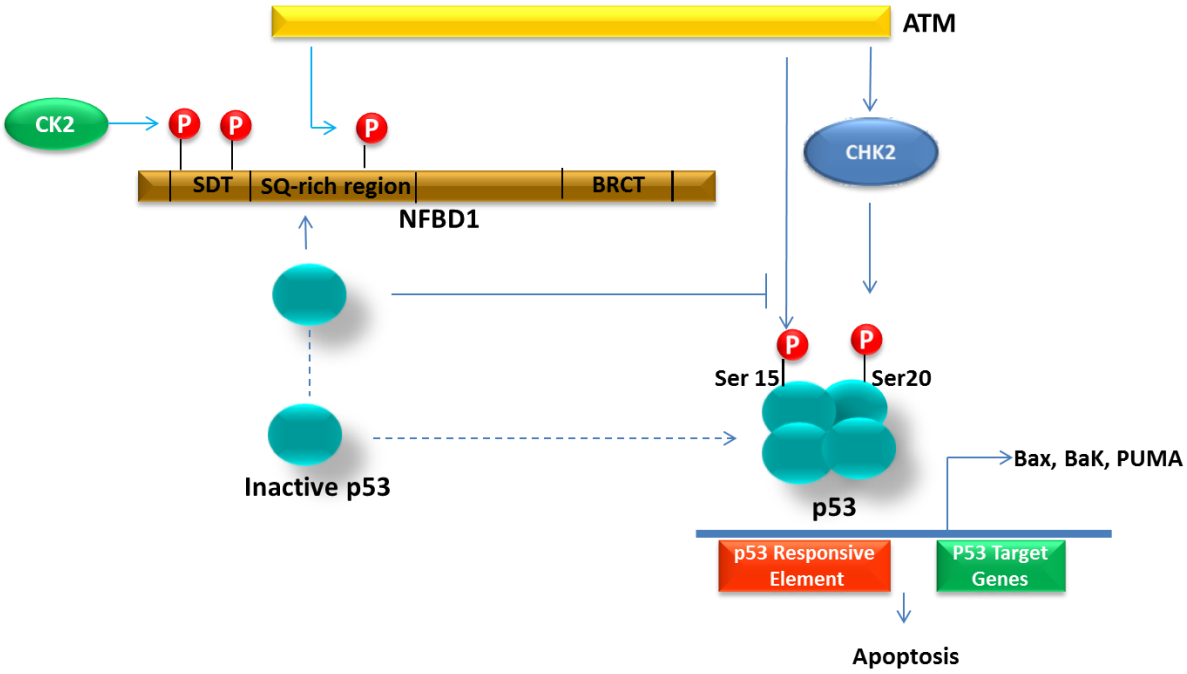

Figure 3: A hypothetical model explaining the interaction of MDC1 with p53 and control of its apoptotic activity during early DNA damage response.

Apart from this, MDC1 also participates in decatenation checkpoint MDC1. The decatenation checkpoint prevents entry into mitosis when sister chromatids are still entangled after replication thus, avoiding DNA breakage during chromosome separation. The cells are arrested at the G2 phase delaying the onset of mitosis until sister chromatids are fully separated (Deming *et al*., 2001). With tBRCT domain of MDC1 as bait, three proteins were identified to play an important role in the checkpoint: TopoIIα, DNA ligase III and XRCC1 (Luo *et al*., 2009). MDC1 interacts with TopoIIα around Ser1524 residue through its tBRCT domain which is a deviation from the known consensus binding site for tBRCT i.e. pS-X-X-Y/F-COOH. The

binding site has an Asp residue rather than a Tyr/Phe at position +3 from the pSer and is not located at the C-terminus of TopoIIα (Stucki *et al*., 2005). It has been shown that downregulation of either MDC1 or TopoIIα prevented the proper activation of the decatenation checkpoint. Thus, MDC1–Topo IIα interaction is important in maintaining genomic stability following chromosome entanglement.

MDC1 as Novel Mitotic Regulator

MDC1 is a mitotic regulator required for cell cycle progression from metaphase to anaphase because of its interaction with one of the many subunits of anaphase promoting complex/cyclosome (APC/C), a ubiquitin ligase which regulates mitosis (Costar *et al*., 2007). The separation of cohesion between the sister chromatids is the main event after DNA replication during which S phase is completed and chromosomes are bioriented. The error proof separation of the sister chromatids ensures equal distribution of genetic material into each daughter cell. Through its ubiquitin activity, APC/C marks B-type cyclins of cyclin-dependent kinase 1 (CDK1) and cohesion for degradation by 26S proteasome. This degradation is necessary for the activation of protein separase which cleaves cohesion, a complex that mediates sister chromatid cohesion and hence, results in their separation (Peters *et al*.,1996; Zacchariae *et al*., 1996; Sudakin *et al*., 1995). MDC1 regulates metaphase to anaphase transition by mediating the interaction of CDC-20 with anaphase promoting complex (APC/C). CDC-20 is necessary for the full ubiquitin ligase activity of APC/C complex during anaphase. Mitotic cells lacking MDC1 have been shown to exhibit reduced levels of APC/C activity and Cdc20 and the interaction between the two and hence, the APC/C activation was a failure (Townsend *et al*., 2009). MDC1 has also been reported to be critical for SAC activation as it localizes at mitotic kinetochores following SAC activation in an ATM-dependent manner. ATM and MDC1 are needed for kinetochore localization of the inhibitory mitotic checkpoint complex (MCC) components, Mad2 and Cdc20 and for the maintenance of the MCC integrity. The MCC participates in SAC by binding to Cdc20 to prevent APC/C activity. ATM and MDC1 regulate the SAC together through an interaction with the MCC. The integrity of the MCC is crucial for an intact SAC which when de-regulated can cause chromosomal aberrations and genomic instability (Eliezer *et al*., 2014).

MDC1 maintains chromosomal stability when DNA double-strand breaks occur during mitosis and this function is mediated through interaction with TOPBP1 possibly by tethering broken chromosomes together via intra and inter-chromosomal bridges until DNA-repair pathways are reactivated in the following G1 phase (Leimbacher *et al*., 2019). Therefore, loss of MDC1 or

disruption of the MDC1-TOPBP1 interaction leads to increased radio-sensitivity in mitotic cells and increased formation of micronuclei that mostly contains acentric chromatin fragments. It can be said that DSBs are not properly stabilized in the absence of MDC1 and TOPBP1 recruitment and acentric fragments are not segregated into the daughter cells along with the chromosome from which they have broken off.

Conclusion

The cell has an intricate network of DDR proteins taking care of DSBs and preserving the integrity of the genome. Eventhough numerous studies have been reported in this direction, the clear mechanism of DDR remains elusive. This review summarizes the importance of one of the central players in the pathway, MDC1, which is not just a regulator of the DDR but also has several significant roles apart from it. It is a scaffold protein which binds several other proteins through its multiple domains and enables an interaction among them. The downregulation of MDC1 leads complex phenotypes as increased radiation sensitivity, impaired NHEJ repair, reduced apoptosis, and a defect in the early G2 checkpoint and intra-S-phase checkpoint (Lou *et al*., 2003; Stewart *et al*., 2003). As discussed in detail, protein interactions mediated by MDC1 mostly follow a general rule of need of post-translational modifications primarily, phosphorylation that are programmed for faster and efficient amplification of the DNA damage signal. Although there are always some exceptions to general rule, for example, the binding of MDC1 to Rad51 does not seem to require phosphorylation whereas it's binding to ATM occurs via a phospho-Ser motif rather than an expected phospho-Thr motif. Another noteworthy property of the domains of MDC1 is their repetitive nature. The domains TQXF, SDT, and PST have imperfect repeats and share very similar characteristics. As far as binding is concerned, both SDT and PST domains require phosphorylation to interact and a single motif is sufficient for binding even though there is a multiple repeat of required motifs. In case of NBS1, the interaction with SDT repeats of MDC1 is kind of bipartite binding, that is, the six SDT repeats may constitute up to three potential NBS1-binding sites. The reason for these repetitive motifs is not clear but two main hypotheses can fit in; first, this allows a greater number of molecules of interacting proteins like RNF8 and NBS1 onto a single MDC1 molecule which would lead to a higher concentration of RNF8 and NBS1 at the break site contributing towards efficient signal amplification and second, the local concentration of several binding sites increases the likelihood of a single molecule to bind MDC1 thus, enhancing their binding affinities. Interestingly, the PST repeats have duplicated so much that they comprise about a third of human MDC1 (Coster & Goldberg, 2010).

MDC1 is indispensable to DDR and there are many reports on the involvement of this protein in other biological processes. As mentioned, some of the novel roles of MDC1 include protecting chromosomes from breakage in the decatenation checkpoint and in the metaphase to anaphase transition in mitosis.

Acknowledgment

The author would like to thank department of biological sciences and biotechnology, Institute of advanced research, Gandhinagar.

References

Chan DW, Chen BPC, Prithivirajsingh S, Kurimasa A, Story MD, Qin J, *et al*. (2002). Autophosphorylation of the DNA-dependent protein kinase catalytic subunit is required for rejoining of DNA double-strand breaks. Genes Dev; 16:2333-8.

Chapman JR, Jackson SP. (2008). Phospho-dependent interactions between NBS1 and MDC1 mediate chromatin retention of the MRN complex at sites of DNA damage. EMBO Rep; 9:795-801.

Cook PJ, Ju BG, Telese F, Wang XT, Glass CK, Rosenfeld MG. (2009).Tyrosine dephosphorylation of H2AX modulates apoptosis and survival decisions. Nature; 458:553-91.
Coster, G., & Goldberg, M. (2010). The cellular response to DNA damage: a focus on MDC1 and its interacting proteins. Nucleus; 1(2): 166–178.

D'Amours D, Jackson SP. (2002). The Mre11 complex: At the crossroads of dna repair and checkpoint signalling, Nat Rev Mol Cell Biol; 3:317–27.

Daniel JA, Pellegrini M, Lee JH, Paull TT, Feigenbaum L, Nussenzweig A. (2008). Multiple autophosphorylation sites are dispensable for murine ATM activation in vivo. J Cell Biol; 183:777-83.

Das, C., Lucia, M.S., Hansen, K.C., and Tyler, J.K. (2009). CBP/p300-mediatedacetylation of histone H3 on lysine 56. Nature; 459, 113–117.

Durocher D, Jackson SP. (2002). The FHA domain. FEBS Lett; 513:58-66.

Eliezer Y, Argaman L, Rhie A, Doherty AJ, Goldberg M. (2009). The Direct Interaction between 53BP1 and MDC1 Is Required for the Recruitment of 53BP1 to Sites of Damage. J Biol Chem; 284:426-35.

Fernandez-Capetillo O, Chen HT, Celeste A, Ward I, Romanienko PJ, Morales JC, *et al*. (2002).DNA damageinduced G(2)-M checkpoint activation by histone H2AX and 53BP1. Nat Cell Biol; 4:993-7.

Goldberg M, Stucki M, Falck J, D'Amours D, Rahman D, Pappin D, *et al*. (2003). MDC1 is required for the intra-S-phase DNA damage checkpoint. Nature; 421:952-6.

Heyer WD, Ehmsen KT, Liu J. (2010). Regulation of homologous recombination in eukaryotes. Annu Rev Genet; 44:113–139.

Huen MSY, Grant R, Manke I, Minn K, Yu XC, Yaffe MB, *et al*. (2007). RNF8 transduces the DNA-damage signal via histone ubiquitylation and checkpoint protein assembly. Cell; 131:901-14.

Inoue K, Nakanjishi M, Kikuchi H, Yamamoto H, Todo S, Nakagawara A, *et al*. (2008). NFBD1/MDC1 stabilizes oncogenic MDM2 to contribute to cell fate determina-tion in response to DNA damage. Biochem Biophys Res Commun; 371:829-33.

Kolas NK, Chapman JR, Nakada S, Ylanko J, Chahwan R, Sweeney FD, *et al*. (2007). Orchestration of the DNAdamage response by the RNF8 ubiquitin ligase. Science; 318:1637-40.

Kuntian Luo, Jian Yuan and Zhenkun Lou. (2011). Oligomerization of MDC1 Protein Is Important for Proper DNA Damage Response. J Biol Chem;286(32):28192-9.

Lavin, M. F., and Kozlov, S. (2007). ATM activation and DNA damage response. Cell Cycle; 6, 931–942.

Lee K, Im J, Shibata E, Dutta A. (2017). ASF1a Promotes Non-homologous End Joining Repair by Facilitating Phosphorylation of MDC1 by ATM at Double-Strand Breaks. Molecular Cell; 68: 1,61-75.

Limbo O, Chahwan C, Yamada Y, de Bruin RA, Wittenberg C, Russell P. (2007). Ctp1 is a cell-cycle-regulated protein that functions with Mre11 complex to control double-strand break repair by homologous recombination. Mol Cell; 28:134–146.

Lloyd J, Chapman JR, Clapperton JA, Haire LF, Hartsuiker E, Li JJ, *et al*. (2009). A Supramodular FHA/BRCTRepeat Architecture Mediates Nbs1 Adaptor Function in Response to DNA Damage. Cell; 139:100- 11. 66.

Lou Z, Minter-Dykhouse K, Franco S, Gostissa M, Rivera M, Celeste A, *et al*. (2006). MDC1 maintains genomic stability by participating in the amplification of ATM dependent DNA damage signals. Mol Cell; 21:187-200.

Lou Z, Minter-Dykhouse K, Wu X, Chen J. (2003). MDC1 is coupled to activated CHK2 in mammalian DNA damage response pathways. Nature; 421:957-61.

Luo KT, Yuan J, Chen JJ, Lou ZK. (2009). Topoisomerase II alpha control the decatenation checkpoint. Nature Cell Biol; 11:196-204.

Mailand N, Bekker-Jensen S, Faustrup H, Melander F, Bartek J, Lukas C, et al. (2007). RNF8 ubiquitylates histones at DNA double-strand breaks and promotes assembly of repair proteins. Cell; 131:887-900.

Meek K, Gupta S, Ramsden DA, Lees-Miller SP. (2004). The DNA-dependent protein kinase: the director at the end. Immunol Rev; 200:132-41. 75.

Melander F, Bekker-Jensen S, Falck J, Bartek J, Mailand N, Lukas J. (2008). Phosphorylation of SDT repeats in the MDC1 N terminus triggers retention of NBS1 at the DNA damage-modified chromatin. J Cell Biol; 181:213-26. 64.

Mello, J.A., Sillje, H.H., Roche, D.M., Kirschner, D.B., Nigg, E.A., and Almouzni,G. (2002). Human Asf1 and CAF-1 interact and synergize in a repair-couplednucleosome assembly pathway. EMBO Rep; 3, 329–334.

Mochan TA, Venere M, DiTullio RA, Halazonetis TD. (2003). 53BP1 and NFBD1/MDC1-Nbs1 function in parallel interacting pathways activating ataxia-telangiectasia mutated (ATM) in response to DNA damage. Cancer Research; 63:8586-91. 14.

Nakanishi M, Ozaki T, Yamamoto H, Hanamoto T, Kikuchi H, Furuya K, *et al*. (2007). NFBD1/MDC1 associates with p53 and regulates its function at the crossroad between cell survival and death in response to DNA damage. J Biol Chem; 282:22993-3004.

Pellegrini M, Celeste A, Difilippantonio S, Guo R, Wang WD, Feigenbaum L, *et al*. (2006). Autophosphorylation at serine 1987 is dispensable for murine Atm activation *in vivo*. Nature; 443:222-5. 56.

Peters JM, King RW, Höög C, Kirschner MW. (1996). Identification of BIME as a subunit of the anaphase-promoting complex. Science; 274(5290):1199–1201.

Sartori AA, Lukas C, Coates J, Mistrik M, Fu S, Bartek J, Baer R, Lukas J, Jackson SP (2007). Human CtIP promotes DNA end resection. Nature; 450:509–514.

Shahar OD, Gabizon R, Feine O, Alhadeff R, Ganoth A, Argaman L, *et al*.(2013). Acetylation of lysine 382 and phosphorylation of serine 392 in p53 modulate the interaction between p53 and MDC1 *in vitro*. PLoS One; 8(10):e78472.

Soutoglou E, Misteli T. (2008). Activation of the cellular DNA damage response in the absence of DNA lesions. Science; 320:1507-10.

Stewart G, Wang B, Bignell C, Taylor A, Elledge S. (2003). MDC1 is a mediator of the mammalian DNA damage checkpoint. Nature; 421:961-6.

Stracker TH, Petrini JH. (2011). The MRE11 complex: starting from the ends. Nat Rev Mol Cell Biol; 12:90–103.

Stucki M, Clapperton J, Mohammad D, Yaffe M, Smerdon S, Jackson S. (2005). MDC1 directly binds phosphorylated histone H2AX to regulate cellular responses to DNA double-strand breaks. Cell; 123:1213-26.

Sudakin V, et al. (1995). The cyclosome, a large complex containing cyclin-selective ubiquitin ligase activity, targets cyclins for destruction at the end of mitosis. Mol Biol Cell; 6(2):185–197.

Sugiyama T, Zaitseva EM, Kowalczykowski SC: A single-stranded DNAbinding protein is needed for efficient presynaptic complex formation by the Saccharomyces cerevisiae Rad51 protein. J Biol Chem 1997; 272:7940–7945.

Uziel T, Lerenthal Y, Moyal L, Andegeko Y, Mittelman L, Shiloh Y. (2003). Requirement of the MRN complex for ATM activation by DNA damage. EMBO J; 22:5612-21.

Watanabe, S., Iimori, M., Chan, D.V. (2018). MDC1 methylation mediated by lysine methyltransferases EHMT1 and EHMT2 regulates active ATM accumulation flanking DNA damage sites. *Sci Rep*; **8,** 10888.

Williams RS, Dodson GE, Limbo O, Yamada Y, Williams JS, Guenther G, *et al*. (2009). Nbs1 Flexibly Tethers Ctp1 and Mre11-Rad50 to Coordinate DNA DoubleStrand Break Processing and Repair. Cell; 139:87- 99.

Xiao A, Li HT, Shechter D, Ahn SH, Fabrizio LA, Erdjument-Bromage H, *et al*. (2009). WSTF regulates the H2A.X DNA damage response via a novel tyrosine kinase activity. Nature; 457:57.

Zachariae W, Shin TH, Galova M, Obermaier B, Nasmyth K. (1996). Identification of subunits of the anaphase-promoting complex of Saccharomyces cerevisiae. Science; 274(5290):1201–1204.

Zgheib O, Pataky K, Brugger J, Halazonetis TD. (2009). An Oligomerized 53BP1 Tudor Domain Suffices for Recognition of DNA Double-Strand Breaks. Mol Cell Biol; 29:1050-8. 72.

Zhang J, Ma Z, Treszezamsky A, Powell S. (2005). MDC1 interacts with Rad51 and facilitates homologous recombination. Nat Struct Mol Biol; 12:902-9.

EMIM IONIC LIQUIDS: APPLICATIONS IN ORGANIC SYNTHESIS AND CATALYSIS

Yash B Barot[1], Roli Mishra[1*]

[1]Department of Engineering and Physical Sciences, Institute of Advanced Research, Koba Institutional Area, Gandhinagar, Gujarat, 382426 India
*Corresponding Author: E-mail: roli.mishra@iar.ac.in

Abstract

Ionic liquids (ILs) exhibited various chemical applications and are known as an environment friendly alternative to the volatile organic solvents. Cationic and anionic components in ILs can be tuned to improve its desired properties. Being designer solvents, ionic liquids can be altered to suit the reaction conditions therefore called as 'task specific ionic liquids. Additionally, ILs are used as neoteric solvents for chemical transformations. The aim of present review is to discuss the applications of 1-ethyl-3-methylimidazolium (EMIM) based ionic liquids as catalysts and solvents in various organic transformations.

Keywords: Ionic liquids, EMIM, Mannich reaction, Acetylation, Tritylation, Media, Catalysis

Introduction

Ionic Liquids (ILs) have attracted considerable attention due to their special properties such as non-volatility, high thermal stability, high polarity, non-explosive, superior catalytic activity, and simple operation at liquid state. ILs is referred as class of purely ionic salt like materials that are liquid at low temperature. Currently, ILs is defined as salts having melting point below the boiling point of water [Hallett *et al.* 2011]. They are also well-known liquid organic salt, molten salts, fused salt, and extraordinary magical fluids, as room temperature ILs (RTILs) [Sugden *et al.* 1928; Gorman *et al.* 2001]. The typical preparations of an ILs mainly involve a quaternization reaction such as the alkylation of a 1-alkylimidazole by a halo alkane. This step is usually followed by an acid-base neutralization or metathesis of the resulting halide salt with a Group 1A metal, ammonium salt, or silver salt of the desired anion to afford the IL together, with a stoichiometric amount of by-product (HX or MX, respectively) which must subsequently be removed. These ILs are entirely composed of various types of known common bulky organic cations like, imidazoilum [Bonĥte *et al.,* 1996; Fannin *et al.,* 1984,. Wilkes *et al.,* 2014; Hurley *et al.* 1951, pyrazolium [Hill *et al.,* 1991], ammonium [Sun *et al.,* 1998; Gale *et al.,* 1980], pyridinium, [Tait *et al.,* 1984], pyrrolidinium [Miyatake *et al.,* 1998], triazolium [MacFarlane *et*

al., 1999], morpholinium [Vestergaard *et al.,* 1993], sulfonium [Hussey *et al.,* 1994], oxazolium [Cha *et al.,* 2005], thiazolium [Davis *et al.*,1999], and inorganic anion [Handy *et al.*,2005] with specific functional groups developed unique physical and chemical properties.

As solvents, ionic liquids have established applications in a number of reactions [Song *et al.,* 2004; Xiao *et al.*, 2004; Anjaiah *et al.*, 2004; Mastrorilli *et al.* 2004; Lombardo *et al.*, 2009; Shen *et al.*, 2008; Feng *et al.*, 2010; Singh *et al.*, 2010; Fukuyama *et al.*, 2007; Schenzel *et al.*, 2014]. Application of ionic liquids as catalytic phase in various organometallic reactions have evaluated by Dupont et al. 2002. Catalytic applications of metal nanoparticles have been also investigated in ionic liquid [Migowski *et al.*, 2007; Dupont *et al.*, 2002]. In addition to the use of ionic liquids as alternate solvents, recently, further work on ionic liquids led to the design and development of functional ionic liquids. Functional ionic liquids are also referred as 'task specific ionic liquids' (TSIL) [Chen *et al.,* 2012]. Nowadays, ILs is often employed as green solvents. Green Chemistry is classified as "the design, manufacture, and application of chemical products and processes to decrease or to eradicate the use and generation of hazardous substances". Room temperature ILs is usually considered chemically and thermally stable because they are often based on the imidazolium or other stable cations.

Applications in Organic Synthesis

Ionic liquids were used as an alternative to green reaction media and catalyst in organic transformations because of their inimitable physical and chemical properties. There are a number of ionic liquids which have been widely used in organic transformations. Herein, we are reviewing application of 1-ethyl-3- methyl-imidazolium in organic transformations. Fu *et al*. designed Biginelli-type reaction involving aliphatic aldehydes, aromatic aldehydes, and urea to give a series of highly diverse 3,4-dihydropyrimidin-2-(1H)-one products in 58-88 % yields with high regioselectivity in the presence of 30 % aqueous solution of ionic liquid (1-ethyl-3-methylimidazolium tetrafluoroborate) as a green reaction medium (Figure1). The catalyst was easily recycled and reused with comparable efficacy for at least four cycles [Fu *et al*., 2019].

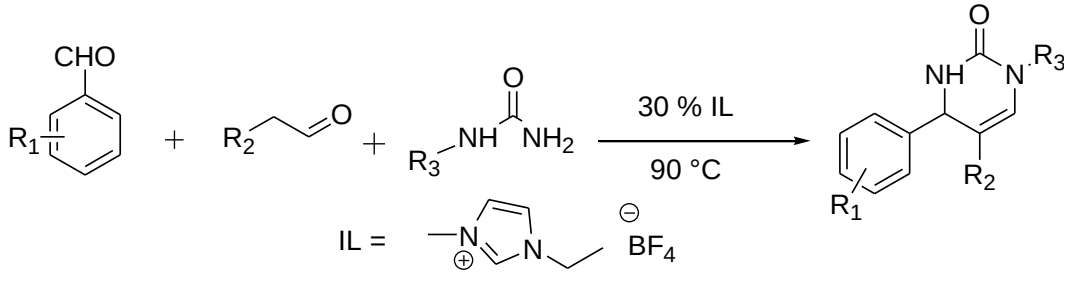

[EMIM][BF4]

Figure 1: Synthesis of Dihydropyrimidin via Biginelli-type reaction using [EMIM] [BF_4]

Chaubey *et al*. reported a new efficient approach for the tritylation of primary alcohols over secondary alcohols using triphenyl methyl alcohol and 4-monomethoxyl trityl alcohols in the presence of 5 mol % imidazolium-based ionic liquid 1- ethyl-3-methylimidazolium tetrachloroaluminate [EMIM] [$AlCl_4$] as catalyst at room temperature (Figure 2). Dichloromethane and acetonitrile exhibited excellent tritylation product of benzyl alcohol and other alcohols. This method was compatible with labile protecting viz. Fmoc, acetyl, tert-butyldiphenylsilyl ether group, etc. Additionally, the catalyst was reusable up to four catalytic cycles with little loss of catalytic activity [Chaubey *et al*., 2020].

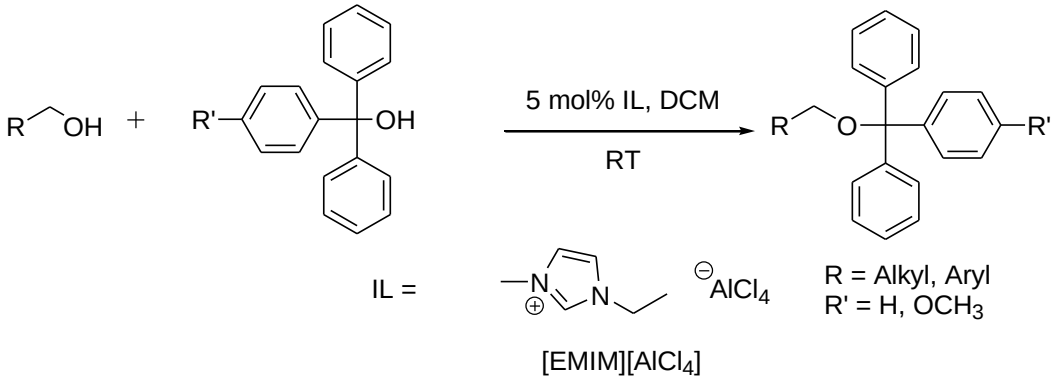

Figure 2: Tritylation of aliphatic and aromatic primary alcohol using 1- ethyl-3-methylimidazolium tetrachloroaluminate [EMIM] [$AlCl_4$] as catalyst

Ionic liquid (IL) 1-ethyl-3-methylimidazolium bis (trifluoromethylsulfonyl) imide [EMIM][NTf_2] and dimethylformamide (DMF) as a co-solvent tremendously promoted the catalytic epoxidation of cis-cyclooctene over Vanadium exchanged faujasite zeolite catalysts [Bai *et al.*, 2016] in presence of oxidant tert-butyl hydroperoxide (TBHP) (Figure 3). It was also anticipated that the activation energy of the kinetically relevant step was reduced in the fragile acidic environment offered by the imidazolium cation of [EMIM] [NTf_2].

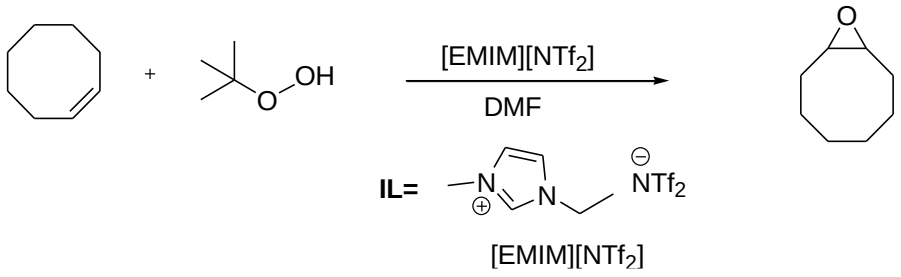

Figure 3: Epoxidation of cis-cyclooctene over vanadium-exchanged faujasite zeolite catalyst in presence of Ionic Liquid [EMIM][NTf_2]

Palladium complex in ethyl-methyl imidazolium hexafluorophosphate [EMIM] [PF_6] ionic liquid at ambient temperature demonstrated highly efficient catalytic activity towards Heck and Suzuki cross-coupling reactions (Figure 4). This catalytic system offers a stable and reusable method for the Heck reaction. Using a very modest amount of catalyst, good-to-excellent yields were accomplished [Ramakrishna *et al.,* 2019]. The reaction conditions were mild and significantly, the catalytic system was easily recyclable and reusable for up to six times without much loss in the catalytic activity.

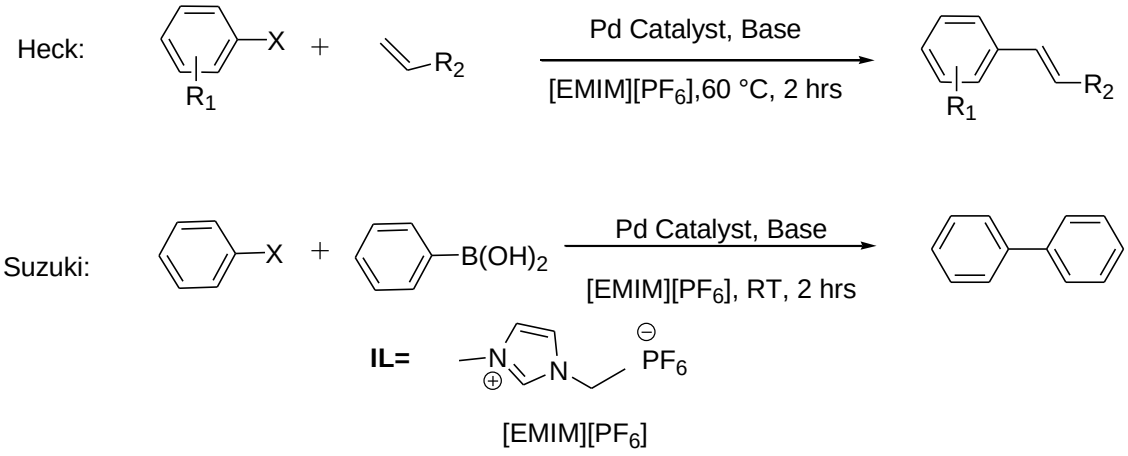

Figure 4: Heck and Suzuki reactions in presence of Pd complex in [EMIM] [PF_6]

Task specific ionic liquids were synthesized by the reaction of methyl imidazole with 1, 3-propane sultone and 1, 4-butane sultone to explore their catalytic activity in the preparation of Mannich bases. Synthesized protic ionic liquids (ILs) catalysed the Mannich reaction at 25°C to afford high yield of Mannich bases in lesser time (Figure 5). This ionic liquid has dual work in the reaction i.e., as a catalyst as well as a solvent. This is also recyclable up to 4 times without

any significant loss in the activity [Sardar *et al.,* 2016]. This study offers a convenient and effective way for the synthesis of Mannich bases at room temperature in short reaction duration.

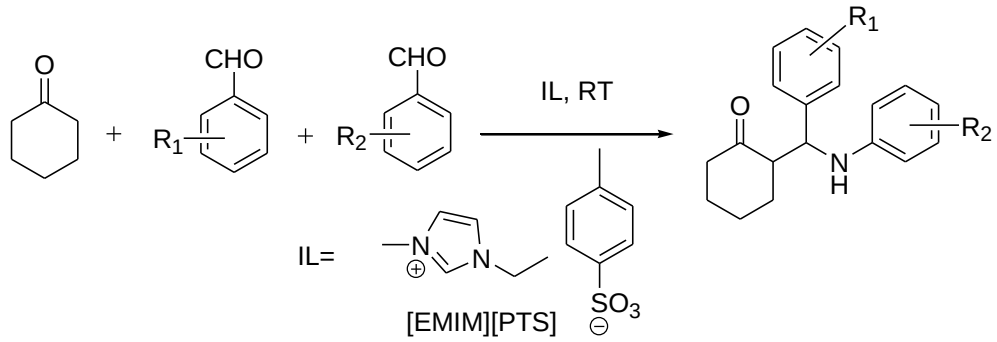

Figure 5: Imidazolium based ionic liquids (1-ethyl-3-methylimidazolium ptoluenesulfonate) [EMIM][PST] catalyzed Mannich reaction

The Mannich type reaction of silyl enolates with aldimines took place smoothly in presence of [EMIM] [OTf] as a solvent and yield β-amino carbonyl compounds in excellent yields without the addition of an activator (Figure 6). The outcome of result explains that ionic liquids bearing an OTf anion are essential. The ionic liquid was recycled 5 times without loss of reactivity [Akiyama *et al.*, 2005].

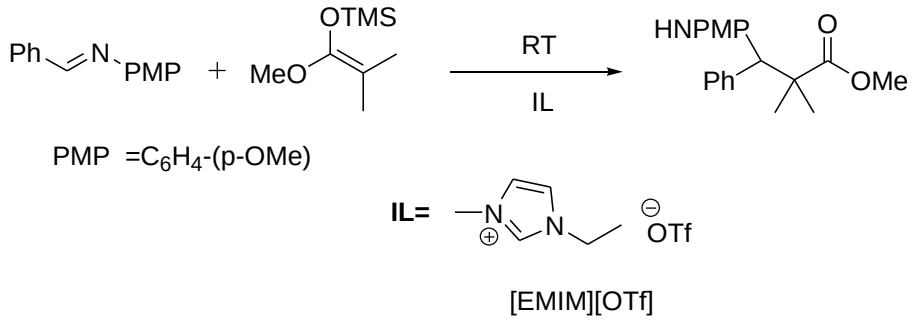

Figure 6: Three-component Mannich-type reactions in [EMIM] [OTf]

The ionic liquid 1-ethyl-3-methylimidazole acetate ([EMIM] [OAc] was found to be a mild and effective catalyst for the efficient one-pot three-component synthesis of 1,4-dihydropyridines from aryl aldehydes, ethylacetoacetate/acetyl acetone, and ammonium acetate at room temperature under sonication (Figure 7). The developed procedure has several advantages like; alternative of unsafe catalysts, higher yields and simple methodology at room temperature [Palakshi *et al.* 2015].

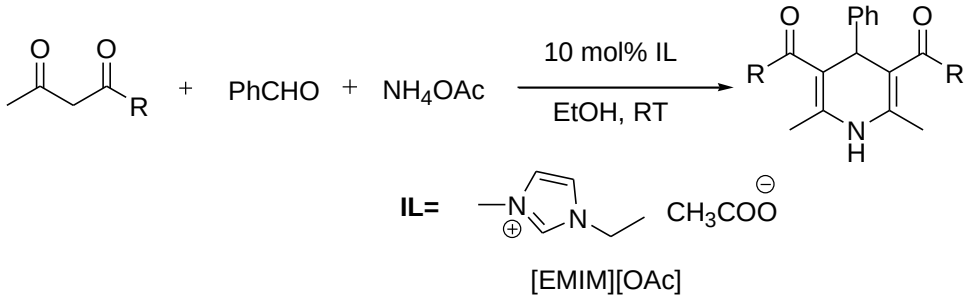

Figure 7: Ionic liquid [EMIM][OAc] catalyzed synthesis of various substituted 1,4-dihydropyridines

Task-specific amino-functionalized imidazolium ionic liquid, acetate1-(2-tert-butoxycarbonylamino-ethyl)-3-methyl-3H-imidazol-1-ium; (Boc-NH-EMIM.OAc) has been developed as an efficient catalyst for the acetylation of alcohols, phenols, and amines in the presence of acetic anhydride (Figure 8). Notably, 10 mol% of catalyst (Boc-NH-EMIM.OAc) demonstrated excellent yields of acetylated product in shorter time under neat system. This catalyst can be reused up to four cycles without any considerable loss of its catalytic activity [Chaubey *et al.* 2020].

In situ strategy of immobilization of a copper complex onto an ionic liquid support has been reported by [Dileep & Rudresha 2015]. A sensible approach of terminal olefin and terpene epoxidation by immobilizing a copper complex and 1-ethyl-3-methylimidazolium hexafluorophosphate using H_2O_2 as the terminal oxidant was developed (Figure 9). The advantages of this oxidation system are that hydrogen peroxide and catalyst are entirely soluble in [EMIM] [PF_6], give a homogeneous oxidation solution, and provide an exceptionally clean environment for catalytic epoxidation.

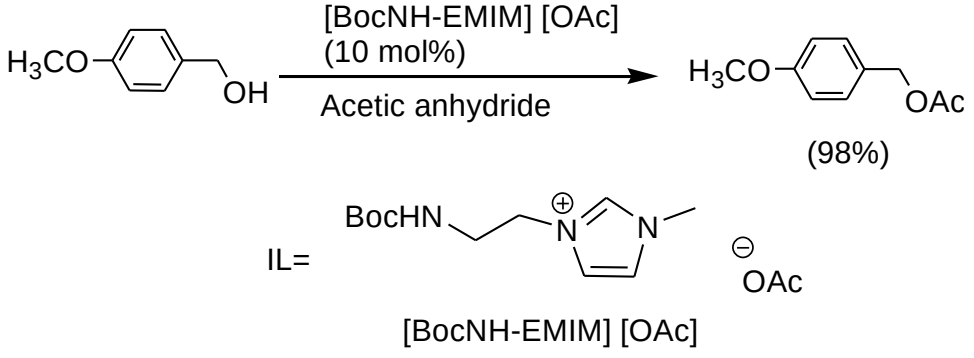

Figure 8: Acetylation of alcohol in presence of [Boc-NH-EMIM] [OAc] and acetic anhydride at room temperature

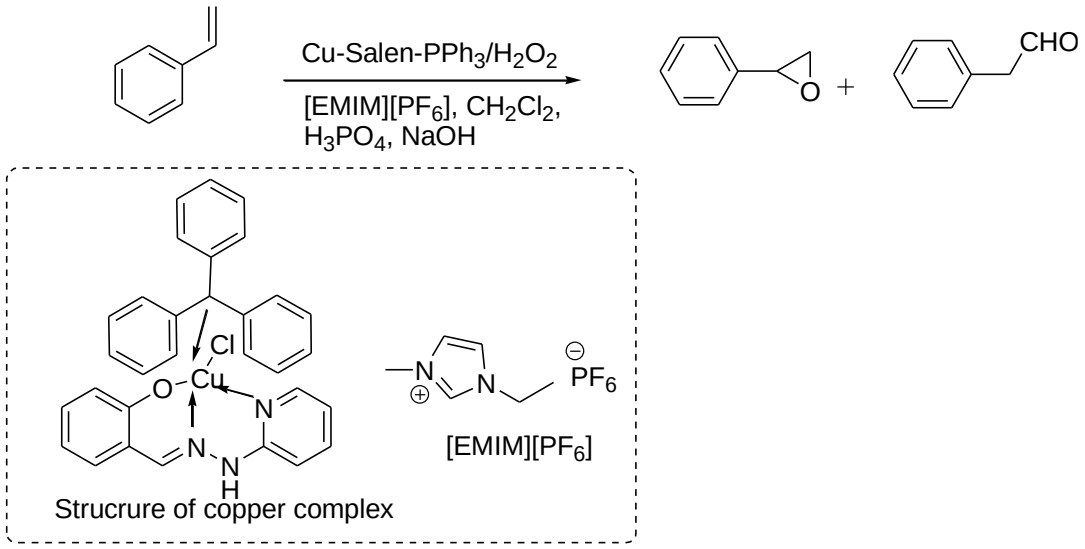

Figure 9: The epoxidation of alkenes by hydrogen peroxide catalyzed by copper complex in [EMIM] [PF_6]

The aerobic oxidation of 1-phenylethanol over a carbon nanotube supported palladium catalyst was improved in the presence of ionic liquid additive [EMIM][NTf_2] and this can be recycled for 5 runs (Figure 10) [Chen *et al.*,2011].

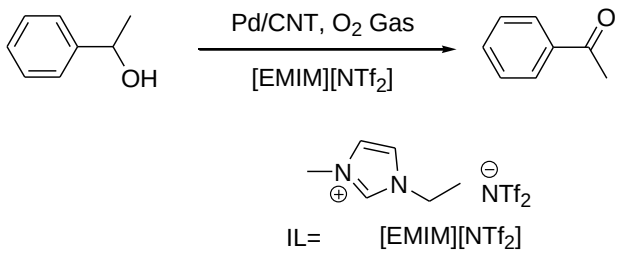

Figure 10: Palladium-catalyzed aerobic oxidation of 1-phenylethanol in presence of ionic liquid additive [EMIM][NTf_2]

Luo et al. 2012 investigated the catalytic activities of Lewis acidic ILs such as [EMIM] Cl-AlCl3, [Bmim] Cl-AlCl3, and [Omim] Cl-AlCl3 for the acetylation of pyrene with acetyl chloride under various experimental conditions. Chloroaluminate ionic liquids and metal chloride catalyses the acetylation of pyrene to furnish 1-acetylpyrene in excellent yield. Ionic liquid [EMIM] [$AlCl_4$] was found to be the most active and selective catalyst in the acylation of pyrene (Figure 11).

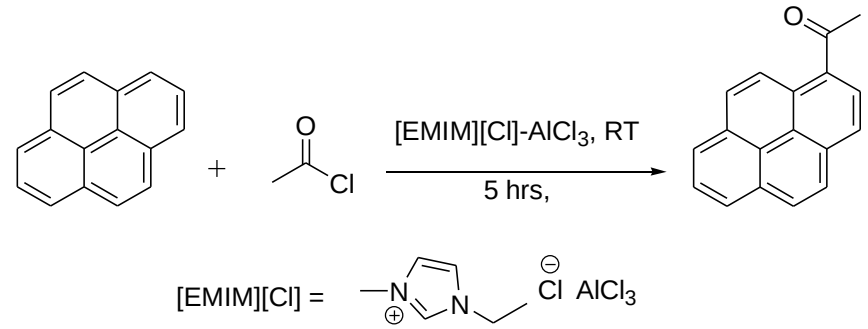

Figure 11: Friedel-Crafts acetylation of pyrene to 1-acetylpyrene in presence of [EMIM] [$AlCl_4$]

Using the minor toxic and biodegradable ionic liquid 1-ethyl-3- methyl-imidazolium acetate [EMIM] [OAc], homogeneous acylation of cellulose was carried out with a high to moderate control over substitution pattern with even satirically demanding nonpolar side chains. The reaction proceeds in the absence of any additional catalyst. Glucose- and cellulose- esters with chain lengths of C8 to C16 were easily prepared by using equimolar amounts of acyl donor. The highest degree of substitution (DS) was achieved at 80°C in two hours (Figure 12). This novel process was extended by further acyl donors like vinyl benzoate, pivalate, and 2-ethylhexanoate to demonstrate the applicability of the vinyl ester-based cellulose modification in [EMIM] [OAc] which was recycled with an efficiency of ~90% and reused for a subsequent synthesis [Hinner *et al.*, 2016].

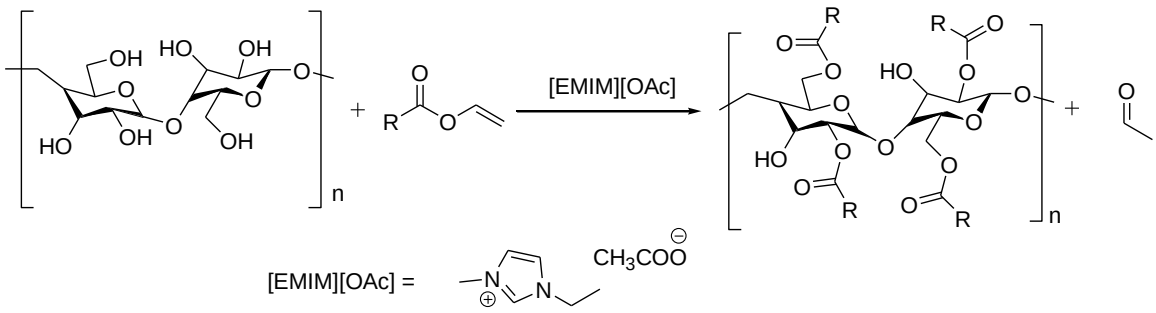

Figure 12: Acetylation of glucose and cellulose in presence of ionic liquid [EMIM] [OAc]

The careful dehydration of pinacol derivatives to branched 1, 3-dienes is very demanding due to the predominance of pinacol rearrangement. This goal can be effectively realized by use of recyclable solid acid/ionic liquid catalyst system. The dehydration of alkyl and cycloalkyl derived diols in presence of Amberlyst-15/[EMIM] [Cl] system furnished the corresponding

1,3-dienes in good yields, whereas Nafion/[EMIM] [Cl] was established to be a better catalyst system for the dehydration of aryl substituted substrates (Figure 13). The presence of [EMIM] [Cl] ionic liquid considerably enhanced the diene selectivity [Hu *et al.* 2017].

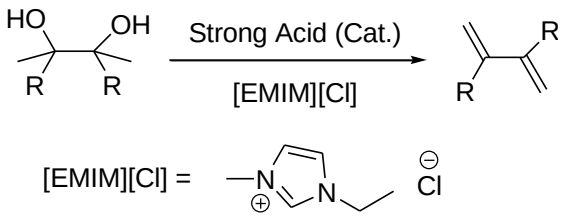

Figure 13: Pinacol Dehydration to 2, 3-Dimethylbutadiene in presence of [EMIM] [Cl]

In the petroleum refining industry, alkylation of isobutane using 2-butene yields products with high octane numbers and clean burning characteristics. Alkylation of isobutane and 2-butene was carried out in presence of binary mixtures of acidic ionic liquids (ILs) and strong acids (sulfuric acid and triflic acid). Presence of ILs very much enhanced the catalytic performance of H_2SO_4 and CF_3SO_3H (Figure 14). The incorporation of a small amount of ILs with Cu-ions to H_2SO_4 or CF_3SO_3H increase the C_8 content of alkylate. The modified ILs such as [EMIM] [HSO_4] CuCl and [EMIM][OTf]-CuCl were found to produce the optimal alkylate quality [Cong *et al.* 2014].

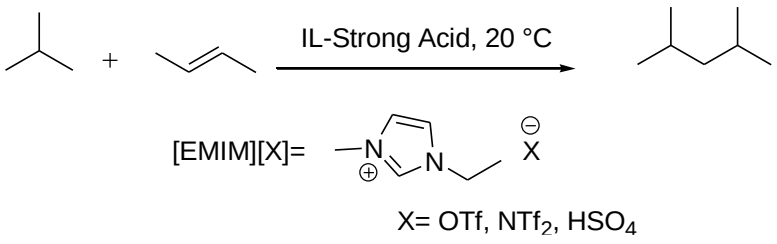

Figure 14: Alkylation of Isobutane/2-Butene in presence of IL-strong acid [EMIM][HSO_4]-CuCl

Conclusion

Over the past decades, ILs has been used extensively as a medium and catalyst for many reactions. Their scope has strolled ahead of academic research laboratories to industries wherever their practical applications have been leading to various sustainable technologies. More emphasis is given on applications of ionic liquids towards organic reactions. Herein applications of 1-ethyl-3- methyl-imidazolium based ionic liquids were discussed for numerous

organic transformations. It can be believed that in the near future, ionic liquids will have more technical as well as chemical applications.

References

Akiyama, T., Suzuki, A., & Fuchibe, K. (2005). Mannich-type reaction promoted by an ionic liquid. *Synlett*, *6*, 1024–1026. https://doi.org/10.1055/s-2005-864816.

Anjaiah, S., Chandrasekhar, S., & Grée, R. (2004). Carbon-Ferrier rearrangements in ionic liquids using Yb(OTf)3 as catalyst. Journal of Molecular Catalysis A: Chemical, 214(1), 133–136. https://doi.org/10.1016/j.molcata.2003.10.063.

Bai, L., Li, K., Yan, Y., Jia, X., Lee, J. M., & Yang, Y. (2016). Catalytic Epoxidation of cis-Cyclooctene over Vanadium-Exchanged Faujasite Zeolite Catalyst with Ionic Liquid as Cosolvent. *ACS Sustainable Chemistry and Engineering*, *4*(2), 437–444. https://doi.org/10.1021/acssuschemeng.5b00854.

Bonĥte, P., Dias, A. P., Papageorgiou, N., Kalyanasundaram, K., & Grätzel, M. (1996). Hydrophobic, Highly Conductive Ambient-Temperature Molten Salts. *Inorganic Chemistry*, *35*(5), 1168–1178. https://doi.org/10.1021/ic951325x.

Cha, J. H., Kim, K. S., Choi, S., Yeon, S. H., Lee, H., Kim, H. S., & Kim, H. (2005). Thermal and electrochemical properties of morpholinium salts with bromide anion. *Korean Journal of Chemical Engineering*, *22*(6), 945–948. https://doi.org/10.1007/BF02705680.

Chen, J., Li, Z., Yang, L., Han, F., Song, H., Zhao, Y., Xia, C. (2012). Catalysis and applications of task-specific ionic liquids. *SCIENTIA SINICA Chimica*, *42*(4), 502–524. https://doi.org/10.1360/032011-727.

Chen, Y., Bai, L., Zhou, C., Lee, J. M., & Yang, Y. (2011). Palladium-catalyzed aerobic oxidation of 1-phenylethanol with an ionic liquid additive. *Chemical Communications*, *47*(22), 6452–6454. https://doi.org/10.1039/c1cc11643f.

Chaubey, S. A., Mishra, J. S., & Mishra, R. (2018). Efficient Approach for the Tritylation of Alcohols Using Recyclable Lewis Acid-Based Ionic Liquid (EMIM·AlCl4) [Research-article]. *ACS Omega*, *3*(8), 9607–9612. https://doi.org/10.1021/acsomega.8b00691.

Chaubey, S.A., Mishra, R. Synthesis of task-specific imidazolium ionic liquid as an efficient catalyst in acetylation of alcohols, phenols, and amines. *Chem. Pap.* (2020). https://doi.org/10.1007/s11696-020-01150-0.

Cong, Y., Liu, Y., & Hu, R. (2014). Isobutane/2-butene alkylation catalyzed by strong acids in the presence of ionic liquid additives. *Petroleum Science and Technology*, *32*(16), 1981–1987. https://doi.org/10.1080/10916466.2012.742540.

Davis, J. H., & Forrester, K. J. (1999). Thiazolium-ion based organic ionic liquids (OILs). Novel oils which promote the benzoin condensation. *Tetrahedron Letters*, *40*(9), 1621–1622. https://doi.org/10.1016/S0040-4039(99)00025-8.

Dileep, R., & Rudresha, B. J. (2015). An ionic liquid immobilized copper complex for catalytic epoxidation. *RSC Advances*, *5*(81), 65870–65873. https://doi.org/10.1039/c5ra12175b.

Dupont, J., De Souza, R. F., & Suarez, P. A. Z. (2002). Ionic liquid (molten salt) phase organometallic catalysis. *Chemical Reviews*, *102*(10), 3667–3692. https://doi.org/10.1021/cr010338r.

Dupont, J., Fonseca, G. S., Umpierre, A. P., Fichtner, P. F. P., & Teixeira, S. R. (2002). Transition-metal nanoparticles in imidazolium ionic liquids: Recycable catalysts for biphasic hydrogenation reactions. *Journal of the American Chemical Society*, *124*(16), 4228–4229. https://doi.org/10.1021/ja025818u.

Fannin, A. A., Floreani, D. A., King, L. A., Landers, J. S., Piersma, B. J., Stech, D. J., Vaughn, R. L., Wilkes, J. S., & Williams, J. L. (1984). Properties of 1,3-dialkylimidazolium chloride-aluminum chloride ionic liquids. 2. Phase transitions, densities, electrical conductivities, and viscosities. *Journal of Physical Chemistry*, *88*(12), 2614–2621. https://doi.org/10.1021/j150656a038.

Feng, L. C., Sun, Y. W., Tang, W. J., Xu, L. J., Lam, K. L., Zhou, Z., & Chan, A. S. C. (2010). Highly efficient chemoselective construction of 2,2-dimethyl-6-substituted 4-piperidones via multi-component tandem Mannich reaction in ionic liquids. *Green Chemistry*, *12*(6), 949–952. https://doi.org/10.1039/b926498a.

Fu, L. H., Xie, Z. B., Chen, G. Q., Lan, J., Hu, Z. Y., & Le, Z. G. (2019). An ionic liquid-based green synthesis strategy: Synthesis of dihydropyrimidinones by three-component Biginelli-type reaction of aliphatic aldehydes, aromatic aldehydes and urea. *Heterocycles*, *98*(8). https://doi.org/10.3987/COM-19-14137.

Fukuyama, T., Inouye, T., & Ryu, I. (2007). *Atom transfer carbonylation using ionic liquids as reaction media*. *692*(February 2006), 685–690. https://doi.org/10.1016/j.jorganchem.2006.08.072.

Gale, R. J., & Osteryoung, R. A. (1980). Infrared spectral investigations of room-temperature aluminum chloride-1-butylpyridinium chloride melts. *Inorganic Chemistry*, *19*(8), 2240–2242. https://doi.org/10.1021/ic50210a009.

Gorman, J. (2001). Faster, Better, Cleaner? *Science News*, *160*(10), 156. https://doi.org/10.2307/4012654.

Hallett, J. P., & Welton, T. (2011). ChemInform Abstract: Room-Temperature Ionic Liquids: Solvents for Synthesis and Catalysis. Part 2. *ChemInform*, *42*(36), no-no. https://doi.org/10.1002/chin.201136231.

Handy, S. T., & Okello, M. (2005). The 2-position of imidazolium ionic liquids: Substitution and exchange. *Journal of Organic Chemistry*, *70*(5), 1915–1918. https://doi.org/10.1021/jo0480850.

Hill, M. G., Mann, K. R., & Lamanna, W. M. (1991). Tetrabutylammonium Tetrakis[3,5-bis(trifluoromethyl)phenyl]borate as a Noncoordinating Electrolyte: Reversible 1e− Oxidations of Ruthenocene, Osmocene, and Rh2(TM4)42+ (TM4 = 2,5-Diisocyano-2,5-dimethylhexane). *Inorganic Chemistry*, *30*(25), 4687–4690. https://doi.org/10.1021/ic00025a003.

Hinner, L. P., Wissner, J. L., Beurer, A., Nebel, B. A., & Hauer, B. (2016). Homogeneous vinyl ester-based synthesis of different cellulose derivatives in 1-ethyl-3-methyl-imidazolium acetate. *Green Chemistry*, *18*(22), 6099–6107. https://doi.org/10.1039/c6gc02005d.

Hsu, J. C., Yen, Y. H., & Chu, Y. H. (2004). Baylis-Hillman reaction in [bdmim][PF6] ionic liquid. *Tetrahedron Letters*, *45*(24), 4673–4676. https://doi.org/10.1016/j.tetlet.2004.04.099.

Hu, Y., Li, N., Li, G., Wang, A., Cong, Y., Wang, X., & Zhang, T. (2017). Solid Acid-Catalyzed Dehydration of Pinacol Derivatives in Ionic Liquid: Simple and Efficient Access to Branched 1,3-Dienes. *ACS Catalysis*, *7*(4), 2576–2582. https://doi.org/10.1021/acscatal.7b00066.

Hurley, F. H., & WIer, T. P. (1951). Electrodeposition of Metals from Fused Quaternary Ammonium Salts. *Journal of The Electrochemical Society*, *98*(5), 203.

Hussey, C.L. The electrochemistry of room temperature haloaluminate molten salts. In Chemistry of Nonaqueous Solutions: Current Progress; Mamantov, G., Popov, A.I., Eds.; VCH: New York, NY, USA, 1994; pp. 227–275.

Lombardo, M., Chiarucci, M., & Trombini, C. (2009). A recyclable triethylammonium ion-tagged diphenylphosphine palladium complex for the Suzuki-Miyaura reaction in ionic liquids. *Green Chemistry*, *11*(4), 574–579. https://doi.org/10.1039/b815568b.

Luo, Y., Pan, A., Xing, M., Chen, M., & Xie, J. (2012). Synthesis of 1-acetylpyrene via Friedel-Crafts reaction using chloroaluminate ionic liquids as dual catalyst and solvent. *Advanced Materials Research*, *443–444*, 917–922. https://doi.org/10.4028/www.scientific.net/AMR.443-444.917.

MacFarlane, D. R., Meakin, P., Sun, J., Amini, N., & Forsyth, M. (1999). Pyrrolidinium imides: A new family of molten salts and conductive plastic crystal phases. *Journal of Physical Chemistry B*, *103*(20), 4164–4170. https://doi.org/10.1021/jp984145s.

Mastrorilli, P., Nobile, C. F., Paolillo, R., & Suranna, G. P. (2004). Catalytic Pauson-Khand reaction in ionic liquids. *Journal of Molecular Catalysis A: Chemical*, *214*(1), 103–106. https://doi.org/10.1016/j.molcata.2003.11.033.

Migowski, P., & Dupont, J. (2007). Catalytic applications of metal nanoparticles in imidazolium ionic liquids. *Chemistry - A European Journal*, *13*(1), 32–39. https://doi.org/10.1002/chem.200601438.

Miyatake, K., Yamamoto, K., Endo, K., & Tsuchida, E. (1998). Superacidified reaction of sulfides and esters for the direct synthesis of sulfonium derivatives. *Journal of Organic Chemistry*, *63*(21), 7522–7524. https://doi.org/10.1021/jo980473c.

Palakshi Reddy, B., Rajesh, K., & Vijayakumar, V. (2015). Ionic liquid [tbmim]Cl2/AlCl3 under ultrasonic irradiation towards synthesis of 1,4-DHP's. *Arabian Journal of Chemistry*, *8*(1), 138–141. https://doi.org/10.1016/j.arabjc.2011.01.027.

Ramakrishna, D. (2019). An Ionic Liquid Immobilized Palladium Complex for an Effective Heck and Suzuki Coupling Reactions. *Chemistry Africa*, *2*(1), 21–28. https://doi.org/10.1007/s42250-018-00038-7.

Sardar, S., Wilfred, C. D., & Marc, L. J. (2016). Synthesis of task specific and reusable protic ionic liquids for one-pot multicomponent syntheses. *AIP Conference Proceedings*, *1787*. https://doi.org/10.1063/1.4968075.

Schenzel, A., Hufendisk, A.,& Barner, C.(2014).Catalytic transesterification of cellulose in ionic liquids: sustainable access to cellulose ester. Green Chemistry. *Green Chemistry*, *16*(2014), 3266–3271. https://doi.org/10.1039/C4GC00312H.

Shen, Z., Zhou, W., Liu, Y., Ji, S., & Loh, T. (2008). *One-pot chemoenzymatic syntheses of enantiomerically-enriched O -acetyl cyanohydrins from aldehydes in ionic liquid †*. *entry 8*, 283–286. https://doi.org/10.1039/b717235d.

Singh, D., Narayanaperumal, S., Gul, K., Godoi, M., Endrigo, O., Rodrigues, D., & Luiz, A. (2010). *Efficient synthesis of selenoesters from acyl chlorides mediated by CuO nanopowder in ionic liquid*. *3*, 957–960. https://doi.org/10.1039/c002648d.

Song, C. E. (2004). Enantioselective chemo- and bio-catalysis in ionic liquids. 82(July 2003).1033-1043.

Sugden, B. S. (1928). CLXVI1.-The Parachor and Chemical Constitution. Part X I I . Fused Metals and Salts. *J. Chem. Soc.*, 1291–1298.

Sun, J., Forsyth, M., & MacFarlane, D. R. (1998). Room-temperature molten salts based on the

quaternary ammonium ion. *Journal of Physical Chemistry B*, *102*(44), 8858–8864. https://doi.org/10.1021/jp981159p.

Tait, S., & Osteryoung, R. A. (1984). Infrared study of ambient-temperature chloroaluminates as a function of melt acidity. *Inorganic Chemistry*, *23*(25), 4352–4360. https://doi.org/10.1021/ic00193a049.

Vestergaard, B. (1993). Molten Triazolium Chloride Systems as New Aluminum Battery Electrolytes. *Journal of The Electrochemical Society*, *140*(11), 3108. https://doi.org/10.1149/1.2220994.

Wilkes, J. S., Levisky, J. A., Wilson, R. A., & Hussey, C. L. (2014).Dialkylimidazolium chloroaluminate melts: A new class of room temprature ILs for electroscopy and synthesis. *Encyclopedia of Lubricants and Lubrication*, *237*(1980), 374–374. https://doi.org/10.1007/978-3-642-22647-2_100172.

Xiao, Y., & Malhotra, S. V. (2004). Diels-Alder reactions in pyridinium based ionic liquids. Tetrahedron Letters, 45(45), 8339–8342. https://doi.org/10.1016/j.tetlet.2004.09.070

AN OVERVIEW OF PHENOMENON, MECHANISM, AND APPLICATION OF AGGREGATION-INDUCED EMISSION

Vivek Anand

Department of Engineering and Physical Science, Institute ofAdvanced Research, Koba Institutional Area, Gandhinagar - 382 426, Gujarat– India

*Corresponding Author, E-mail: vivek.anand@iar.ac.in

Abstract

Organic conjugated polymers and small molecules, owing to their extended conjugation, have wide applications in the fields of organic light-emitting diodes (OLEDs), field-effect transistors (FETs), dye-sensitized solar cells (DSSCs), and chemical sensors. Hence, there is a trend in engineering new organic fluorophores (OFs) exhibiting aggregation-induced emission (AIE) behaviour. AIE is a phenomenon in which a luminogen, non-emissive in suitable solvents, becomes highly emissive when allowed to aggregate in poor solvents or thin films. If a CM shows AIE property, then the fluorescence quenching in film form can be tackled. The physical phenomenon responsible for AIE is found to be the restriction of intramolecular rotation (RIR) in the aggregated state. Since its discovery, increasing attention has been paid to the synthesis and development of AIE active conjugated molecules, as they are rare and can find intense application as OLED materials. This review attempts to explain the mechanism of AIE through various mechanistic studies, the application of AIE molecules in optoelectronics, and recent interesting trends in developing new mechanoluminiscent materials possessing AIE traits.

Keywords: conjugated organic molecules, aggregation-induced emission, organic light emitting diodes, field effect transistor, sonogashira coupling reaction, hexaphenyisilole, intramolecular charge transfer, mechanoluminescence

Conjugated Organic Molecules for Optoelectronic Applications

Organic polymers and small molecules possessing extended conjugation have a tremendous demand in advanced electronic materials. They have already found practical applications in the fields of light-emitting diodes (LEDs), field-effect transistors (FETs), dye-sensitized solar cells (DSSCs), and chemical sensors (Grimsdale *et al.,* 2009). For the synthesis of these conjugated organic materials, transition metal (TM) catalyzed cross-coupling methodologies have evolved as one of the most potential and versatile tools (Xu *et al.,* 2014). Among the TM-catalyzed cross-coupling methodologies, Pd-catalyzed reaction between aryl or alkenyl halides and organometals containing Al, Zn, Zr (Negishi), B (Suzuki), Sn (Stille) and terminal alkenes (Heck) or alkynes (Sonogashira) are central (Verheyen *et al.,* 2017). Sonogashira coupling is

one of the most popular cross-coupling reactions for the formation of C (sp^2)-C (sp) bonds between aromatic halides and terminal alkynes in the presence of catalytic CuI (Chinchilla *et al.,* 2011). The salient features of this cross-coupling are its compatibility with various functional groups, ambient temperature, and milder reaction conditions.

Sonogashira Coupling Reaction

The Sonogashira coupling comprises two independent catalytic cycles. First is the oxidative addition of electron-deficient palladium (Pd) onto an aromatic halide, which generates aryl-PdX complex. While the second is the reaction among the alkyne, Cu(I) salt and a base to produce Cu-acetylide intermediate. Then, the two cycles converge *via* transmetalation to generate an aryl-Pd-acetylide species. Finally, through reductive elimination, the alkyne is formed along with an electron-deficient Pd. The catalytic cycle is shown in Scheme 1. Literature is abundant with efficient and fascinating conjugated molecules (CMs) synthesized *via* Sonogashira coupling reaction for many optoelectronic applications. For instance, highly luminescent (quantum yield Φ_F = 77-98%) anthracene derivatives with bulky carbazolyl-fluorene or carbazolyl-carbazole units were synthesized in excellent yield for OLED applications (Slodek *et al.,* 2016). Furthermore, ethynyl-pyrene substituted phenothiazine based organic dyes were synthesized by the same coupling reaction with 12% conversion efficiency (Nagarajan *et al.,* 2017). Additionally, porphyrin-diketopyrrolopyrrole based conjugated polymers (CPs) were synthesized for ambipolar FET application with a hole mobility of 0.1 $cm^2V^{-1}s^{-1}$ (Zhou *et al.,* 2017).

For all the aforementioned optoelectronic applications (OAs), the CMs are desired in the aggregated states (film or solid forms). But in the solid-state, aggregation caused quenching (ACQ) comes into play which significantly hampers their efficiency. ACQ is a phenomenon in which the molecule in aggregated state decays *via* non-radiative pathways, leading to decreased quantum efficiency. The reason for ACQ is the formation of sandwich-shaped excimers and exciplexes in the CMs aided by a collision among the molecules between their excited and ground states. Several approaches have been developed to overcome this phenomenon. For instance, aromatic rings were covalently attached to branched chains, bulky cyclic groups, spiro kinks, and dendritic wedges (Nguyen *et al.,* 2006). Furthermore, fluorophores have been physically passivated *via* surfactant encapsulation. Doping with non-conjugated polymer films like poly (methyl methacrylate) (PMMA) has also been explored (Kulkarni *et al.,* 2003).

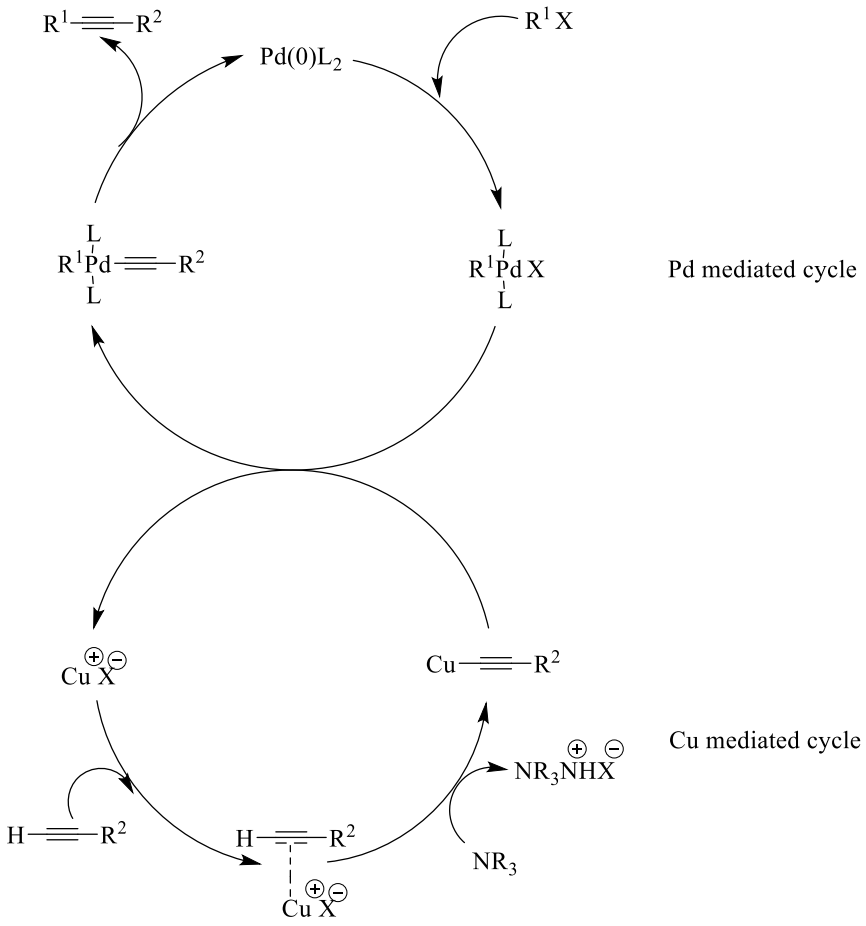

Scheme 1: Mechanism of the Pd/Cu catalyzed Sonogashira reaction (Xu *et al.,* 2014)

Nevertheless, all these approaches are tedious from both synthetic and engineering point of view. For example, the attachment of the bulky pendant substrate can threaten the extended π-electron conjugation of the molecule. In addition, the doping may lead to hindrance in charge mobility and reduction in luminogen density (Hong *et al.,* 2009). Therefore, conjugated systems are needed in which light emission is enhanced instead of quenched upon aggregation.

Introduction to Aggregation-Induced Emission (AIE)

Aggregation-induced emission (AIE) was discovered in 2001, serendipitously, by Tang *et al*. They synthesized an extensively conjugated hexaphenylsilole moiety (HPS, Figure 1) that was expected to show intense emission in the solution phase. To their surprise, the molecule was found to be non-luminescent in the solution phase but highly emissive in the aggregated state. This contradictory phenomenon was coined as aggregation-induced emission (AIE). Since then, AIE has opened a new perspective in the application of CMs for vivid optoelectronic applications.

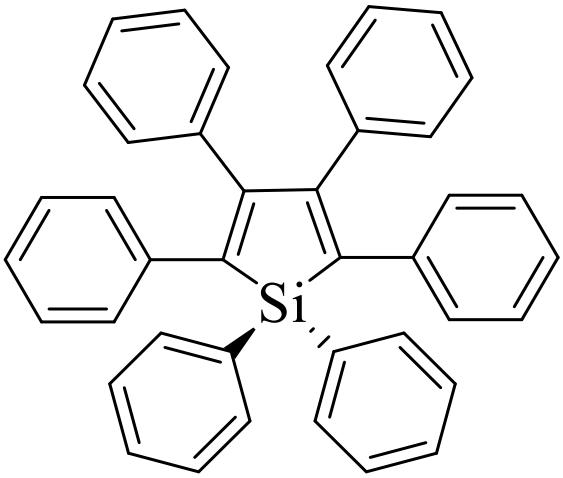

Figure 1: Structure of hexaphenylsilole (HPS) [Reproduced with permission from the American Chemical Society (Chen *et al.*, 2003)]

Through various rigorous experiments, it was concluded that restriction of intramolecular rotation (RIR) in the aggregated state was the fundamental reason for AIE (Hong *et al.*, 2009). The ACQ (ordinary for traditional conjugated molecules like pyrene) and AIE for HPS are depicted in Figure 2. The phenomenon and the mechanism of AIE are elaborately discussed in the following sections.

Phenomenon

As discussed above, HPS was non-luminescent in acetonitrile solution. The gradual addition of water (which is a non-solvent for HPS) to the acetonitrile solution of HPS caused

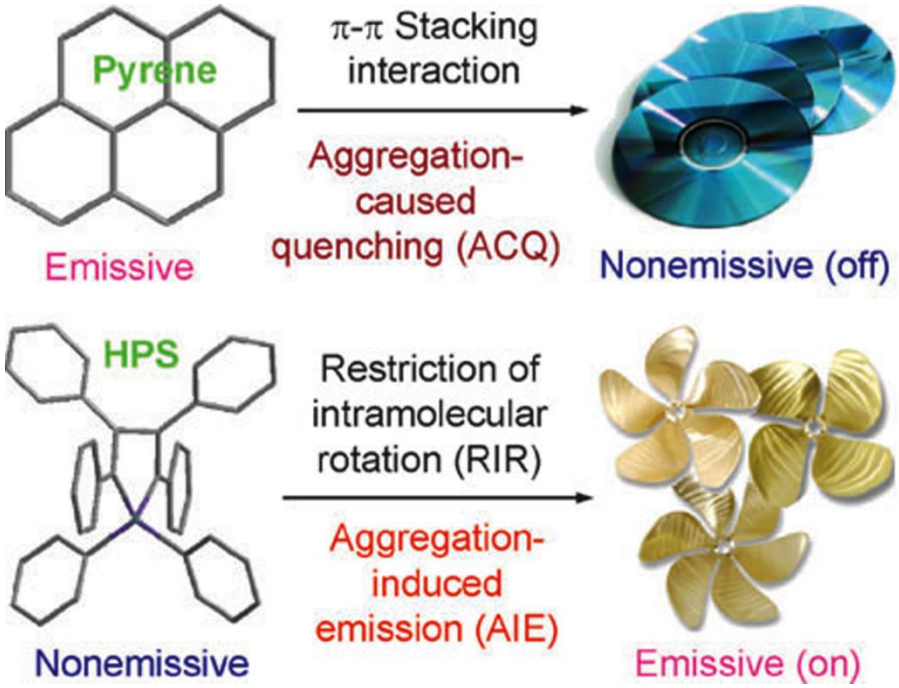

Figure 2: Planar luminogens such as pyrene tend to aggregate just as discs pile up whereas non-planar propeller shape luminogen like HPS behaves differently due to RIR [Reproduced with permission from the Royal Society of Chemistry (Hong *et al.*, 2009)].

its aggregation (Chen *et al.*, 2003). This aggregation led to efficient emission inducement. Hence, HPS is AIE active. The photoluminescence (PL) spectrum of HPS in acetonitrile was negligible (Figure 3) with a fluorescence quantum yield (Φ_F) of 0.22%. In 99% water, the Φ_F value was 56% which is 255 times higher than that in pure acetonitrile. Thus, AIE had enabled the HPS to emit in the aggregated state. The PL spectra and quantum yield *versus* solvent composition of the mixture of HPS in different acetonitrile/water mixtures are shown in Figure 3. Like HPS, a variety of other silole derivatives were synthesized. All the molecules showed the AIE effect, proving that AIE is not an isolated phenomenon for HPS but is a frequent phenomenon for all the molecules which carry structural features capable of restricting the intramolecular rotation in the aggregated state.

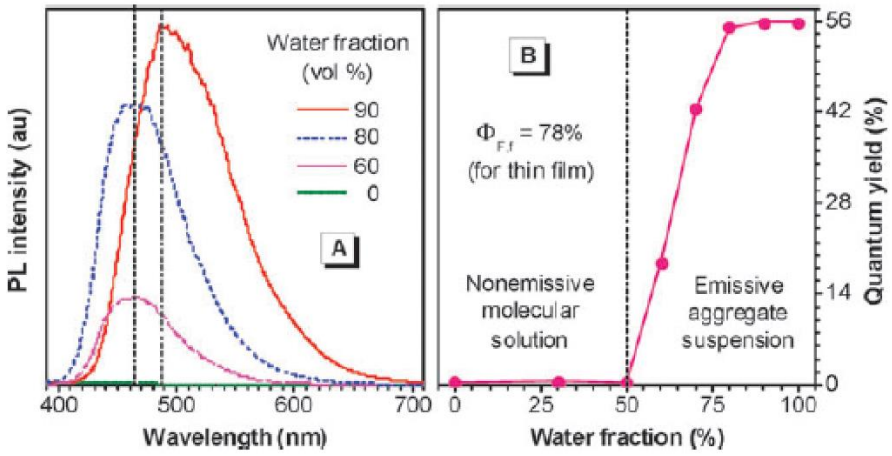

Figure 3 (A) PL spectra of HPS in acetonitrile-water solution mixtures (B) Fluorescence quantum yield (Φ_f) *vs.* solvent composition of the mixture [Reproduced with permission from the American Chemical Society (Chen *et al.*, 2003)]

Mechanism

To understand the mechanism behind AIE, several mechanistic pathways were investigated. Conformational planarization, *J*-aggregate formation, twisted intramolecular charge transfer (TICT), and RIR are the prominent phenomena that were considered for this study. However, none of these phenomena found experimental support except RIR. RIR in HPS

was attributed to its unique structural attributes. For instance, in HPS, six phenyl rings (rotors) are connected to one silole core (stator) *via* single bonds (Figure 1). Consequently, the rotations of these C-C single bonds are prevalent in the dilute solution phase, leading to the non-radiative dissipation of energy. Nevertheless, in the aggregated state, HPS molecules are in close contact with each other, which hinders the free rotations, leading to the inducement of radiative decay (Hong *et al.*, 2009). To prove the RIR hypothesis, several experiments were performed.

Viscochromism

The increase in viscosity impedes the intramolecular rotation hence, should boost the silole emission. This experiment was conducted by Chen *et al.* 2003. In this experiment, glycerol (solvent with high viscosity) was added to a methanol solution of HPS. For mixtures with glycerol fractions < 50%, the PL intensity increased linearly with viscosity. The increment in this region was mainly due to the viscosity effect. For glycerol fractions > 50%, the PL intensity increased rapidly due to aggregate formation. The effect of different glycerol/methanol mixtures on the PL intensity of HPS is shown in Figure 4(A).

Piezochromism

Application of pressure introduced an antagonistic effect on the PL spectrum of HPS (Fan *et al.*, 2008). The emission increased first and then slowly decreased from the plateau, as shown in Figure 4(B). It was proposed that initially, pressurization led to the shortening of distance among the HPS molecules, and hence application of pressure strengthened the RIR process. Nonetheless, the further application of pressure promoted excimer formation, which eventually weakened the light emission. The quenching in fluorescence on the application of pressure is commonly observed for conventional luminophores, as shown for the solid film of tris (8-hydroxyquinolinato) aluminium (ALq_3) in panel B of Figure 4(B)

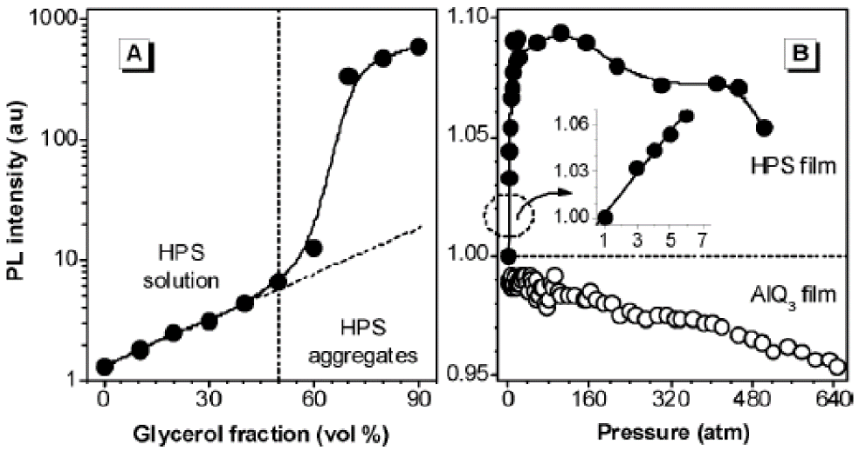

Figure 4: Effects of (A) composition of glycerol-methanol mixture and (B) externally applied pressure on the PL intensity of HPS (Chen *et al*., 2003). Data for an Alq_3 film is shown in panel B for comparison **[**Reproduced with permission from the Royal Society of Chemistry (Fan *et al*., 2008)].

Thermochromism

Fortification of intramolecular rotation could also be achieved by cooling the solution to lower temperatures. Thus, the effect of temperature on silole solution emission was also studied by Chen *et al.* 2003. THF was used as a solvent for this investigation because of its low melting point and strong solvating power for silole. In fact, on lowering the temperature to -196 °C (using Liq. nitrogen), a considerable increase in the PL intensity was observed. It was concluded that the cooling of the solution froze the thermally susceptible intramolecular rotations present in solole molecules, which enhanced the emission intensity. The effect of temperature on HPS emission in THF is shown in Figure 5(A).

To further verify the effect of temperature, dynamic NMR studies were carried out by Chen *et al.* 2003. At room temperature, sharp NMR peaks were observed owing to the rapid intramolecular rotations. Nevertheless, the broadening of the peaks was noticed on cooling the solution. As anticipated, the broadening of HPS NMR peaks at lower temperatures is due to RIR. The results are shown in Figure 5 (B).

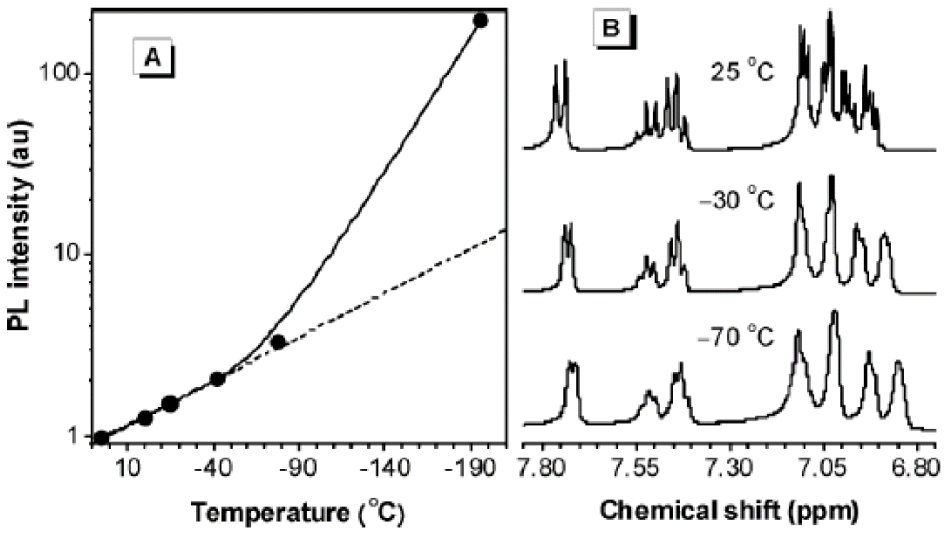

Figure 5 (A) Effects of temperature on PL intensity of HPS in THF (B) ^{1H} NMR spectra of HPS in dicholoromethane-d_2 at different temperatures [Reproduced with permission from the American Chemical Society (Chen *et al*., 2003)].

Fluorescence Lifetime Studies

The lifetime studies for the emission from HPS solution were carried out by Ren *et al.* 2005. For this study, the lifetime of different water-DMF mixture solutions of HPS was investigated. In pure DMF, HPS solution deactivated *via* a single pathway with a lifetime of 0.04 ns. However, on slowly increasing the fraction of water, the excited state of the solution started decaying *via* two relaxation pathways. For example, in the 30:70 ratio of water: DMF, the molecule relaxed by two channels: fast (0.10 ns) and slow (3.75 ns). As the concentration of water was increased further, the decay *via* slow channel became prominent. For example, for 90% water, the excited state decayed mainly by the slow channel with a lifetime of 7.16 ns.

Lowering of temperature also increased the lifetime *via* the slow channel. At 150 K, the decay was 1.23 ns through the fast channel and 7.19 ns by the slow channel. However, at 30 K, the lifetime changed to 10.39 ns for the slow pathway. Thus, both aggregation and lowering of temperature restricted the intramolecular rotation as the decay *via* slow channel increased in both cases. The decay dynamics of HPS for different water/DMF mixtures and at different temperatures are listed in Table 1. Therefore, from all the studies, it was concluded that the twisted motion of the phenyl peripheral rings of HPS was restricted by increasing viscosity, aggregation, and freezing, which enhanced the PL intensity.

Table 1: Fluorescence Decay Parameters of HPS Solutions[a] (Ren *et al*., 2005)

No.	Solvent	T/K	A_1 (%)	A_2 (%)	τ_1 /ns	τ_2 /ns
1	H_2O-DMF (0:10)	295	100	0	0.04	_
2	H_2O-DMF (3:7)	295	80	20	0.10	3.75
3	H_2O-DMF (7:3)	295	50	50	0.82	4.98
4	H_2O-DMF (9:1)	295	43	57	1.27	7.16
5	DMF	295	100	0	0.04	_
6	DMF	200	51	49	0.31	2.89
7	DMF	150	43	57	1.23	7.19
8	DMF	30	34	66	2.49	10.39

a

Determined from I =A_1 exp(-t/τ_1) + A_2 exp(-t/τ_2), where A and τ are the fraction amount and fluorescence lifetime of the shorter and longer-lived species

Structural Modification

To verify the RIR mechanism, structural tuning was also carried out by attaching two bulky isopropyl groups to the outer phenyl groups of HPS (Li *et al.*, in 2005), as shown in Figure 6(B). The isopropyl groups, due to their bulky size, restricted the intramolecular rotation. Thus, the molecule was fluorescent in the solution state with a fluorescence quantum yield of 83% in acetone. This study reflects that, by bringing internal structural changes in the HPS molecule, RIR can be promoted in the solution phase itself and hence, PL behaviour can be tuned. The PL spectrum of sterically hindered HPS derivative, along with its structure and the photograph of its solution, is shown in Figure 6.

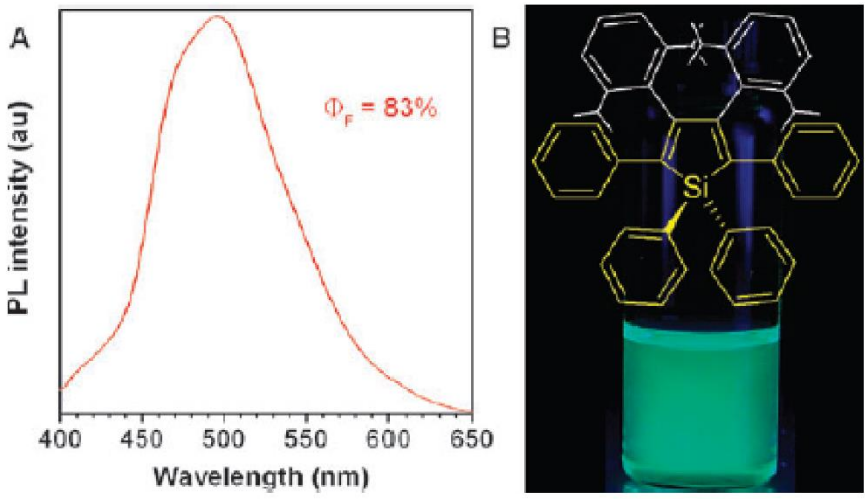

Figure 6 (A) PL spectrum of a sterically hindered HPS derivative 1 in acetone (B) Chemical structure of 1 and photograph of its solution taken under illumination with a UV lamp [Reproduced with permission from the American Chemical Society (Li *et al.*, 2005)].

Particle Size Analysis

The absorption spectra of HPS measured in a solvent mixture (acetonitrile and water) with high water content showed tailing-off in the higher wavelength region. This phenomenon is called the Mie effect. The tailing-off or Mie effect is a signature for nanoparticle formation. The evidence gained by UV-visible spectra was also supported by particle size analysis (Chen *et al.*, 2003). The dynamic light scattering (DLS) experiment revealed that the particle size was 190 nm and 130 nm in the solvent mixture with 80% and 90% water, respectively. UV-visible spectra of HPS for different water-acetonitrile mixtures and particle size analysis for the mixtures are shown in Figure 7.

Other AIE Systems

If the propeller-like shape and RIR are responsible for the AIE effect, then AIE should not be a special attribute of the HPS molecule but a common property of any molecule which has similar structural features. Guided by the above fact, many silole derivatives were

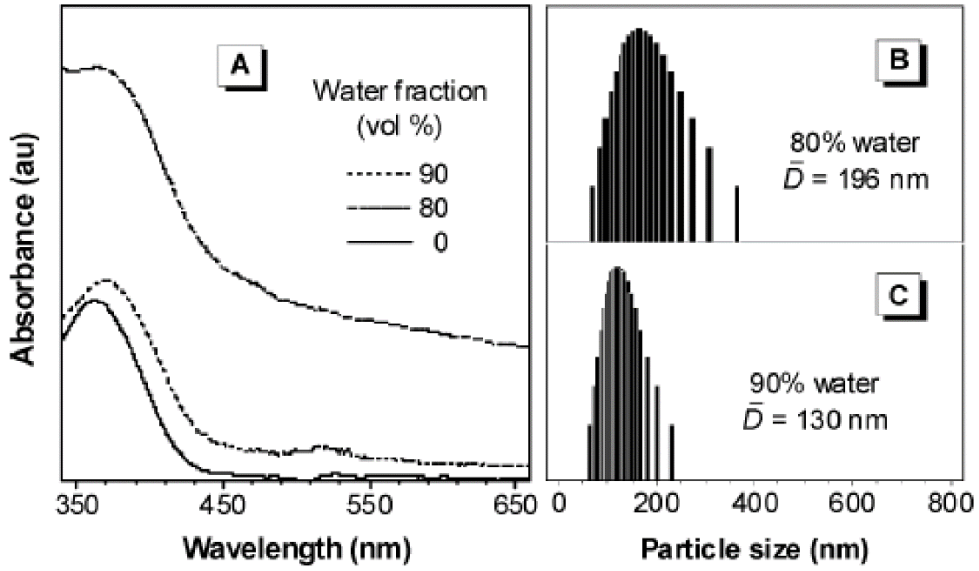

Figure 7 (A) Absorption spectra of HPS in acetonitrile-water mixtures. Size distribution of nanoparticles of HPS in acetonitrile-water mixtures containing (B) 80 % and (**C**) 90 % water [Reproduced with permission from the American Chemical Society (Chen *et al.*, 2003)].

synthesized by Zeng *et al*. The structures of a few of these molecules are shown in Figure 8 (Zeng *et al.*, 2007). All these molecules are propeller-shaped and composed of rotors and stators (a-h). As expected, all these molecules showed AIE property.

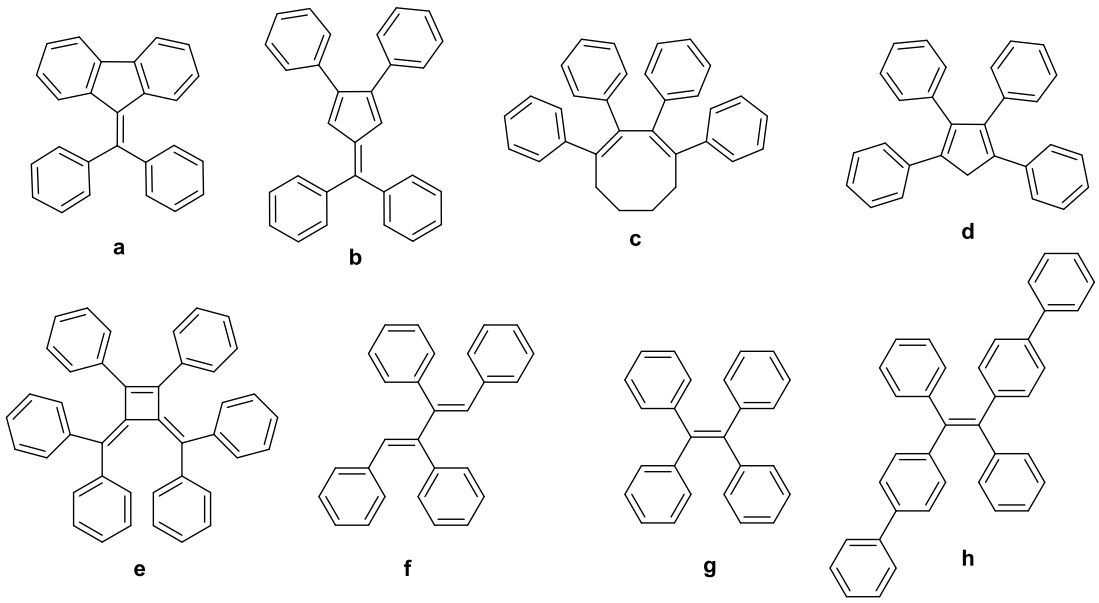

Figure 8: Examples of different AIE fluorophores (a-h) that emit visible light of various colors **[**Reproduced with permission from the Royal Society of Chemistry (Zeng *et al.*, 2007)].

Introducing polar groups into AIE fluorophores decorates the molecules with vivid coloured emission. For example, the molecule shown in Figure 9 is a butterfly-shaped push-pull (donor-acceptor) conjugated system synthesized by Tong *et al*. This molecule emitted green, orange, and red light in THF-water mixtures with 40%, 90%, and 99% water, respectively (Tong *et al.*, 2007). The photographs of the three colours obtained under UV light irradiation are also shown in Figure 9. Thus, AIE has opened a new endeavour of research where new potent and interesting molecules can be synthesized for optoelectronic applications and eloquent colour tuning. Other interesting examples of molecules exhibiting AIE are also discussed below. The mechanistic studies of these fascinating CMs bring into light interesting facts about AIE systems.

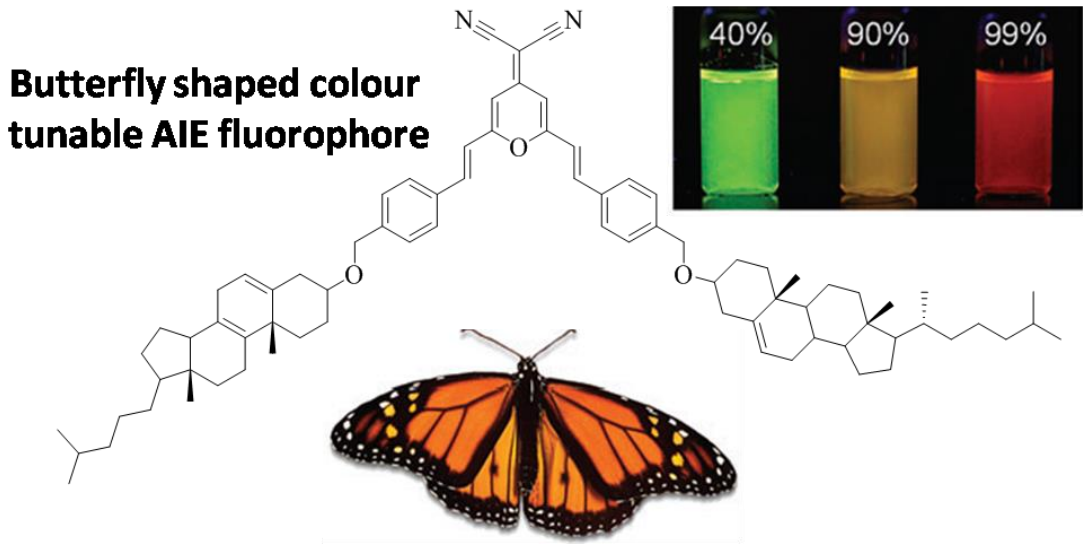

Figure 9: The nano aggregates of butterfly-shaped AIE fluorophore suspended in THF-water mixtures with water contents of 40 %, 90 % and 99 % emit green, yellow and red light, respectively under UV light illumination [Reproduced with permission from the American Chemical Society (Tong *et al.*, 2007)].

Oligo(phenothiazine)s for Twisted Intramolecular Charge Transfer and Aggregation-Induced Emission

Some interesting examples are 9, 10 divinylanthracene oligomers containing phenothiazine (AnPHZ2 and AnPHZ4), as shown in Figure 10 (Zhang *et al.*, 2013). These molecules showed interesting properties *viz.* twisted intramolecular charge transfer (TICT) and AIE. TICT is an attribute shown by typical donor-acceptor (D-A) type molecules possessing electron donor and acceptor functionalities. Such molecules show a change in PL spectra on changing the polarity of the solvent, which is known as solvatochromism. The TICT mechanism explains the influence of polarity on emission behaviour. In the non-polar solvent, the molecule remained in coplanar conformation, hence exhibited intense emission with a normal Stokes shift. However, in the polar solvents, the planar conformation was no longer stable, leading to the existence of a charge transfer (CT) state, or the twisted conformation. The polar solvent adequately stabilized the twisted or non-coplanar state. Therefore, low energy emission, with obvious solvatochromism and a decrease in fluorescence intensity was observed. The reduction in PL intensity was attributed to the increase in non-radiative transitions, which became possible in the CT state.

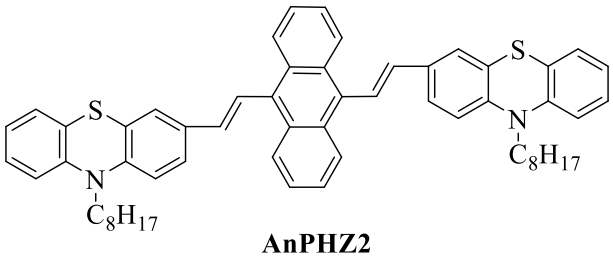

AnPHZ2

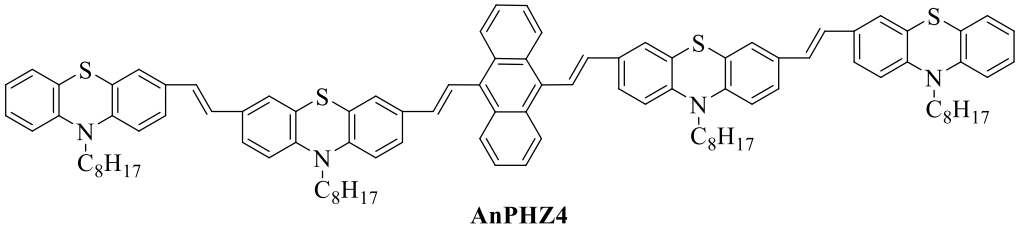

AnPHZ4

Figure 10: Molecular structures of AnPHZ2 and AnPHZ4 [Reproduced with permission from the American Chemical Society (Zhang *et al.*, 2013)].

For example, both AnPHZ2 and AnPHZ4 showed solvatochromic emission. In these molecules, the phenothiazine moiety acts as a donor, and the divinylanthracene is the acceptor. The spectral properties of AnPHZ2 in different solvents are shown in Figure 11. In cyclohexane, the emission peak was observed at 613 nm, while in the solvent of high polarity, i.e., DMSO, the peak appeared at 692 nm. Thus, a 79 nm red shift was observed on moving from non-polar to strongly polar solvent along with the decrease in fluorescence intensity. To get an insight into the ICT nature, the Lippert-Mataga plot was studied. This emission energy *versus* solvent polarity plot is shown in Figure 12. The plot showed two straight lines, which indicated the existence of two excited states. The locally excited (LE) and the charge transfer (CT) states. Moreover, the ICT study revealed that the molecule showed positive solvatochromism. The CT state also quenched the fluorescence in polar solvents because of the excessive interaction between the solvent and solute species. Thus, the low fluorescence quantum efficiency of 0.06 and 0.07 in THF for AnPHZ2 and AnPHZ4, respectively, was observed. The twisted and coplanar conformations of the molecule in polar and non-polar solvents are shown in Figure 13.

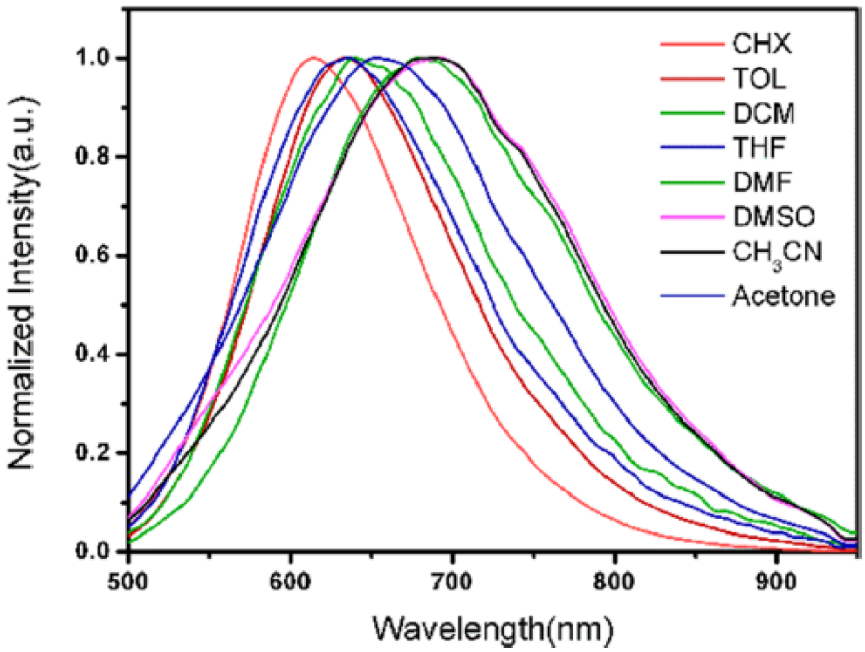

Figure 11: Fluorescence spectra of AnPHZ2 in different solutions. All emission spectra were collected with an excitation at 405 nm [Reproduced with permission from the American Chemical Society (Zhang *et al.*, 2013)].

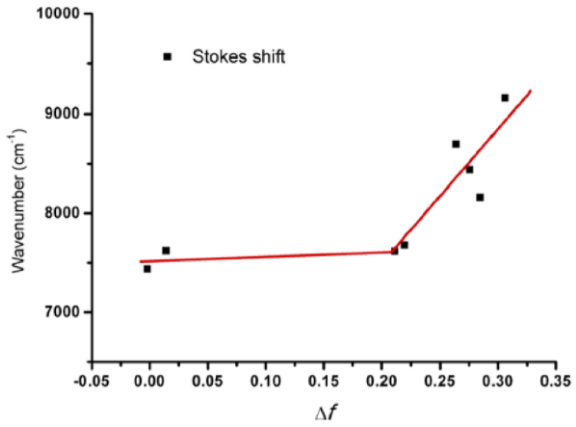

Figure 12: Fluorescence stokes shifts as a function of orientation polarizability *Δf* in different solvents [Reproduced with permission from the American Chemical Society (Zhang *et al.*, 2013)].

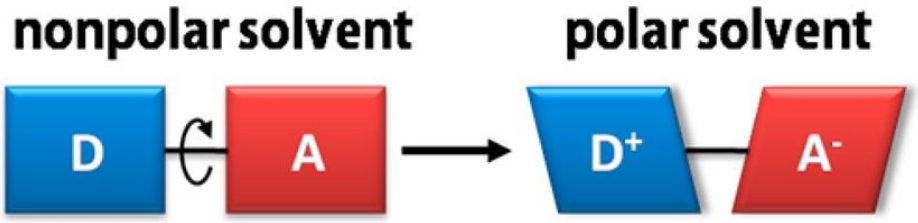

Figure 13: Schematic of the TICTstate in polar solvents [Reproduced with permission from the American Chemical Society (Zhang *et al.*, 2013)].

AIE Properties

The PL spectra of AnPHZ2 in different water/THF mixtures are shown in Figure 14. In pure THF, the molecule showed weak and broad emission. When a small amount of water was added, the solute did not aggregate, although the emission was slightly red-shifted and weakened. With the addition of a large amount of water (> 70%), on the other hand, the intensity of emission was significantly increased, along with a slight blue shift. In fact, for 90% water, the PL intensity was six times larger than that for pure THF. The same experiment was repeated for DMF/water mixture, and similar results were observed. Hence, the experiment is universal and not specific for THF/water mixture. Thus, for low water concentration, the TICT

state was more pronounced. Nevertheless, excessive addition of water leads to the prominence of AIE behaviour.

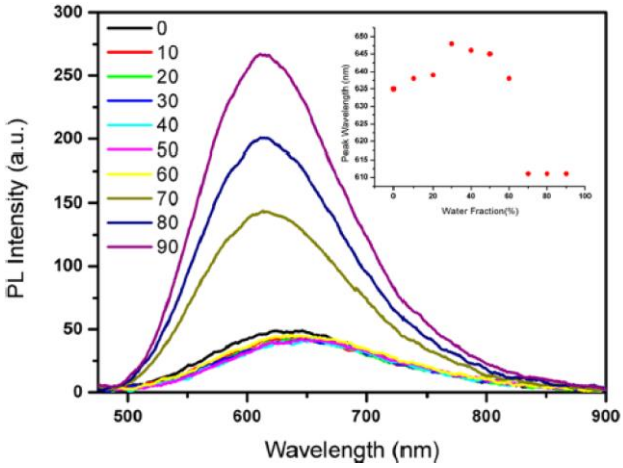

Figure 14: Emission spectra of AnPHZ2 in water/THF mixtureswith different fractions of water [Reproduced with permission from the American Chemical Society (Zhang *et al.*, 2013)].

Restriction of Intramolecular Motion as a General Mechanism for AIE

In this review, until now, AIE is mainly attributed to the RIR mechanism. However, RIR could not fully explain the AIE phenomenon. Leung *et al.,* proposed the restriction of intramolecular vibration (RIV) as one of the attributes for AIE apart from RIR (Leung *et al.*, 2014). They synthesized two annulenylidene based molecules: 10, 10', 11, 11'- tetrahydro-5, 5'-bidibenzo [a, d][7] annulenylidene (THBDBA) and 5,5' bidibenzo [a, d] [7] annulenylidene (BDBA). The fluorescence properties of these two molecules were compared with the archetypal AIE molecule tetraphenylethene (TPE) for the mechanistic study of AIE. The molecular structures of all three molecules are shown in Figure 15. In both THBDBA and BDBA, unlike TPE, the phenyl rings are covalently locked. So, considering the RIR mechanism, both the molecules should not show AIE behaviour. To their surprise, on analyzing the PL properties, both the molecules showed AIE activity. The molecules were non-emissive in the suitable solvent (THF) but showed enhancement in emission intensity on the addition of non-solvent (water). This analogous behaviour was explained by the RIV mechanism.

The single-crystal structure of THBDBA and TPE and the optimized structure of BDBA are shown in Figure 16. From the figure, the locked phenyl rings in THBDBA and BDBA can be visualized. It was hypothesized that if THBDBA was fully solvated, it could adopt the relaxed 'chair' conformation, leading to free vibrational relaxation. In the aggregated state, on the other

hand, it adopted a more strained ‘boat’ form, which restricted the vibrational relaxations (Figure 17). Hence, the RIV mechanism could be the reason for AIE in these molecules. This hypothesis was verified by computational QM/MM model studies as well. Eventually, it is not just RIR or RIV but a combination of both, i.e., restriction of intramolecular motion (RIM), which is responsible for AIE attributes.

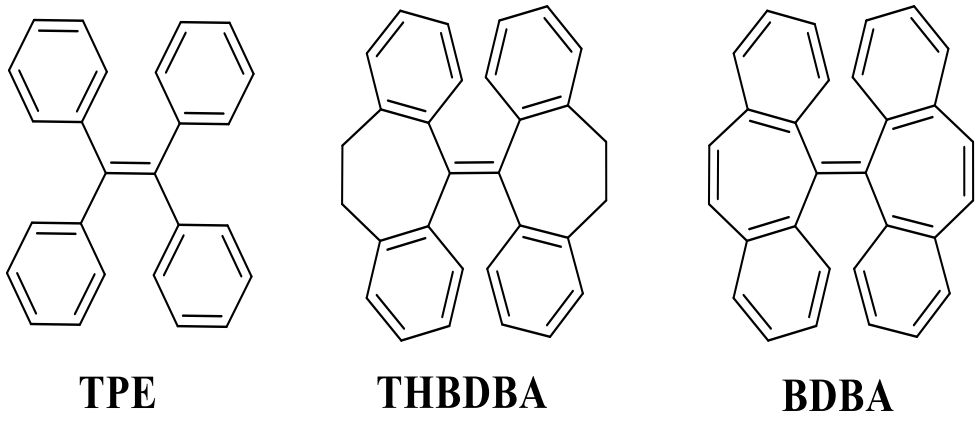

Figure 15: Molecular structures of TPE, THBDBA, and BDBA [Reproduced with permission from Wiley (Leung *et al.*, 2014)].

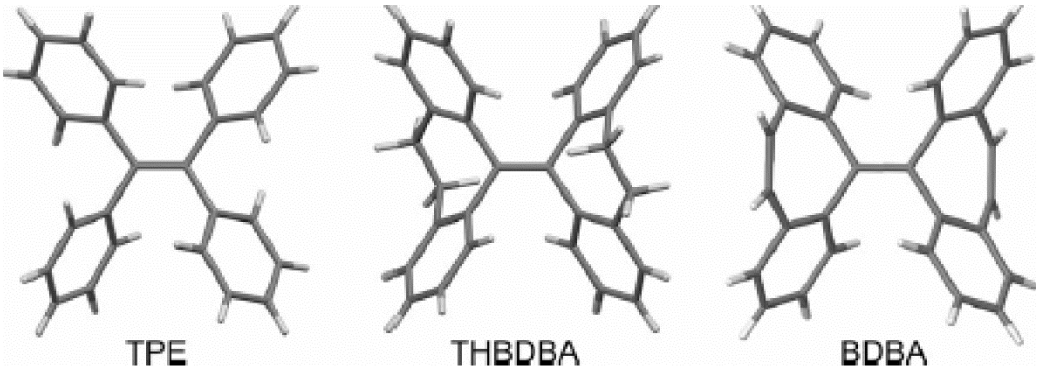

Figure 16: Single-crystal structures of TPE, THBDBA, and optimized structure of BDBA [Reproduced with permission from Wiley (Leung *et al.*, 2014)].

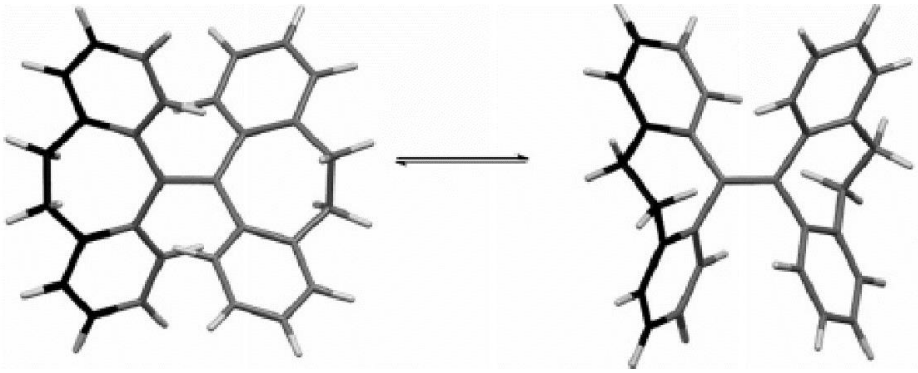

Figure 17: Calculated possible structural conformations of THBDBA. Left: 'chair' conformation; Right: 'boat' conformation [Reproduced with permission from Wiley (Leung *et al.*, 2014)].

AIE Strategy for Developing New Mechanoluminescent Materials

An interesting revelation was made about the effect of AIE on designing novel mechanoluminescent conjugated molecules by Yu *et al*. Mechanoluminescence is a phenomenon in which a molecule changes its PL properties on the application of mechanical pressure. These smart materials find special applications in storage devices, pressure sensors, rewritable media, and security ink. In this work, the hydrogen-bonded organic framework (HOFs) titled HOFTPE4F based on nitro-substituted tetraphenylethene (TPE) was synthesized (Yu *et al.*, 2017). The molecular structure is shown in Figure 18. The molecule showed no PL in the crystalline state, but considerable emission enhancement was observed in the amorphous state. The molecule HOFTPE4N had a highly porous structure in the crystalline form. X-ray diffraction studies revealed two types of pores with pore sizes of 5.855 × 5.855 Å (α-pore) and 7.218 × 7.218 Å (β-pore). It is the α-pore that was responsible for the quenching of fluorescence, as intramolecular rotations were rampant. Nevertheless, when the crystalline molecule was ground, the rupture of α-pore occurred, resulting in the inducement of RIR. Hence, efficient PL intensity was observed in the amorphous form. This experiment shows that AIE in the solid-state may vary in crystalline and amorphous forms, which can be used in developing new mechanoluminescent materials.

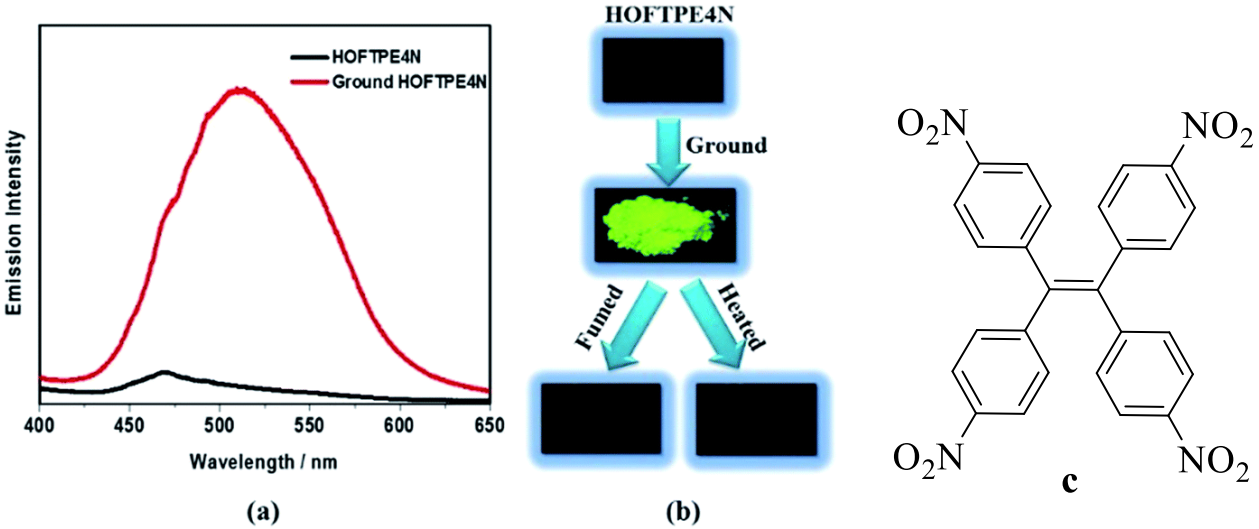

Figure 18 (A) Emission spectra of TPE4N and ground TPE4N (B) Photographs of the mechanoluminescent properties of HOFTPE4N and the quenching process (C) Molecular

structure of HOFTPE4N [Reproduced with permission from the Royal Society of Chemistry (Yu *et al.*, 2017)].

Applications of AIE Molecules

AIE luminogens are ideal candidates for various applications because of their high emission in the aggregated state. In the following sections, the various significant applications of AIE molecules have been discussed with examples.

Chemical Sensors

Dong *et al.* (2007) applied AIE fluorophores to detect volatile organic compounds (VOCs). The solution of diphenyltetraphenylethene (TPE) derivative 1 was spotted on a TLC plate, as shown

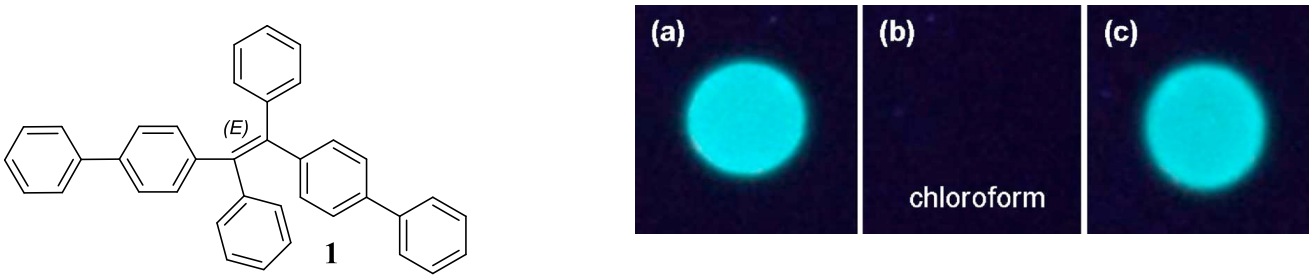

in Figure 19. The fluorescence of the spot was quenched on saturation with the chloroform vapour. However, the luminescence reappeared when the solvent was evaporated. A similar effect was observed for other VOCs, such as dichloromethane, acetonitrile, acetone and THF. Such chemosensors used for VOCs have hygienic and environmental implications (Dong *et al.*, 2007).

Figure 19: (Left) Chemical structure of 1. (Right) Spots of 1 on TLC plates placed in Petri-dish sets (a) without and (b) saturated with chloroform vapour. The photograph in panel taken after the organic vapour in panel b has been evacuated [Reproduced with permission from the American Institute of Physics (Dong *et al.*, 2007)].

In another important example, an aminated HPS derivative A_2HPS was utilized for the detection of nitroaromatic based warfare explosives: 2,4,6-trinitrotoluene (TNT) and 2,4-dinitrotoluene (DNT). Because of the unavailability of DNT and TNT, picric acid (PA) was used. On the sequential addition of PA into the aqueous solution of A_2HPS, the emission intensity was progressively quenched, as shown in Figure 20 (Dong *et al.*, 2007). The quenching constant

(K_{SV}) of 1.65 × 10^5 M^{-1} was obtained by the Stern-Volmer plot. Thus, nano-aggregates of A_2HPS were successfully utilized for the detection of explosives.

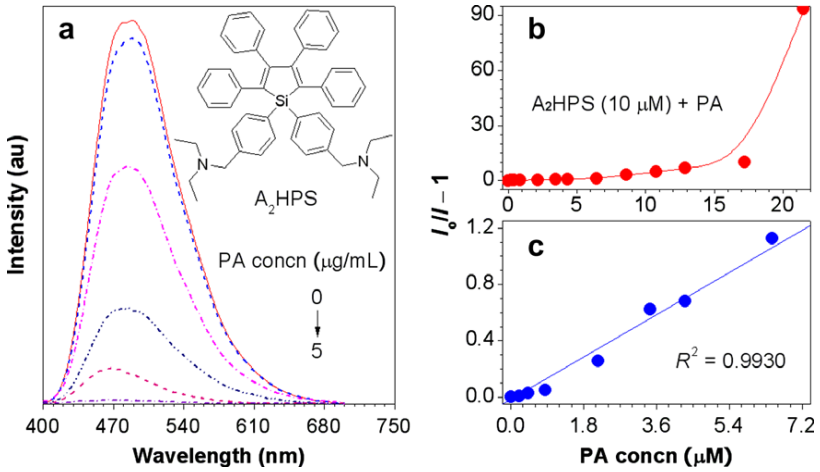

Figure 20 (A) Emission spectra of A_2HPS in THF/water mixtures (1:99 v/v) containing different amounts of PA. (B) Plot of emission intensity versus PA concentration. (C) Linear region of the (I_0/I -1) – [PA] plot [Reproduced with permission from the American Institute of Physics (Dong *et al.*, 2007)].

Biological Probes

AIE dyes are covalently attached to hydrophilic functional groups such as hydroxyl, amino, sulfonate, and boronate to impart solubility in water for use as biological probes. Thus, the luminogens are non-fluorescent in the aqueous buffer but become emissive when bound to biological species. Such turn-on sensors are advantageous over their turnoff counterparts.

An example is sulfonated tetraphenylethene TPE (Figure 21), which was used as a turn-on biosensor for protein bovine serum albumin (BSA). It was found that the PL intensity for 500 mgL^{-1} BSA was ~240 times higher than that for 0 mgL^{-1} of BSA (Tong *et al.*, 2007). It was proposed that TPE derivative in the presence of water owing to complete solubility was non-emissive. However, in the presence of BSA, which contained hydrophobic binding sites, the TPE derivative gave immense emission. The hydrophobic nature of BSA led to the aggregation of TPE derivative, and hence, the AIE was observed. Nevertheless, the addition of sodium dodecyl sulfate (SDS) into the BSA solution of the TPE derivative resulted in the quenching of fluorescence. The SDS is known to rupture the hydrophobic binding sites. Hence, because of the release of the TPE derivative back to the aqueous solution, the fluorescence was quenched.

The PL spectra of TPE sulfonate in the presence of BSA and SDS are shown in Figure 22. Thus, such turn-on sensors are sensitive, specific, and faster for implications in the biological field.

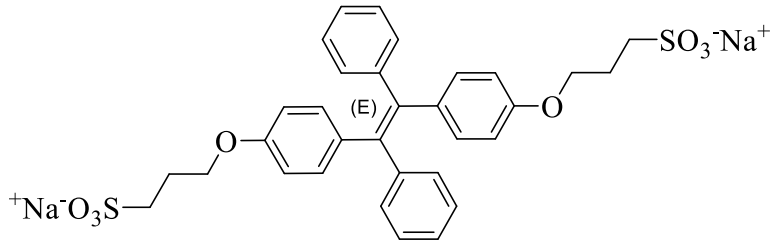

Figure 21: Chemical structure of TPE sulfonate [Reproduced with permission from the American Chemical Society (Tong *et al.*, 2007)].

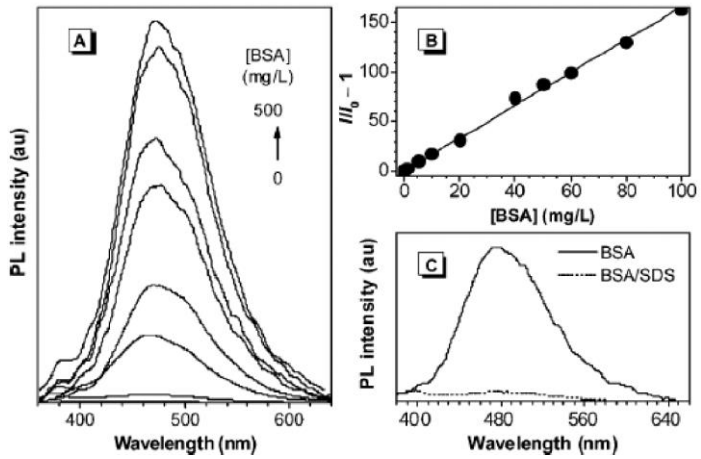

Figure 22 (A) PL spectra of sulfonated TPE salt in phosphate buffer (pH = 7.0) containing different amounts of bovine serum albumin (BSA). (B) Plot of [BSA] *versus* $I/I_0 - 1$; I_0 = intensity at [BSA] = 0 mg/L. (C) Effect of BSA on the PL spectrum of a buffered solution of 1 in the absence and presence of sodium dodecyl sulphate (SDS). [Reproduced with permission from the American Chemical Society (Tong *et al.*, 2007)].

Another significant application of AIE fluorophore is in the sensing of sugar by molecule 2 (Figure 23). Sugar plays a pivotal role in the metabolic activity of our body. Hence, convenient methods for the selective and sensitive recognition of sugar in the aqueous medium are of paramount importance in the medicinal field. For instance, monitoring glucose levels in human fluids such as urine and blood are crucial for the treatment of diabetes. Compound 2 was synthesized by attaching boronic acid chelating groups to phenyl rings of triphenyl ethylene (TPE). This molecule is soluble in water. In the presence of D-glucose, 2 showed a significant

increase in the PL intensity, whereas no such dramatic change was observed with D-mannose or D-galactose. Conformational matching between D-glucose and compound 2 may be responsible for the specificity (Dong *et al.,* 2007).

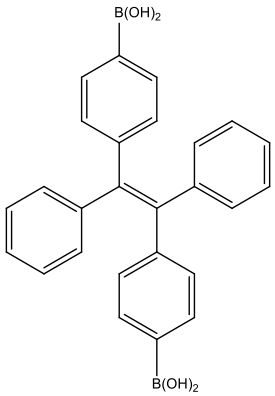

Figure 23: Chemical structure of TPE-bisboronic acid used for sugar sensing in biological fluids

Conclusion

This review explains the phenomenon and mechanism of aggregation-induced emission (AIE). Restriction of intramolecular rotation (RIR) is the sole source for AIE, which has been elucidated through several mechanistic studies *viz.* viscochromism, piezochromism, thermochromism, and lifetime studies. Furthermore, particle size analysis demonstrated that the formation of nano aggregates is responsible for the AIE phenomenon. The elaborate mechanistic studies have enabled scientists to develop new interesting AIE fluorophores with eloquent colour tuning. The application of these fluorophores as chemical sensors and biological probes has also been discussed. To conclude, the synthesis of conjugated organic molecules for AIE applications is a growing field. This field, although well studied, still has vast scope in optoelectronics, which can open new endeavours in the near future. Fluorophores in the aggregated state have immense utility as most optoelectronic devices need them in solid or film form. Keeping these points in mind, the synthesis of new organic conjugated systems which can find practical applications is crucial.

References

Chen J., C. C. W. Law, J. W. Y. Lam, Y. Dong, S. M. F. Lo, I. D. Williams, D. Zhu, B. Z. Tang (2003) Synthesis, light emission, nanoaggregation and restricted intramolecular rotation of 1,1-substituted 2,3,4,5-tetraphenylsiloles. *Chem. Mater., 15*: 1535-1546.

Chinchilla R., C. Najera (2011) Recent advances in Sonogashira reactions. *Chem. Soc. Rev., 40*: 5084-5121.

Dong Y., J. W. Y. Lam, A. Qin, J. Liu, Z. Li and B. Z. Tang (2007) Aggregation-induced emission of tetraphenylethene derivatives and their utilities as chemical vapor sensors and in organic light-emitting diodes. *Appl. Phys. Lett., 91*: 011111.

Dong Y., J. W. Y. Lam, A. Qin, J. Liu, Z. Li, J. Liu, J. Sun, Y. Dong and B. Z. Tang (2007) Endowing hexaphenylsilole with chemical sensory and biological probing properties by attaching amino pendants to the silolyl core. *Chem. Phys.Lett., 446*: 124-127.

Fan X., J. Sun, F. Wang, Z. Chu, P. Wang, Y. Dong, R. Hu, B. Z. Tang, D. Zou (2008) Photoluminescence and electroluminescence of hexaphenylsilole are enhanced by pressurization in the solid state. *Chem. Commun.*, 2989-2991.

Grimsdale A. C., K. L. Chan, R. E. Martin, P. G. Jokisz and A. B. Holmes (2009) Synthesis of light-emitting conjugated polymers for applications inelectroluminescent devices. *Chem. Rev., 109*: 897-1091.

Hong Y., J. W. Y. Lam and B. Z. Tang (2009) Aggregation-induced emission: phenomenon, mechanism and applications. *Chem. Commun.*, 4332-4353.

Kulkarni A. P. and S. A. Jenekhe (2003) Blue light-emitting diodes with good spectral stability based on blends of poly-9,9-dioctylfluorene): interplay between morphology, photophysics and device performance. *Macromolecules, 36:* 5285-5296.

Leung N. L. C., N. Xie, W. Yuan, Y. Liu, Q. Wu, Q. Peng, Q. Miao, J. W. Y. Lam and B. Z. Tang (2014) Restriction of intramolecular motions: the general mechanism behind aggregation-induced emission.*Chem. Eur. J.***,** *20:* 15349-15353**.**

Li Z., Y. Dong, B. Mi, Y. Tang, M. Häussler, H. Tong, Y. Dong, J. W. Y. Lam, Y. Ren, H. H. Y. Sung, K. S. Wong, P. Gao, I. D. Williams, H. S. Kwok and B. Z. Tang (2005) Structural control of the photoluminescence of siloleregioisomers and their utility as sensitive regiodiscriminatingchemosensors and efficient electroluminescent materials. *J. Phys. Chem. B***,** *109:* 10061-10066.

Nagarajan B., S. Kushwaha, R. Elumalai, S. Mandal, K. Ramanujam and D. Raghavachari (2017) Novel ethynyl-pyrene substituted phenothiazine-based metal free organic dyes in DSSC with 12 % conversion efficiency. *J. Mater. Chem. A***,** *5:* 10289-10300.

Nguyen B. T., J. E. Gautrot, C. Ji, P. l. Brumer, M. T. Nguyen and X. X. Zhu (2006) Enhancing the photoluminescence intensity of conjugated polycationic polymers by using quantum dots as antiaggregation reagents. *Langmuir, 22:* 4799-4803.

Ren Y., J. W. Y. Lam, Y. Dong, B. Z. Tang and K. S. Wong (2005) Enhanced emission efficiency and excited state lifetime due to restricted intramolecular motion in silole aggregates. *J. Phys. Chem. B, 109*: 1135-1140.

Slodek A., M. Filapek, E. S. Balcerzak, M. Grucela, S. Kotowicz, H. Janeczek, K. Smolarek, S. Mackowski, J. G. Malecki, A. Jedrzejowska, G. s. Gorol, A. Chrobok, B. Marcol, S. Krompiec and M. Matussek (2016) Highly luminescence anthracene derivatives as promising materials for OLED applications. *Eur. J. Org. Chem.*, 4020-4031.

Tang B. Z., X. Zhan, G. Yu, P. P. S. Lee, Y. Liu and D. Zhu (2001) Efficient blue emission from siloles. *J. Mater. Chem., 11*: 2974-2978.

Tong H., Y. Hong, Y. Dong, M. Häussler, Z. Li, J. W. Y. Lam, Y. Dong, H. H. Y. Sung, I. D. Williams and B. Z. Tang(2007) Protein detection and quantitation by tetraphenylethene-based fluorescent probes with aggregation-induced emission characteristics. *J. Phys. Chem. B, 111:* 11817-11823.

Tong H., Y. Hong, Y. Dong, Y. Ren, M. Häussler, J. W. Y. Lam, K. S. Wong and B. Z. Tang (2007) Color-tunable, aggregation-induced emission of a butterfly-shaped molecule comprising a pyran skeleton and two cholesteryl wings. *J. Phys. Chem. B, 111:* 2000-2007.

Verheyen L., P. Leysen, M. P. V. D. Eede, W. Ceunen, T. Hardeman and G. Koeckelberghs (2017) Advances in the controlled polymerization of conjugated polymers. *Polymer, 108:* 521-546.

Xu S., E. H. kim, A. Wei and E. Negishi (2014) Pd- and Ni- catalyzed cross coupling reactions in the synthesis of organic electronic materials. *Adv. Mater., 15:* 1-23.

Yu T., D. Ou, Z. Yang, Q. Huang, Z. Mao, J. Chen, Y. Zhang, S. Liu, J. Xu, M. R. Bryce and Z. Chi (2017) The HOF structures of nitrotetraphenylethene derivatives provide new insights into the nature of AIE and a way to design mechanoluminescent materials. *Chem. Sci., 8:* 1163-1168.

Zeng Q., Z. Li, Y. Dong, C. Di, A Qin, Y. Hong, L. Ji, Z. Zhu, C. K. W. Jim, G. Yu, Q. Li, Z. Li, Y. Liu, J. Qin, and B. Z. Tang(2007) Fluorescence enhancement of benzene-cored luminophors by restricted intramolecular rotations: AIE and AIEE effects. *Chem. Commun.*, 70-72.

Zhang J., B. Xu, J. Chem, L. Wang and W. Tian (2013) Oligo(phenothiazine)s: Twisted intramolecular charge transfer and aggregation-induced emission. *J. Phys. Chem. C, 117:* 23117-23125.

Zhou, S., C. Li, J. Zhang, Y. Yu, A. Zhang, Y. Wu and W. Li (2017) Diketopyrrolopyrrole-porphyrin based conjugated polymers for ambipolar field-effect transistors. *Chem. Asian J., 12:* 1861-1864.

STRUCTURE-FUNCTION RELATIONSHIP: ITS TRANSLATION FROM LIVING ORGANISMS TO NANOSTRUCTURED MATERIALS

Chiranjib Banerjee*

Dept. of Engineering and Physical Sciences, Institute of Advanced Research, Gandhinagar, Gujarat 382426, India

*Corresponding Author, E-mail: banerjeec@gmail.com

Abstract

Structure-function relationship, one of the significant aspects of nature, refers to origin of certain functionalities of a living or non-living specimen depending upon the structure of a part of the specimen or the specimen as a whole. In nature, such structure-function relationship is ubiquitous and scientists are striving continuously to mimic those unique structural features in materials so that useful functionalities can be derived out of them. Such endeavor is neither trivial and simple but requires large precision, subtle control of particle arrangement and creativity. The current article highlights some of these unique structural aspects in biological species and how they can be replicated to form novel nanostructured materials with technologically important functionalities.

Keywords: Structure, Function, Template, Nanomaterials, Biological

Introduction

The aphorism, *structure determines function* is a universal fact that can be observed at different levels of our environment. Whether it is a tiny sub-microscopic particle or a large macroscopic object, almost always it can be found that the function of an object is actually the outcome of its characteristic structural features. Mother Nature has created unique structures in the living organisms which can generate new functions, suitable for their survival. In fact, the primary essence of evolution is actually a gradual and continuous change in the structures of simple organisms, so that higher level organisms evolve with more complex structures and functions. For the last three decades, the prime interest of researchers is to exploit this structure-function relationship and design new nanomaterials so as to derive useful functional responses out of

them. These novel materials, the so-called ‘functional or smart materials’, have been designed by mimicking biological structures, and such bio-inspired science have earned a significant place in today’s nanoscience. The present paper intends to highlight examples of certain structural features from the living world that give rise to useful functions, and how this structure-function combination can be translated to nanostructured materials to bestow new functionalities upon them.

The Bio-inspired Nanoscience

Fabrication of micro- and macro scale materials with well-defined and controllable nanometer scale features is very challenging, and such materials are generally fabricated using either lithographic techniques or template mediated approaches. Several artificial templates have been used to serve the purpose;[1-5] however, they generally lack the structural sophistication necessary to yield the intricate details that the lithographic techniques typically provide. Inspired by the fascinating structures found in the living world, researchers attempted to replicate them in synthetic materials. To this end, using biological templates showed great success in transferring biological structural features to unique nanoarchitectures.

The Essence of Biological Templating

Primarily, bio-templating has been adopted either to replicate the structural features and functionality of a living species or to direct the assembly of nanomaterials employing a biological structure.[6]

The species selected for replication typically possess attractive morphological features, e.g. diatoms or butterfly wing scales, and the final material represents a copy of the template. These natural templates possess a wide variety of interesting characteristics, such as nanoporosity in diatoms, channel structures in viruses, or complex architectures in butterfly wings. Producing the correct morphology with high degree of precision is essential to realize the desired functional output.

In the second case, a biological species acts as a moderator to regulate the assembly of nanoparticles into some pre-determined patterns or architecture. Such control is generally achieved via self-assembly, van der Waals forces, electrostatic interactions and other molecular recognition processes. As a prerequisite, the biologicals employed must carry specific chemical or morphological attributes to direct the particles to form the required structure.

Although a vast number of organisms have been used as biological templates, only a few havepractical significance. In the current article, some of the important biologicals will be discussed in brief, whose interesting structures had been translated into synthetic materials, which in turngave rise to novel properties and functional responses in those smart materials.

Butterfly Wings

The beautiful colors exhibited by butterfly wings are usually contributed by two sources: pigments and periodical submicrometer structures which are also referred to as 'chemical' and'physical' colors, respectively.[7] For the purpose of structure and property replication, the 'physical' color is the prerequisite for choosing the right type of butterfly templates. Butterflywing scales (150 µm x 50 µm) exhibit extremely complex morphology which consists of lamellas arranged in highly ordered architectures to form pores and layers. This complex structure has been used as biotemplate to generate tubular ZnO structures of micrometer dimensions.[8] Furthermore, photonic devices behaving as optical waveguides and beam splitters have also been developed by replicating the structural hierarchy of butterfly wing using atomiclayer deposition of Al_2O_3 coatings.[9]

Bacteria

Bacteria are another attractive species for bio-templating of nanomaterials because of the several advantages they offer. Among them, the wide variety of morphological features is the most relevant to the generation of a variety of interesting nanostructures. For example, bacilli-, cocci-, or spirilli-shaped bacteria can lead to the formation of corresponding 3D hollow nanostructures which cannot be realized by other means. Zhou et al. showed that two kinds oflactobacillus, viz. *Streptococcus thermophilus* and *Lactobacillus bulgaricus* can be used as templates to initiate the formation of ZnS hollow nano spheres and nano tubes, respectively.[10]Bacterial threads have also been templated to form silica fibers consisting of densely packed silica nanoparticles. Further calcination of these bacteria-silicate structures removed the organic matrix and resulted in an organized array of 0.5 µm wide channels.[11] *Deinococcus radiodurans*, *Escherichia coli*, and *Rhodospirilium rubrum* were all used in the same study astemplates for magnetic Ni nanoparticles. The cells were first activated by catalytic Pt, followedby deposition of Ni nanoparticles from $NiSO_4$ solution. Different nanostructures, viz. nanospheres, nanofilaments (45-80 nm long) and nanocoils (9 µm long) were obtained.[12] Some studies have taken advantage of the high affinity of some live bacteria toward certain specific chemicals. For example, *Bacillus cereus* has high affinity for lysine. These bacteria have been

coated with lysine-functionalized gold nanoparticles to produce an electrically conducting monolayer. The selectivity and high density of the nanoparticle pattern exhibited a dramatic increase in conductivity. By using electroluminescent nanoparticles or quantum dots, the above technique can be further extended to fabricate electro-optical devices.[13]

Viruses

Among the plethora of virus-templated nano structures reported in the literature, the work of Belcher and co-workers from Massachusetts Institute of Technology was innovative. The researchers used M13 bacteriophage as a universal template to control the patterning of semiconducting, metallic, oxide and magnetic materials. They modified the protein of the viral capsid with substrate-specific peptides and generated ZnS and CdS nanoparticles at specific sites in a very controlled way. Moreover, virus-templated gold nanoparticles were also synthesized, which in turn were used for nucleation and growth of cobalt oxide nanowires over large scales.[14] A well-dispersed Au-Co hybrid nanomaterial was obtained. In another study, virus-virus interactions were organized via self-assembly to create 2D liquid crystalline layer on polyelectrolyte films. Applying these ensembles in lithium-battery, a high cycling rate was achieved with capacity remaining practically stable for up to 10 charge/discharge cycles. Moreover, the devices could be operated at equivalent or higher capacitance values compared with that of the conventional Li batteries.[15, 16]

Mosaic viruses (e.g., tobacco, cowpea, red clover) have also gained large attention as biotemplates because of their high stability under extreme pH and temperature conditions. Additionally, the charged amino acids in their capsids can be tailored through chemical functionalization according to substrate-specific necessity. Stephen Mann et al. were the first to demonstrate that TMV viruses can be used to synthesize a variety of nanoparticles, such as CdS (5 nm), PbS (30 nm), FeO (22 nm).[17] The nucleation and growth of these particles were guided by the charge residues located on the outer surface of the virus. Thin silica-coated virion surfaces formed through sol-gel chemistry have also been reported. Interestingly, the silica-coated virions showed even higher level of ordered structure by self-assembling into linear chains.[17]

Diatoms

Diatoms are single-celled photosynthetic algae whose cell walls are composed of opaline silica. These silica cell walls are decorated with striking nanostructured patterns (~ 50 nm), such as circular, hexagonal, or rod-shaped depending on the species. Mirkin et al. were the first to show

that diatom cell walls can be chemically engineered to interact with nanoparticles.[18] Using piranha solution (H_2SO_4/H_2O_2 mixture), the organic components of the diatoms were first digested, followed by functionalization of the cell walls with aminosilane. The functionalized diatoms were reacted further with ssDNA and used as a template to arrange cDNA-functionalized Au nanoparticles. The same researchers were also successful in fabricating Ti and Ag coated diatom cells, and Ag micro shell structure which retained every detail of the nanostructure originally present on the diatom shell.[19] Since roughened metal surfaces and silver colloids have been proven to be effective substrates for surface enhanced Raman scattering (SERS), these micro shells and metal coated diatoms displayed very high intensity SERS signals and allowed the detection of Rhodamine 6G dye up to 100 nano molar (nM) concentration level. Additionally, by exploiting the optical properties, say photoluminescence that depend upon the nanostructural features of the silica shell and are sensitive to organic vapors and gases, novel nanosensors can be built.[20]

DNA

The double helix structure of DNA along with its nanometer-scale diameter (2 nm) and helical pitch (3.4-3.6 nm) has attracted scientists to use it as a template in nanotechnology.[21] Gold nanoparticles carrying oligonucleotides have been placed in order guided by linear single-stranded DNA. Such nano-assembly was achieved either through molecular recognition of complementary strands or via electrostatic interaction with the DNA template.[22] DNA can also be employed to control the spatial organization of nanoparticles. Single-stranded and cyclic DNAs were used by Adeye et al. to achieve extraordinary control of both spatial position and geometrical assembly of gold nanoparticles. Additionally, the read-write functions realized also show the great potential of DNA templating in forming nanostructures.[23] By controlling the structure of DNA molecules and forming complex 2D or 3D architecture out of it, such as lattices and grids, scientists have used those architectures as templates to generate ordered assemblies of Au nanoparticles (5 nm) with precise lattice spacing of 15-35 nm.[24] The structure of DNA molecule was also extended further to magnetic[25] and metallic nanostructures to obtain good control of dimension, crystallinity and chirality.[26]

Conclusions

To conclude, this short article highlighted some of the unique structures of biological species and how they can be translated into the non-living world so as to achieve smart nanomaterials. The translated structures generated new specialized functions in those materials

and made them important candidates for several technological and scientific applications. Furthermore, such bio-templating approach have great potential in creating exciting nanoarchitectures in a controlled way. Finally, this structure-function relationship is one of the important relationships in science and can open up more innovative research in future.

References

1. Huck, W., Tien, J., and Whitesides, G. (1998). Three-Dimensional Mesoscale Self-Assembly. Journal of the American Chemical Society. 120:8267-8268.
2. Caruso, F., Caruso, R., and Mohwald, H. (1998). Nanoengineering of Inorganic and Hybrid Hollow Spheres by Colloidal Templating. Science. 282:1111-1114.
3. Love, J., Gates, B., Wolfe, D., Paul, K., and Whitesides, G. (2002). Fabrication and Wetting Properties of Metallic Half-Shells with Submicron Diameters. Nano Letters. 2:891-894.
4. Paunov, V., and Cayre, O. (2004). Supraparticles and Janus Particles Fabricated by Replication of Particle Monolayers at Liquid Surfaces Using a Gel Trapping Technique. Advanced Materials. 16:788-791.
5. Lu, Y., Liu, G., Kim, J., Mejia, Y., and Lee, L. (2005). Nanophotonic Crescent Moon Structures with Sharp Edge for Ultrasensitive Biomolecular Detection by Local Electromagnetic Field Enhancement Effect. Nano Letters. 5:119-124.
6. Sotiropoulou, S., Sierra-Sastre, Y., Mark, S., and Batt, C. (2008). Biotemplated Nanostructured Materials†. Chemistry of Materials. 20:821-834.
7. Vukusic, P., Sambles, J., and Lawrence, C. (2000). Color mixing in wing scales of a butterfly. Nature. 404:457-457.
8. Zhang, W., Zhang, D., Fan, T., Ding, J., Guo, Q., and Ogawa, H. (2006). Fabrication of ZnO microtubes with adjustable nanopores on the walls by the templating of butterfly wing scales. Nanotechnology. 17:840-844.
9. Huang, J., Wang, X., and Wang, Z. (2006). Controlled Replication of Butterfly Wings for Achieving Tunable Photonic Properties. Nano Letters. 6:2325-2331.
10. Zhou, H., Fan, T., Zhang, D., Ding, J., Guo, Q., and Ogawa, H. (2007). Novel Bacteria-Templated Sonochemical Route for the in-Situ One-Step Synthesis of ZnS Hollow Nanostructures. Chemistry of Materials. 19:2144-2146.

11. Zhang, B., Davis, S., Mann, S., and Mendelson, N. (2000). Bacterial templating of zeolite fibres with hierarchical structure. Chemical Communications. 9:781-782.

12. Mogul, R., Getz Kelly, J., Cable, M., and Hebard, A. (2006). Synthesis and magnetic characterization of microstructures prepared from microbial templates of differing morphology. Materials Letters. 60:19-22.

13. Berry, V., Rangaswamy, S., and Saraf, R. (2004). Highly Selective, Electrically Conductive Monolayer of Nanoparticles on Live Bacteria. Nano Letters. 4:939-942.

14. Huang, Y., Chiang, C., Lee, S., Gao, Y., Hu, E., and Yoreo, J. et al. (2005). Programmable Assembly of Nanoarchitectures Using Genetically Engineered Viruses. Nano Letters. 5:1429-1434.

15. Ogasawara, T., Débart, A., Holzapfel, M., Novák, P., and Bruce, P. (2006). Rechargeable Li2O2Electrode for Lithium Batteries. Journal of the American Chemical Society. 128:1390-1393.

16. Kunduraci, M., Al-Sharab, J., and Amatucci, G. (2006). High-Power Nanostructured LiMn2-xNixO4High-Voltage Lithium-Ion Battery Electrode Materials: Electrochemical Impact of Electronic Conductivity and Morphology. Chemistry of Materials. 18:3585- 3592.

17. Shenton, W., Douglas, T., Young, M., Stubbs, G., and Mann, S. (1999). Inorganic-Organic Nanotube Composites from Template Mineralization of Tobacco Mosaic Virus. Advanced Materials. 11:253-256.

18. Rosi, N., Thaxton, C., and Mirkin, C. (2004). Control of Nanoparticle Assembly by Using DNA-Modified Diatom Templates. Angewandte Chemie International Edition. 43:5500-5503.

19. Payne, E., Rosi, N., Xue, C., and Mirkin, C. (2005). Sacrificial Biological Templates for the Formation of Nanostructured Metallic Microshells. Angewandte Chemie International Edition. 44:5064-5067.

20. Losic, D., Mitchell, J., and Voelcker, N. (2006). Fabrication of Gold Nanostructures by Templating from Porous Diatom Frustules. New Journal of Chemistry. 30:908-914.

21. Seeman, N. (2003). DNA in a Material World. Nature. 421:427-431.

22. Kumar, A., Pattarkine, M., Bhadbhade, M., Mandale, A., Ganesh, K., and Datar, S. (2001). Linear Superclusters of Colloidal Gold Particles by Electrostatic Assembly on DNA Templates. Advanced Materials. 13:341-344.

23. Aldaye, F., and Sleiman, H. (2007). Dynamic DNA Templates for Discrete Gold Nanoparticle Assemblies: Control of Geometry, Modularity, Write/Erase and Structural Switching. Journal of the American Chemical Society. 129:4130-4131.

24. Zhang, J., Liu, Y., Ke, Y., and Yan, H. (2006). Periodic Square-Like Gold Nanoparticle Arrays Templated by Self-Assembled 2D DNA Nanogrids on a Surface. Nano Letters. 6:248-251.

25. Kinsella, J., and Ivanisevic, A. (2007). DNA-Templated Magnetic Nanowires with Different Compositions: Fabrication and Analysis. Langmuir. 23:3886-3890.

26. Shemer, G., Krichevski, O., Markovich, G., Molotsky, T., Lubitz, I., and Kotlyar, A. (2006). Chirality of Silver Nanoparticles Synthesized on DNA. Journal of the American Chemical Society. 128:11006-11007.

DEGRADATION AND REMOVAL OF PENDIMETHALINHERBICIDE FROM AQUEOUS SOLUTION USING ELECTRO-SORPTION PROCESS

Shubham Dudhane[1], Rutvik Majethiya[2], Isha Jani, Mitesh Patel[2], Ganesh Bajad[2*]

[1]Department of Chemical Engineering, University Institute of Chemical Technology, North Maharashtra University, Jalgaon 425001, India

[2]Department of Engineering and Physical science, Institute of Advanced Research, Gandhinagar 382007, Gujarat, India

*Corresponding Author, E-mail: ganesh.bajad@iar.ac.in

Abstract

Pendimethalin, a di-nitro-aniline class herbicide is frequently used to control most of the annual grasses in India. Due to the extensive use of pendimethalin herbicide, the runoff and pond water samples near to the farms are found to be contaminated. In this work, we have prepared a conductive film of CNT-PVAc composites which is further used as a spiral wound electrode. The electrodes were incorporated in a specially designed electrochemical filter for the degradation of pendimethalin herbicide. We have reduced the concentration of pendimethalin herbicide up to 55% to 60 % using the electrolysis process. The morphologies of CNTs were confirmed using FE-SEM, energy dispersive spectroscopy (EDS)**,** and electrical conductivity test. Further, the % reduction in the concentration of Pendimethalin Herbicide was analysed using UV absorption spectroscopy.

Keywords: electro-sorption, carbon nanotubes, pendimethalin herbicide, polyvinyl acetate, degradation

Introduction

The Pendimethalin ($C_{13}H_{19}N_3O_4$) [3, 4-dimethyl-2, 6-dinitro-N-pentan-3-ylaniline] is the most commonly used herbicides in India. The extensive uses of pesticides and herbicides have alarmed the level of contamination in ground and surface water [1]. The Chlorophenols and Dinitroaniline are the major environmental pollutants that are widely used in the production of pesticides and herbicides. These pollutants get directly mixed with water sources and are also absorbed onto the surfaces of the soil and aquatic sediments and are harmful to human, animal, and fish [2]. To reduce the exceeded concentration of herbicides in the soil, some conventional methods such as incineration, air stripping, adsorption, biological treatments, etc. can be used. However, the economic feasibility of these methods is unsure. Alternatively, the pollutant from

soil can be removed by washing it with water and further treatment of washed water [3]. For the less soluble pollutants, surfactant aided soil washing is generally used [4]. Most of these methods are used to separate the pollutants from fluid to solid [5]. It will be better if one could be able to degrade the removed products.

The adsorption process is very common in the industry for the separation of components [6]. If the adsorption is clubbed with the electrolysis process, both separation and degradation can be achieved. Activated carbon is one of the most promising adsorbents available in the industry; however, it cannot degrade the contaminant as it is not electrically conductive [7].

Since the discovery of carbon nanotubes (CNTs), carbon in the form of conductive material becomes very popular and has been utilized in many applications. CNTs are reported in different forms depending on their chirality, single-walled carbon nanotubes (SWCNTs), multi-walled carbon nanotubes (MWCNTs), metallic, non-metallic, and semiconductor CNTs [8]. In this work, the synthesis of carbon nanotubes was carried out using waste plastic as a precursor and Ni/Mo/MgO as a catalyst using the combustion technique[9]. Further, these CNTs were utilized for the synthesis of PVAc/CNT polymer nano-composites. PVAc polymer can be dissolved in many solvents other than water and does not cross-link[10].

The present work examines the degradation of Pendimethalin by using the electrosorption process. The electrodes are fabricated using CNTs as it has good thermal, electrical, and mechanical properties. PVA_C is merely used as a binder to form a flexible conductive electrode. This study aims to characterize the electrochemical properties and % removal of pendimethalin concentration.

Materials and Methods

Materials

Chemicals such as citric acid, nickel nitrate hex hydrate, ammonium heptamolybdate, magnesium nitrate hexahydrate, sodium dodecyl sulphate, dimethyl-forma-amide, polyvinyl acetate, methanol, acetone, and pendimethalin obtained from Sigma Aldrich with 99% purity was used in the present study.

Synthesis of MWCNTs

Syntheses of MWCNTs was carried out using a chemical vapour deposition method as reported in our previous work [9]. The required amount of shredded HDPE plastic chip was mixed with the desired amount of prepared catalyst. The mixture was kept in a ceramic crucible covered

with aluminium foil and was heated at 800 °C in the muffle furnace. The crucible was removed from the furnace after 10 minutes and was cooled to room temperature. The as-synthesized MWCNTs were further utilized for the synthesis of a conductive film.

Synthesis of CNT/PVA Composite

(A) (B)

Figure 1 (A) Photograph of as-prepared CNT/PVAc composite film, (B) Electrolysis system and treated sample

The CNTs have dispersed in dimethyl forma-amide solution with a 1:1 weight ratio of CNT and sodium dodecyl sulphate (SDS) by using the ultra-sonication process. A desired amount of PVAc was added into the solution and stirred for 8h to get uniform homogeneous black polymeric liquid. Further, the solution was ultra-sonicated for 15 minutes to remove air bubbles. The as prepared black solution was spread over a glass plate and made into a thin sheet (1.5 mm thick) using a solution-casting method and then dipped into distilled water for 24 h. The film Fig 1 (A) was removed from the water and dried for 24 h. Fig 1 (B) shows electrolysis set-up used to treat pendimethalin solution.

Electrolysis

Electrolysis filter was constructed as spiral wound thin-film electrodes with provision for fluid inlet as shown in Fig 2 (B), 1. The fluid is further passed through the holes Fig 2 (A), 9) to the annulus of electrodes. Composite thin film electrodes with spacers in between were placed below and above the holes marked over the tube. A spacer was placed between two composite films to avoid the contact between two electrodes wherein the spacing between the electrodes was kept 0.3 mm. The composite film was then spirally wound to form a compact cylindrical filter. The solution enters the filter from either end of the pipe and further circulated inside thin film through holes inside the pipe. The DC supply wires were connected to the composite layers, one with a positive electrode and another is a negative. Fig 1 (A) shows the cut section

of the spiral wound electrolysis filter and Fig 2 (B) shows multiple layers of the electrode along with spacers. 1-waste water inlet; 9- holes in electrode annulus; 10- fluid out outlet (optional); 3, 5, 6- CNT/PVA films; 2, 4-spacer, 7 & 8- +v ad –ve DC supply respectively.

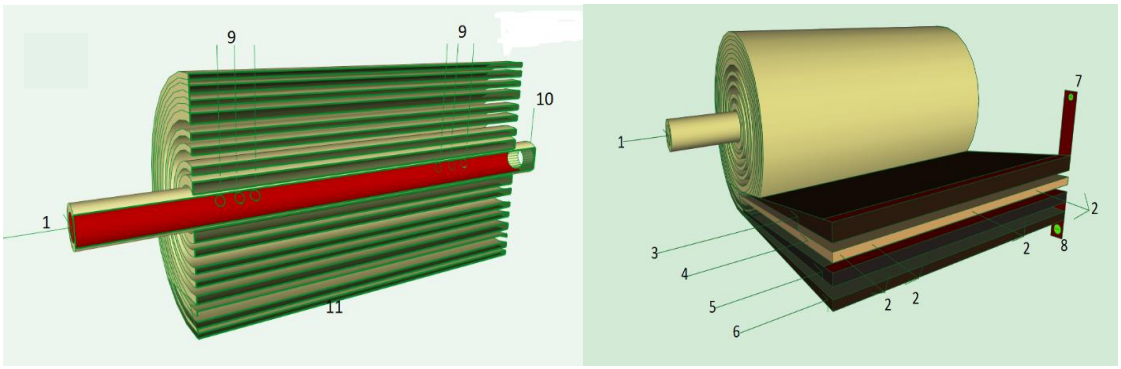

Figure 2: (A) Schematic of electrochemical filter drawn using Google Sketchup cross-section of filter, (B) CNT and spacer arrangement

Various concentrations of pendimethalin herbicide solution were prepared such as 100, 200, 300, 400, 500, and 600 in PPM and passed through electrodes to determine the maximum wavelength (λ_{max}) and absorbance of herbicide by UV spectroscopy. Table 1 represents the detailed specification of the spiral wound electrochemical filter.

Table 1 Detailed specification of the electrochemical system

Electrode specifications	**Units**
Electrode length	42 cm
Electrode width	11.8 cm
Active surface Area	498.6 cm^2
Reactor volume	30 mL
Flow-rate	0.15 mL/s
Voltage supply	9V
Electrode spacing	0.3 cm
Reactor length	20 cm
Reactor diameter	3 cm
RTD	3.2min

Results and Discussions

Characterization of electrode materials and composite electrodes

FESEM is used to analyse the morphology and particle size of MWCNTs. The result obtained by scanning electron microscope (S48000, Hitachi, Japan) indicates that the size of MWCNTs is around 18 to 27 nm (Fig 3).

(A) (B)

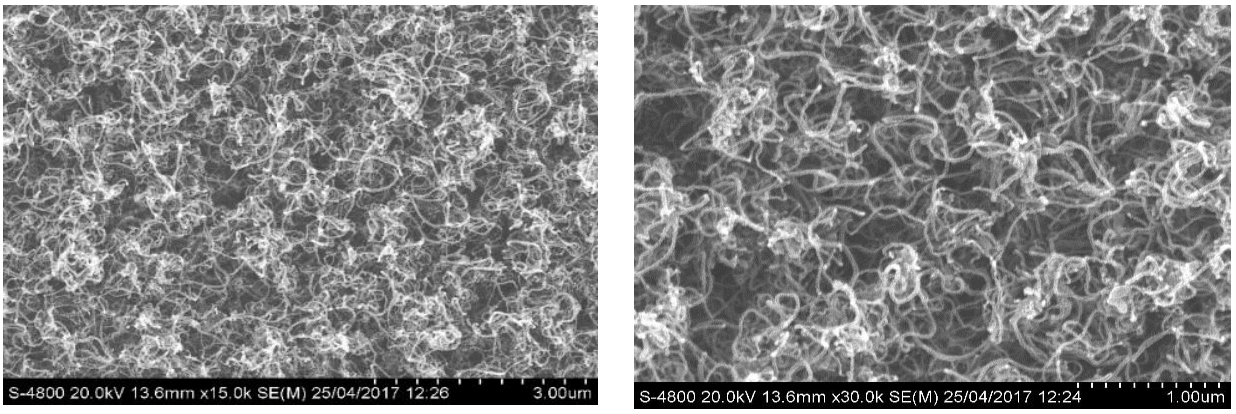

Figure 3: Scanning electron microscopy of as-synthesized CNTs using Ni / Mo / MgO Catalyst.

Energy Dispersive Spectroscopy (EDS) spectra for analysing elemental composition were recorded on spectrometer attached with SEM machine (S48000, Hitachi, Japan) operating at 0.5 to 30 kV (Fig 4). Elemental mapping was also performed using the same technique. The elemental detection has found the C, O, N, Mg, Ni metals.

(A) (B)

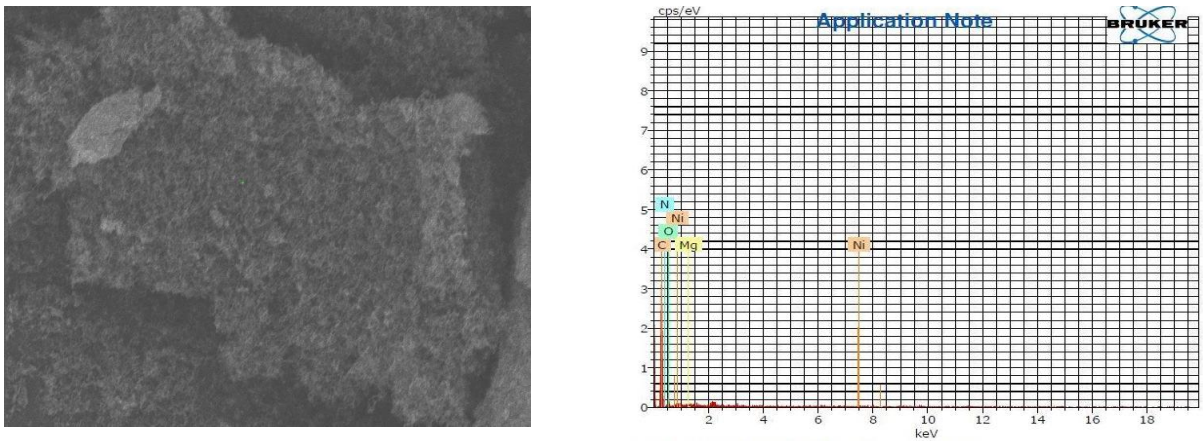

Figure 4: EDS spectra and elemental mapping of MWCNTs

The conductivity of MWCNTs was measured after compressing and making the powder of a tablet shape. Fig 5 (A, B) shows the plot of voltage versus current from which we can conclude that the material's conductivity obeys ohm's law and has a very good conductive.

(A) (B)

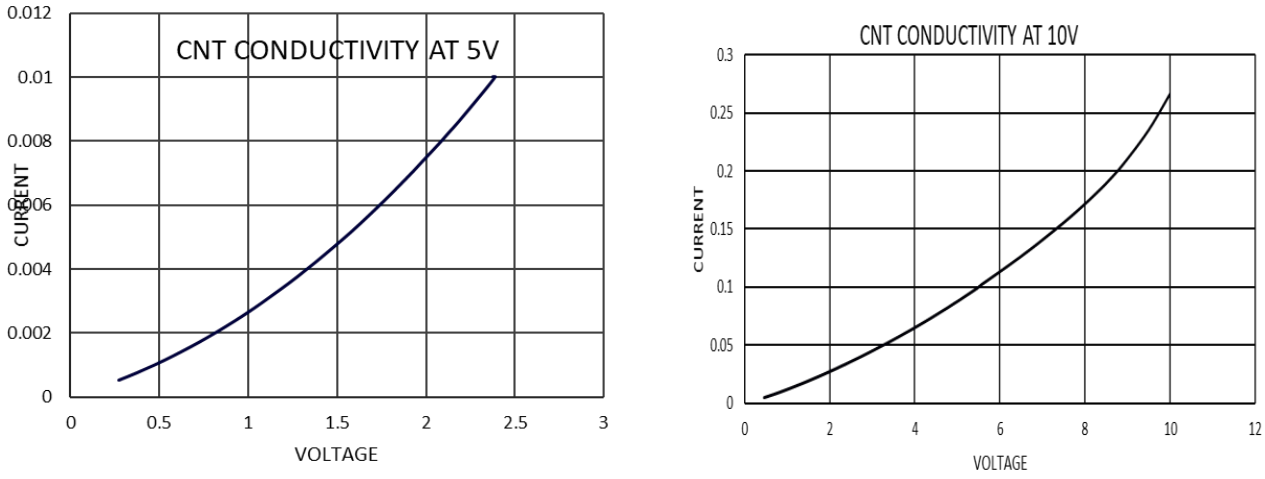

Figure 5: Conductivity of CNTs measured after compressing and making it of a tablet shape

The electrical conductivity of the CNT/PVA composite is shown in Fig. 6. The AC electrical conductivity was measured with a Solartron SI-1287. Electrochemical Interface is equipped with a Solartron 1255B Frequency Response Analyzer at a frequency range of 0.1 Hz to 1 MHz. The composite was found to have good conductivity above 9V.

(A) Sample 1 (Voltage Vs Current)

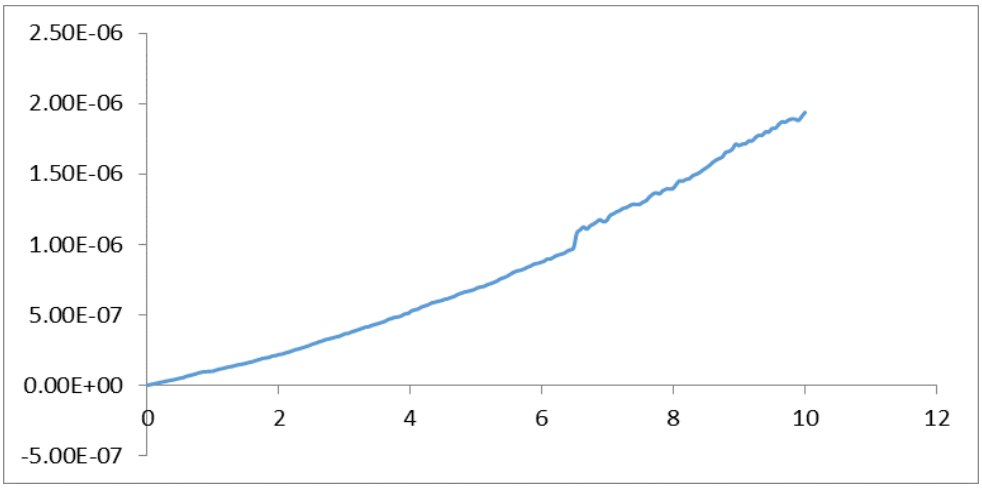

(B) Sample 2 (Voltage Vs Current)

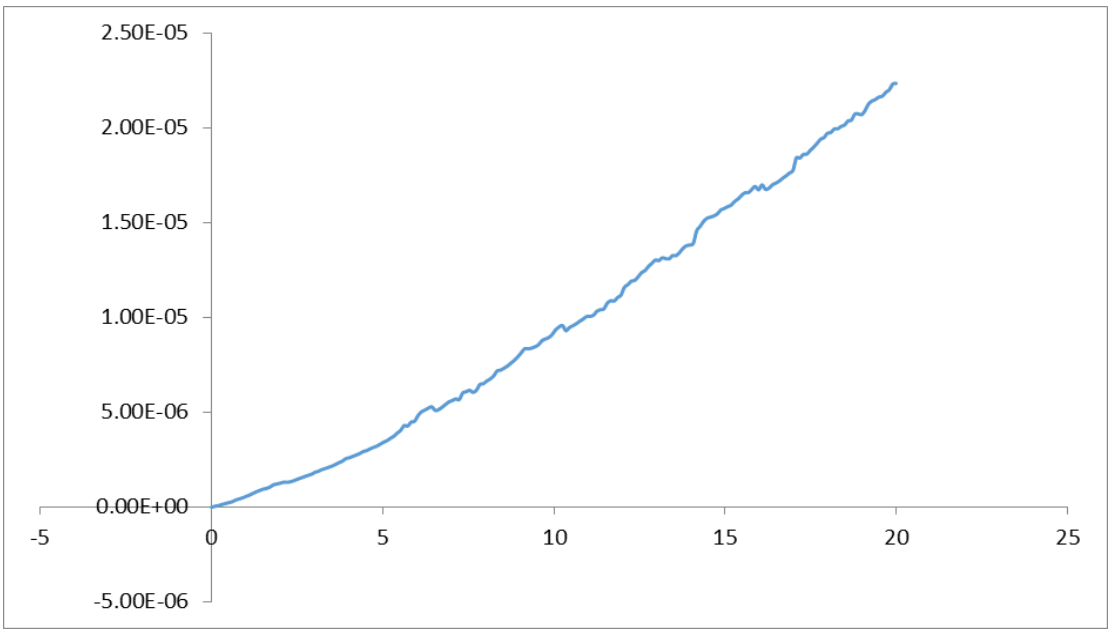

(C) Sample 3 (Voltage Vs Current)

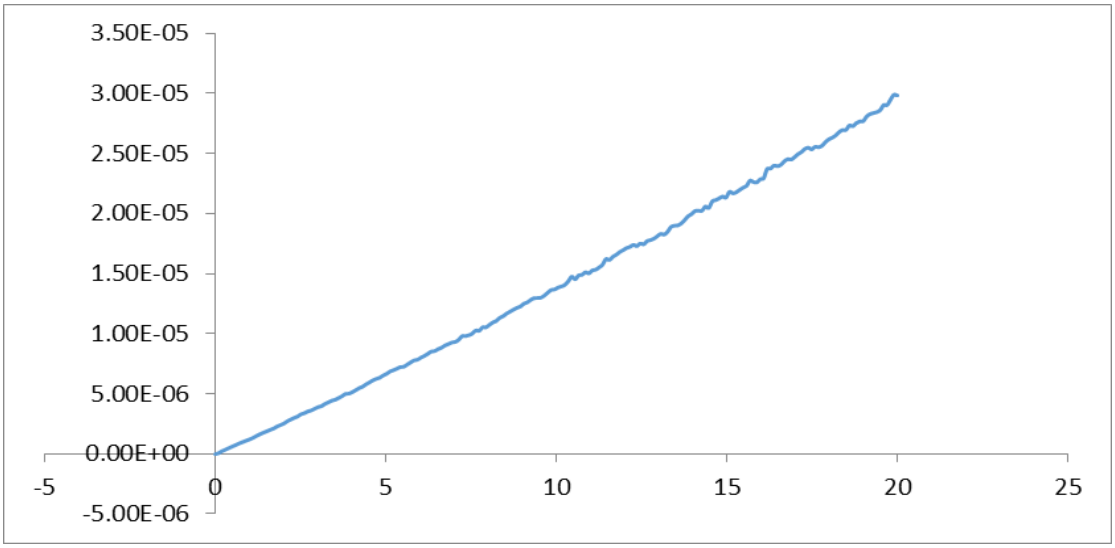

Figure 6: (A, B, C The electrical conductivity of CNT/PVA composites for different samples)

Analysis of samples using UV visible spectrophotometer

The degradation process of pendimethalin herbicides was recorded using a UV visible spectrophotometer. The maximum absorbance wavelength of pendimethalin in water was observed to be at 453 nm (Fig 7). Further, the calibration chart was prepared using different concentration of Pendimethalin in an aqueous solution and their absorbance was recorded. From the graph, slope and intercept of straight line is calculated as, slope (m) = 0.00028 & Intercept (c) = - 0.029.

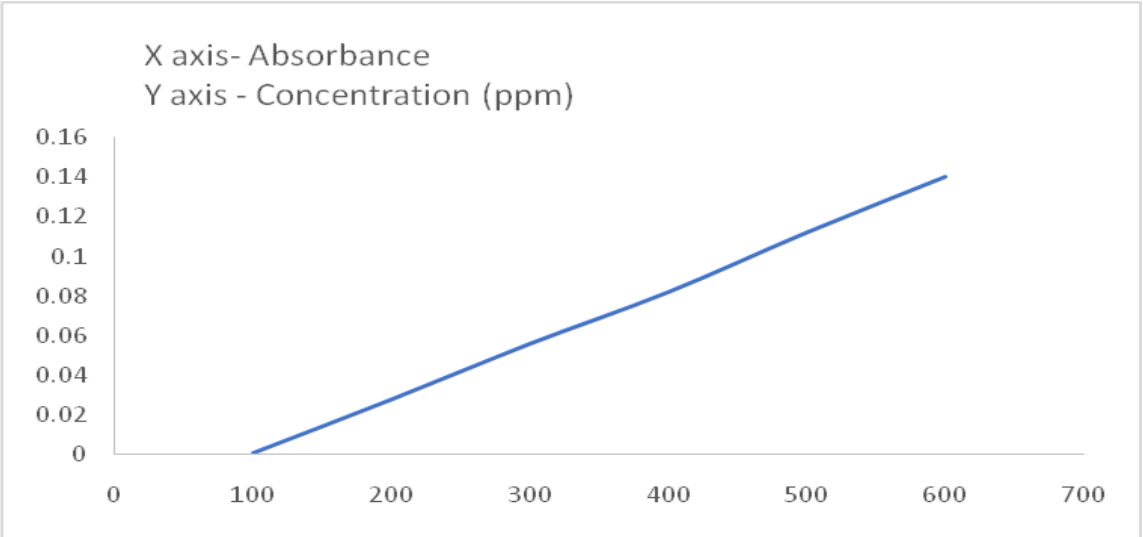

Figure 7: Calibration chart for absorbance of various concentrations pendimethalin herbicides solution at 453nm

Table 2: Reduction in Pendimethalin concentration after electrolysis

Sr. No.	Initial Concentration (PPM)	Absorbance of the treated sample	Final Concentration (PPM)	% Reduction
1	600	0.027	201.43	66.42
2	500	0.020	176.20	64.76
3	400	0.017	165.71	58.57
4	300	0.001	108.57	63.81

Table 2 shows a reduction in pendimethalin herbicide after electrolysis. It is clear from the data that electro-sorption is very efficient to degrade Pendimethalin herbicide in an aqueous solution. In the electrosorption process, the adsorption of certain counter ion and co ion distribution takes place at the electrode surface. The Faradaic side-reaction occurs at one electrode where degradation of either electrode occurs. Further, the breakdown of the electrolyte and catalytic conversion of an impurity species occurs. In the electrolysis of pendimethalin, a range of water and oxygen reactions can occur wherein these reactions yield or consume protons and hydroxides [11].

Conclusion

The MWCNTs were effectively blended with PVAc to form a thin sheet with improved electrical conductivity. The CNT/PVA composite as a spiral wound electrode has shown

excellent electro-sorption capacity. The degradation and removal of Pendimethalin herbicide from an aqueous solution are found to be very effective using spiral wound electrodes. The pendimethalin solution continuously processed through the spiral wound CNT/ PVAc thin film electrodes with the RTD of 3 minutes and 20 seconds. The designed electrochemical system is efficient to degrade the pendimethalin herbicide up to 58% to 66 %. The removal percentage of pendimethalin herbicides increases with the increasing concentration of the solution.

References:

Bajad G. S., R. P. Vijayakumar, A. G. Gupta, V. Jagtap, and Y. Singh. (2015). Synthesis and characterization of CNTs using polypropylene waste as precursor, *Mat. sci. & Eng. B*, 198 (1), 68–77.

Semsarzadeh M. A. and B. Ghalei, (2012). Characterization and gas permeability of polyurethane and polyvinyl acetate blend membranes with polyethylene oxide-polypropylene oxide block copolymer, *J. Memb. Sci*., 401 (2), 97–108.

El-Geundi M. S., T. E. Farrag, and H. M. A. Abd El-Ghany. (2005). Adsorption equilibrium of a herbicide (pendimethalin) onto natural clay, *Adsorpt. Sci. Technol*., 23 (6), 437–453.

Lu Q., J. Yu, and J. Gao, (2006). Degradation of 2, 4-dichlorophenol by using glow discharge electrolysis, *J. Haz. Mtrls*. 136, 526–531.

Cotillas S., S. Cristina, M. J. Solache-r, P. Ca, and M. A. Rodrigo. (2017) Removal of pendimethalin from soil washing effluents using electrolytic and electro-irradiated technologies based on diamond anodes, *Applied Catal. B*, 356, 112-118.

Deokar S. K., G. S. Bajad, P. Bhonde, R. P. Vijayakumar, and S. A. Mandavgane. (2017) Adsorptive Removal of Diuron Herbicide on Carbon Nanotubes Synthesized from Plastic Waste, *J. Polym. Environ*. 25 (2), 165–175.

Ahmad S. N., S. Hakeem, R. A. Alvi, and K. Farooq. (2013) Synthesis of multi-walled carbon nanotubes and their application in resin based nanocomposites, *J. Physics Conf Series.*, 439 (1) 01-08.

Reichenberger S., M. Bach, A. Skitschak, and H. G. Frede. (2007). Mitigation strategies to reduce pesticide inputs into ground- and surface water and their effectiveness; A review, *Sci. Total Environ*., 384 (1–3), 1–35.

Sondhia S. (2014). Herbicides residues in soil, water, plants and non-targeted organisms and human health implications: an Indian perspective, *Indian J. Weed Sci*., 46, (1) 66–85.

Chu W., K. H. Chan, and W. K. Choy. (2006). The partitioning and modelling of pesticide parathion in a surfactant-assisted soil-washing system, *Chemosphere*, 64 (5), 711–716.

Su X. and T. Alan Hatton. (2017). Electrosorption at functional interfaces: from molecular-level interactions to electrochemical cell design, *Phys. Chem.*19 23570-23584.

APPLICATION OF MACHINE LEARNING TO DETECT PHISHING URLS

Azriel Henry, Sunil Gautam*
Department of Engineering and Physical Sciences, Institute of Advanced Research, Gandhinagar
*Corresponding Author, E-mail: sunil.gautam@iar.ac.in

Abstract

Phishing is one of the most common and highly effective cyber-attacks in the cyber world. Phishers, to acquire confidential information or data like credentials, use different tactics to fool users. There are several techniques to detect phishing but still no technique is fully efficient. In this paper, the proposed model shows the use of machine learning technique to detect phishing. In this work, supervised and unsupervised algorithms are used for the detection of phishing and show that random forest outperforms other algorithms with higher classification accuracy.

Keywords: classification, machine learning, phishing, keyloggers

Introduction

Phishing is a common approach to obtain personal information from users. In this attack, the attacker uses different techniques like Clone Phishing, Spear Phishing, Whaling, Link Manipulation,Website Forgery, Filter Evasion, Social Engineering, Covert Redirect, Voice Phishing (Vishing), SMS Phishing, Tabnabbing, and Evil Twins to acquire a user's credentials. The word 'phishing' is said to have been first used in the mid-90s by a well-known spammer and hacker Khan C Smith [1]. The first recorded mention of the word is found in the hacking tool called AOHell which included a method for attempting to steal the financial details including the password of America's online users [2]. According to Wombat 2018 State of Phish, 76% of the organizations had experienced phishing attacks in 2017. Therefore, the digital world is safe from phishing attacks. In these days, all organizations across all fields are routinely targeted. Almost half (48%) the respondents of Wombat's 2018 State of the Phish survey said that the rate of phishing attacks is increasing [3]. Another survey from Millersmile website shows that around 942 attacks have been seen from January 2018 to March 2020 [4]. There are plenty of techniques in phishing that is used by a phisher to attack a user. Some of the techniques are discussed in the next section [5].

The remaining paper is structured as follows: section 2 reviews the related work; section 3 discusses our proposed model work; the experimental work is given in section 4; and the results are discussed in section 5. Finally, the paper will be concluded in section 6.

Phishing Techniques

Link Manipulation

Link manipulation is the phishing technique in which the phisher sends a connection request to a malicious site. At the point when the client clicks on the beguiling connection, it sends the user to the phisher's site instead of the site referenced in the connection. Drifting the mouse over the connection to see the genuine location prevents clients from submitting to interface control.

Keyloggers

Keyloggers is the malware used to distinguish key clicks from the keyboard. The data is sent to the phisher who will unravel passwords and other important data. To keep key lumberjacks from reading or accessing individual data, secure legitimate sites give the alternate option to utilize mouse snaps to make sections through the virtual console.

Trojan

A trojan horse is a sort of malware intended to delude the client with an activity that looks genuine, yet enables unapproved access to the client’s record to gather accreditations through the neighbourhood machine. The obtained data is then transmitted to cyber criminals.

Malvertising

Malvertising is a pernicious activity that contains dynamic contents which are planned or masked to download a drive’s undesirable substance or malware into your system. Adventures in Flash and Adobe PDF are the most widely recognized methods used in malvertisements.

(i) Session Hijacking

In session hijacking, the phisher misuses control component of the web session to acquire data from the user. Session sniffing is the basic session hacking system. Session sniffing allows phishers to catch pertinent data with the aim of getting the targeted person to the internet server unlawfully.

(ii) Content Injection

Content injection is the phishing technique in which the phisher changes a part of the component on the web page of a site. This is carried out to delude the client to go to a webpage outside the legitimate site where the client is then approached to enter individual or personal data.

(iii) Phishing through Search Engines

Some phishing techniques or methods include web crawlers where the client is coordinated to items destinations which may offer minimal effort items or administrations. At the point when the client endeavours to purchase the item by entering the charge card subtleties, the information is gathered by the phishing site. There are many phony banks' sites offering charge cards or credits to clients at a low rate and they are phishing destinations.

(iv) Vishing (Voice Phishing)

In voice or phone phishing, the phisher makes phone calls to the targeted user and asks the user to dial a specific number. The purpose is to get personal information about the bank account through the phone. Phone phishing is mostly done with a fake caller ID.

(v) Smishing (SMS Phishing)

Smishing is phishing conducted via a telephone-based text messaging service SMS i.e. Short Message Service. A smishing text, attempts to entice a victim into revealing personal information via a link that leads to a phishing website.

Related Work

There are many studies which show methods to deal with phishing attacks. Researches have used different approaches against phishing which includee Natural Language Processing (NLP), Heuristic-based Approach, Machine Learning, White List-Black List, Rule based Technique, Image Processing, etc. Buber et al. (2018) have proposed a system that detects phishing using machine learning. This proposed method uses random forest and sequential minimal optimization (SMO) algorithms to perform the classification [6]. Lee et al. (2015) showcased a heuristic approach to detect a phishing attack. This work also focused on the data set used and enhances the same with new features. Machine learning algorithms used in this study for

classification are SVM, decision tree, naïve bayes, KNN, random forest, and random tree. The comparison of the algorithms is carried out based on parameters like specificity, sensitivity and accuracy [7]. Rao et al. (2017) proposed a method to detect behaviour. This methodology performs steps like login check, feed fake credentials, zero links in the body of source code, and common page redirection ratio (CPRR) to ensure the legitimacy of a website. However, this technique fails to detect websites which use single sign-on. [8].

Santhana et al. (2012) shows the use of supervised machine learning algorithms like multilayer perceptron, decision tree induction, and naïve bayes to detect a phishing attack. Their observation shows that out of the three algorithms, decision tree predicts phishing more accurately [9].

Jain et al. (2018) have proposed a client-side solution to detect phishing attack using hyperlink information. They have used various types of classification algorithms and observed that the classification with logistic regression classifier achieved the highest accuracy [10]. Jain et al. (2018) have also developed another phishing detection system called PHISH-SAFE to detect phishing URLs. They have used 33000 phishing and legitimate URLs and 14 features with support vector machine (SVM) and naïve bayes classifier. Their results show that SVM achieves an accuracy of more than 90% [11].

Proposed Model

In two decades, several researchers detected that phishing using machine learning gives promising results than other methods due to its ability to detect zero-day attack. This paper also proposes work that shows the use of Machine Learning algorithms to detect phishing and also apply the classification algorithms for comparative results. The proposed model of our system is shown in Figure 1.

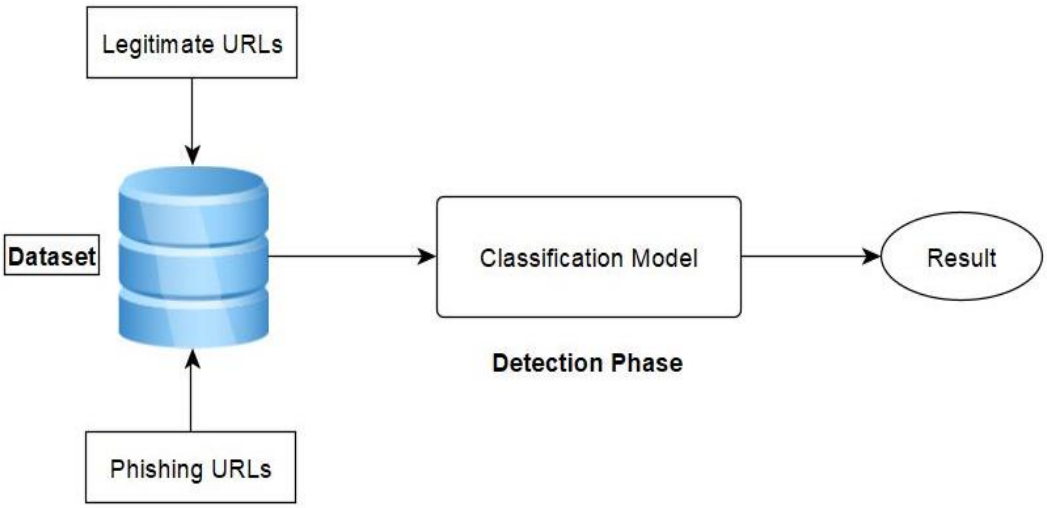

Figure 1: Proposed Model

Classification Process

In this work, different machine learning algorithms such as random forest, decision tree, naïve bayes, k-nearest neighbor, and multilayer perceptron have been used. These techniques are discussed in the next section.

(i) Random Forest

Random forest also known as random decision forest is an ensemble learning method in which combining multiple algorithms are used to generate better results for tasks like regression and classification. To produce excellent results, individual classifier is combined with other classifiers which are weak when used alone. The figure 2 algorithm starts with a tree-like graph or model of decisions and an input is entered at the top. Then, it travels down the graph with data being divided into smaller sets based on specific variables [12].

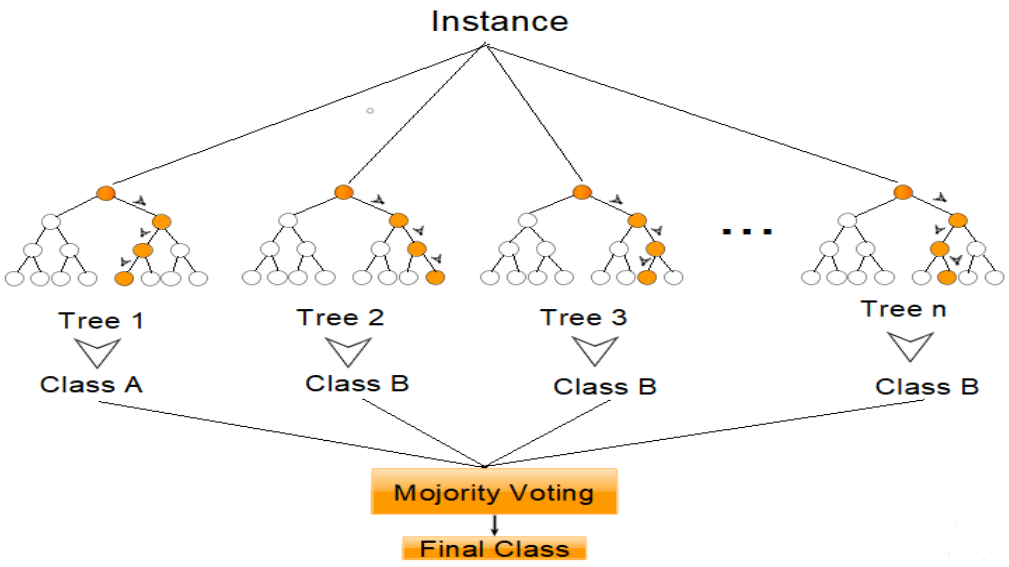

Figure 2: Random Forest Algorithm

(ii) Decision Tree

In a decision tree algorithm, every possible outcome is shown in a branching structure or tree structure like a flow chart. The nodes on the tree represent the test on a variable whereas the branch represents the result or outcome of the test [12]. To determine how nodes branch in the decision tree, entropy is used. The formula of entropy is as follows,

$$\text{Entropy} = \sum_{i=0}^{c} p_i \log_2 p_i \qquad (1)$$

Where c represents the number of classes and the p_i are the ratios of the elements of each label.

(iii) Naïve Bayes

The naïve bayes algorithm performs the classification on every value without considering other values or in other words, it performs independently. Probability is used to predict the class of the instance based on all the given attributes or features. This algorithm is simple than most other algorithms. Nevertheless, it performs well and is widely used on basis of its performance compared to other sophisticated classifiers [12-14].

$$P(x|c) = P\frac{x}{c}(P(c)) \Big/ |P(x)| \qquad (2)$$

Where,

- P(c|x) is the posterior probability of class (target)
- (c|x) is the posterior probability of class (target)

- P(c) is the prior probability of class
- P(x|c) is the likelihood which is the probability of predictor given class
- P(x) is the prior probability of predictor

(iv) K-Nearest Neighbor

The k-nearest-neighbor algorithm estimates the nearness of a data point to that of the other member of one group or another. It looks at the data points around the given data point to define the group of that data point. For example, for a given class- Group X and Group Y, the algorithm to determine its group will look at the data points that are near to the given data point to see the group with the majority of data points [12]. Distance between the members is measured by a distance function.

Algorithm 1: Distance-based index: construction

Step 1: Partition of the data or the data space

Step 2: Choose one reference point for each partition

Step 3: Compute the distance between all the data within the partition and its reference point

Algorithm 2: Distance-based index: KNN search

Step 1: Given a query item Q for which the KNN search is performed, compute the distances between the query item and all the reference points

Step 2: Sort the partitions based on the distances to Q in non-decreasing order

Step 3: Search for KNNs of Q using the triangle inequality from within the closest partition

One of the methods to find the distance with the Euclidean distance formula,

$$\text{Euclidean distance} = \sqrt{\sum_{i=1}^{k} \left(x_i - y_i\right)^2} \qquad (3)$$

Where k is the number of neighbour members to be considered and x and y are the members between whose distance is measured [15-16].

(v) Multilayer Perceptron

A multilayer perceptron (MLP) is a class of feed forward artificial neural network. The figure 3 shows the three layers in a multilayer perceptron namely, an input layer, a hidden layer, and an output layer. Each node is a neuron and uses a nonlinear activation function except for the input

nodes. MLP uses a supervised learning technique-back propagation to perform training. MLP is different compared to linear perceptron due to its multiple layers and non-linear activation. MLP can differentiate data that is not linearly separable [17-18].

Algorithm: Multilayer perceptron learning process

Step 1: Starts with the inputs and operates: Sum of the product of inputs and their weights

Step 2: Bias Factor is added

Step 3: Feeds the sum with the Activation Function

Step 4: The result is the output of the perceptron

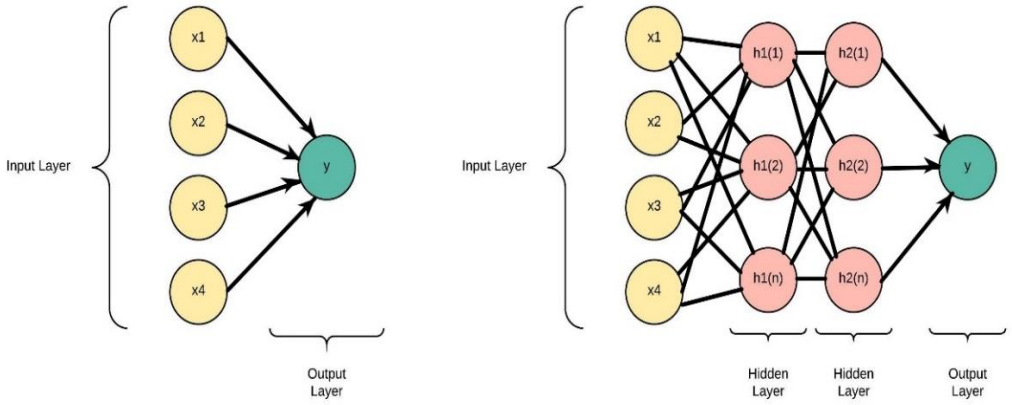

Figure 3: Multilayer Perceptron

Experimental Setup

In this section, all URL features used in the phishing dataset have been listed. In addition, each feature is also described in brief. Lastly, the preliminary setup and the testing metric of the experiments have been defined.

Dataset Description

The phishing dataset used in this research work is acquired from UCI Machine Learning Repository [19]. This dataset contains 11055 numbers of instances and 30 features. Features and their description is shown in the table given below.

Table 4.1: Dataset Features

Sr.no.	Features of Dataset 1	Description

1	Using the IP Address	If the Domain Part has an IP Address then it is a Phishing URL
2	Long URL to Hide the Suspicious Part	URLs having lengths equals to 54 or more are Phishing URLs
3	Using URL Shortening Services “Tiny URL”	URLs considerably smaller and able to redirect are phishing URLs
4	URL’s having “@” Symbol	@ leads the browser to ignore preceeding letters therefore URL with @ is phishing
5	Redirecting using “//”	URLs redirecting using symbol “//” are phishing URLs
6	Adding Prefix or Suffix Separated by (-) to the Domain	URLs using symbol “-” to look like legitimate URLs are phishing URLs
7	Sub Domain and Multi Sub Domains	URLs having more than 2 dots are phishing URLs
8	HTTPS (Hyper Text Transfer Protocol with Secure Sockets Layer)	URLs using HTTPS are legitimate URLs
9	Domain Registration Length	If domain expiration time is less than 1 year then given URL is Phishing
10	Favicon	Usage of graphic image on a domain to redirect is phishing
11	Using Non-Standard Port	If the port is of the preffered status then the given URL is phishing
12	The Existence of “HTTPS” Token in the Domain Part of the URL	URLs having HTTPS in tht domain part are phishing URLs
13	Request URL	Domain with more than 22% request URLs is phishing
14	URL of Anchor	Domain with the use of anchor tag more than 31% is suspicious and phishing
15	Links in <Meta>, <Script> and <Link> tags	Links in <Meta>, <Script> and <Link> tags more than 17% is suspicious and phishing
16	Server Form Handler (SFH)	SFHs with empty string or blank is phishing and different domain name is suspicious
17	Submitting Information to Email	Use of mail() or mailto functions is phishing
18	Abnormal URL	If host name is not the part of URL the it is Phishing URL
19	Website Forwarding	More than 2 times redirection of a page is phishing
20	Status Bar Customization	If onMouseOver() function changes status then it is phishing
21	Disabling Right Click	If right click is disabled the it is phishing
22	Using Pop-up Window	Pop-up windows with text field is phishing
23	IFrame Redirection	Usage of Iframe is phishing
24	Age of Domain	Age of domain less than 6 months is Phishing

25	DNS Record	If no DNS record for the domain then it is phishing
26	Website Traffic	Website rank greater than 100000 is suspicious and phishing
27	PageRank	Page rank less than 0.2 is phishing
28	Google Index	If webpage is indexed by Google then the given URL is legitimate URL
29	Number of Links Pointing to Page	If the number of links pointing to the given URL is zero then it is phishing
30	Statistical-Reports Based Feature	If URL belongs to the top Phishing URLs list (PhishTank, StopBadware) then it is phishing

System Configuration and Testing Metric

The experiments to test the results are performed in the google colab environment using python programming language. The system used to create this environment has the following specifications: Windows OS, Intel I7-6500U CPU processor, and 8GB of RAM. The evaluation was conducted using kf old cross-validation. K-fold cross-validation divides the input data into k wherein k – 1 dataset(s) are used for training and the remaining one is used for validation. This process is performed k times such as, the number in the divided dataset because all datasets can be used for training and validation [7]. This work performs 10-fold cross-validation.

Result and Discussion

The analysis of the performance of the machine learning algorithm is based on the accuracy of each algorithm, the time it takes to execute, and the ROC (Receiver Operating Charecteristic) curve. Accuracy is the measurement of correctly classified instances. Time is the total time taken by the algorithm to execute training and testing the dataset and calculate the accuracy. ROC curve is significant to visualize the performance of the models graphically.

Table 5.1: Accuracy and Time

Sr. no.	**Algorithm**	**Accuracy (%)**	**Time(s)**
1.	Random Forest	97.2016	7.0900
2.	Decision Tree	96.4054	0.8337
3.	Naïve Bayes	60.1492	0.6671
4.	K-Nearest Neighbor (k=1)	95.3321	18.2981
5.	Multilayer Perceptron	93.5472	49.6787

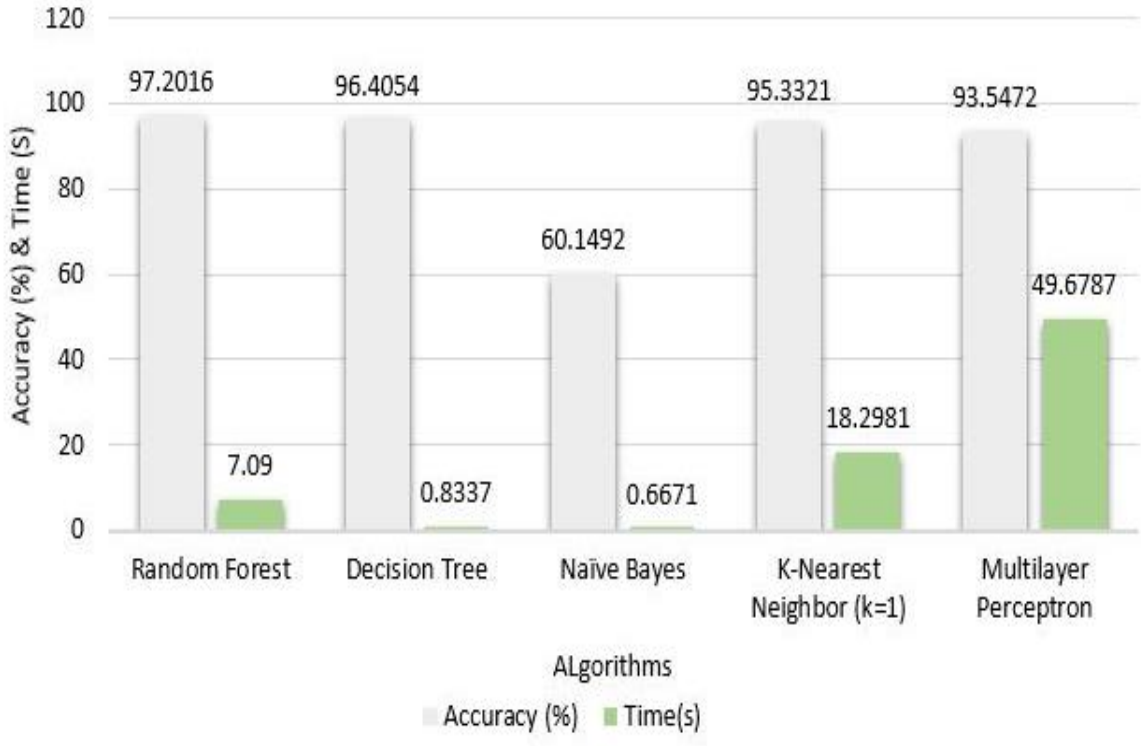

Figure 4: Accuracy and Time Analysis

Table 5.1 shows the accuracy and time results of each algorithm used in the proposed work. Figure 4 shows the performance comparison of the algorithms based on the accuracy and time of the classifiers. Among the algorithms used, random forest has the highest accuracy of 97.20% in around seven seconds of execution time. Decision tree algorithm also performs well with second highest accuracy of 96.40% and execution time less than that of random forest. Random forest performs more accurately due to its ability to select observations for all its decision trees and averaging the same. Naïve bayes takes the lowest amount of execution time but with the lowest accuracy rate. K-nearest neighbor algorithm

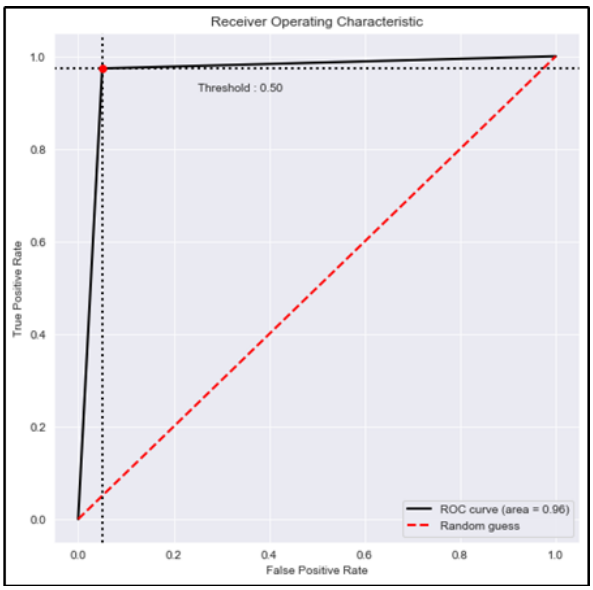

Figure 5: ROC Curve for Random Forest

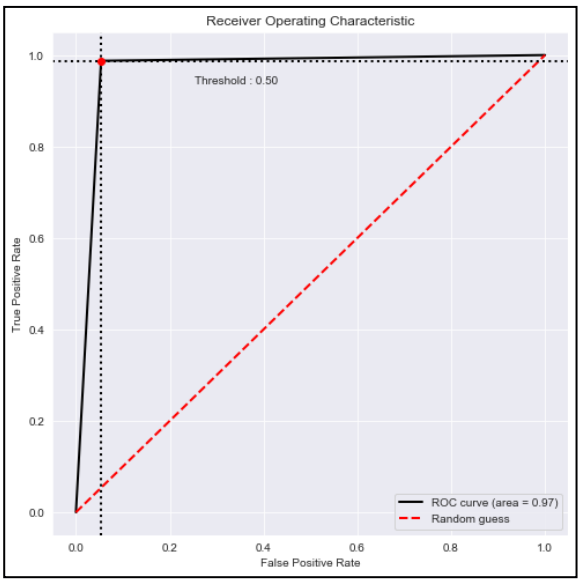

Figure 6: ROC Curve for Decision Tree

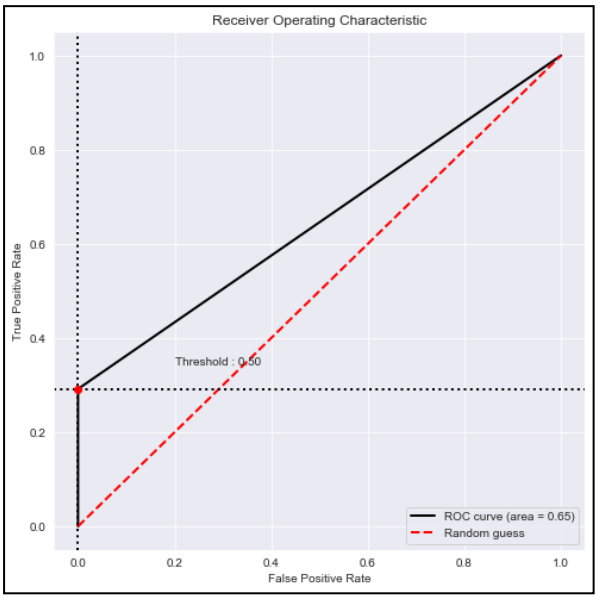

Figure 7: ROC Curve for Naïve Bayes

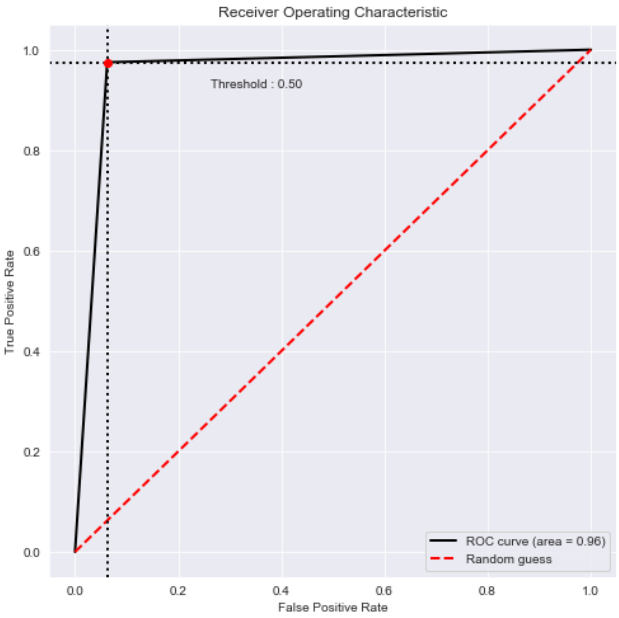

Figure 8: ROC Curve for KNN

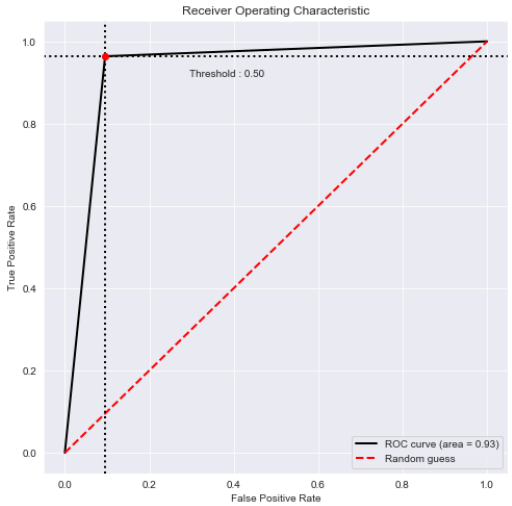

Figure 9: ROC Curve for Multi Layer Perceptron

was tested with the values of k as 1,3,5,7,9 and 11 out of which result in k=1outperformed other values with accuracy more than 95%.

Moreover, multilayer perceptron has the highest execution time concerning all its counterparts. MLP takes more time due to the number of features and the number of hidden layers used to train the algorithm. However, the use of a more powerful system can reduce the execution or training time of multilayer perceptron.

ROC (Receiver Operating Characteristics) curve is one of the most important metrics to evaluate the performance of any classification model. Figures 5-9 show ROC curves of each classification model used in this research. The ROC curve is a graph to plot TPR (True Positive Rate) vs. FPR (False Positive Rate) for a binary classification model. TPR in our case is the probability of the result as phishing given that the true state is phishing. A figure 5 show that the area under the ROC curves i.e. AUC (area under the curve) for the random forest classifier is 0.97 which is the highest among all the classifiers. This shows that random forest is more capable to separate the classes with low false positive rate. Moreover, it is closely followed by k- nearest neighbor and decision tree classifiers.

Therefore, assessing all the classifiers based on three metrics namely, accuracy, time, and AUC/ROC; random forest detects phishing more accurately.

Conclusion

In this research work, the proposed model is designed to detect phishing URLs to secure the system from a phishing attack. Among the five algorithms used in the proposed work, random forest performs the best with the accuracy of 97.20%. However, its execution time is not the best. Naïve bayes has the lowest execution time compared to all other algorithms. The system

can be furthermore enhanced by using pre-processing methods like feature selection and classification methods like ensemble algorithm.

References

"A guide to machine learning algorithms and their applications", https://www.sas.com/en_gb/insights/articles/analytics/machine-learningalgorithms.html\.

Ankit Kumar Jain, B. B. Gupta, "A machine learning based approach for phishing detection using hyperlinks information", Journal of Ambient Intelligence and Humanized Computing, Springer, pp. 2015-2028, 2018.

Ankit Kumar Jain, B. B. Gupta, PHISH-SAFE: URL Features-Based Phishing Detection System Using Machine Learning, Cyber Security, pp 467-474, 2018.

AOL Acts to Thwart Hackers. https://simson.net/clips/1995/95.SJMN.AOL_Hackers.html.
EarthLink wins $25 million lawsuit against junk e-mailer. https://www.bizjournals.com/atlanta/stories/2002/07/22/story4.html?page=all.

Ebubekir Buber, BanuDiri, and OzgurKoraySahingoz, "NLP Based Phishing Attack Detection from URLs", Springer International Publishing AG, vol. 736, pp. 608-618, 2018.

Jin-Lee Lee, Dong-Hyun Kim, Chang-Hoon, Lee, "Heuristic-based Approach for Phishing Site Detection Using URL Features", CEET, pp. 131-135, 2015.

Kiyoung Yang, Cyrus Shahabi, "An efficient k nearest neighbor search for multivariate time series", Information and Computation, Elsevier, pp. 65-98, 2007.

K Nearest Neighbors – Classification, https://www.saedsayad.com/k_nearest_neighbors.htm.

Must-Know Phishing Statistics, the Barkly Team.https://blog.barkly.com/phishing-statistics-2018.

Naïve Bayesian, https://www.saedsayad.com/naive_bayesian.htm.

Perceptrons and Multi-Layer Perceptrons: The Artificial Neuron at the Core of Deep Learning, https://missinglink.ai/guides/neural-network-concepts/perceptrons-and-multi-layer-perceptrons-the-artificial-neuron-at-the-core-of-deep-learning/

Phishing Techniques, http://www.phishing.org/phishing-techniques.

"Phishing Websites Data Set", https://archive.ics.uci.edu/ml/datasets/phishing+websites.

Routhu Srinivasa Rao, Alwyn R Pais, "Detecting Phishing Websites using Automation of Human Behavior", CPSS, pp. 33-42, 2017.

Santhana Lakshmi V, Vijaya MS, “Efficient prediction of phishing websites using supervised learning algorithms”, SciVerseScienceDirect, Elsevier, pp. 798-805, 2012.

Scam report from January 2018 - March 2020, http://www.millersmiles.co.uk/archives.php.

Naive Bayes for Text Classification”, Advanced in Control Engineeringand Information Science, Elsevier, pp. 2160 – 2164, 2011.

Yanping Li ; Wenming Cao, “An Extended Multilayer Perceptron Model Using Reduced Geometric Algebra”, IEEE Access, pp. 129815 – 129823, 2019.

BRIEF OVERVIEW ON DESIGN AND IMPLEMENTATION OF AUTONOMOUS CHESS PLAYING ROBOT

Sachin Sharma
Department of Engineering and Physical Sciences, Institute of Advanced Research, Gandhinagar, India

*Corresponding Author, E-mail: sachin.sharma@iar.ac.in

ABSTRACT:

This paper presents the design and construction of automatic chess playing robot built on artificial intelligence techniques. Magnetic gripper was designed using software solid works. The actual gripper mechanism works by activating an electromagnet at the bottom of a vertically moving beam. Each chess piece has a small metal dowel fitted in a drilled hole on the top. For the actual prototype, laser-cut wooden Legos was used. Detection of the corners of the squares on a chessboard and for image segmentation, a vision system based on Artifical intelligence was made. For detecting the movements of pieces on the board, an image recognition model was trained using convolutional neural networks. In order to locate the manipulator, image-based visual serving system was designed. Experimental results show that the system was able to make game decisions and manipulate the pieces on the board.

Keywords: Artifical Intelligence (AI), Raspberry Pi, Robotic Arm, Image Processing, Camera, OpenCV

INTRODUCTION AND LITERATURE SURVEY:

The first machine to play chess was built in 1769 by Wolfgang von Kempelen and was known as “The Turk” [1]. Apparently, the machine could play chess against a human opponent, but it was actually operated by a chess master. For many years, researchers in the area of artificial intelligence have been working on algorithms to play chess autonomously. Alan Turing and David Champernowne were the first to develop a program capable of playing a full chess game [2], known as “Turing’s paper machine” [3] [4]. Because at the time there were no computers capable of executing the instructions, it was Turing himself who performed the processing tasks using paper and pencil. It was not until 1996 that a fully functional computer program, IBM’s Deep Blue, was able to defeat the world champion Gary Kasparov [5]. Since then, many chess engines have been developed, and simultaneously it has become easier to develop mechanical robots [6] [7]. The chess game is an excellent application that works as a test bed for the

implementation of autonomous robotic systems, as it requires solutions for perception, manipulation, and human–robot interactions for a well-structured problem [8-12]. Several alternatives have been used for the perception of game state in different implementations of autonomous chess systems.

In [13,14], the authors focused on differentiating specific chess pieces, but the high levels of precision required by reliable autonomous systems were not achieved. Most practical implementations address this problem by detecting the movements of the pieces and tracking them from their initial position, assuming that the initial configuration of the board is correct. In [15,16], the researchers used on-board magnetic sensors to detect the movement of the pieces, and a fixed position for the board relative to the robot in order to ease the manipulation. Other works used 2D and depth cameras to follow the development of the game [20-24], while in the investigation carried out in [25], depth cameras were used to detect the occupancy of the board squares and compare the current state with the previous states. In this work, a single 2D fisheye camera mounted on the arm grip was used for all perception tasks. All the above literature survey information's are mentioned in [26] also.

MOTIVATION:

Chess being one of the most popular games in the world, development of chess playing programme and machines has been a challenge of great interest to engineers since decades. Even though excellent chess playing programs have been designed which can easily beat grandmasters under normal conditions, autonomous robots playing chess on real life chess boards are still hard to find. Our aim is to implement a robotic arm that can play chess with humans on a normal chess board just as humans do. Most chess playing robots that currently exist use sensory chess boards to decipher the moves of the players and separate chess engines to generate further moves. We wish to design a robot that can identify the moves by processing images captured through a camera, thus creating a machine that could play chess on any normal chess board without additional requirements.

I. SOFTWARE REQUIREMENTS:

- Python IDE
- OpenCV

II. HARDWARE REQUIREMENTS:

- Raspberry Pi 4

- Camera
- Servo Motors
- Materials to Build Robotic arm
- Chess Board with Magnetic Head on pieces
- Magnetic Gripper Arm
- Motor Driver
- 5 V Charger
- SD Card

III. BLOCK DIAGRAM OF THE PROPOSED SYSTEM AND METHODOLOGY:

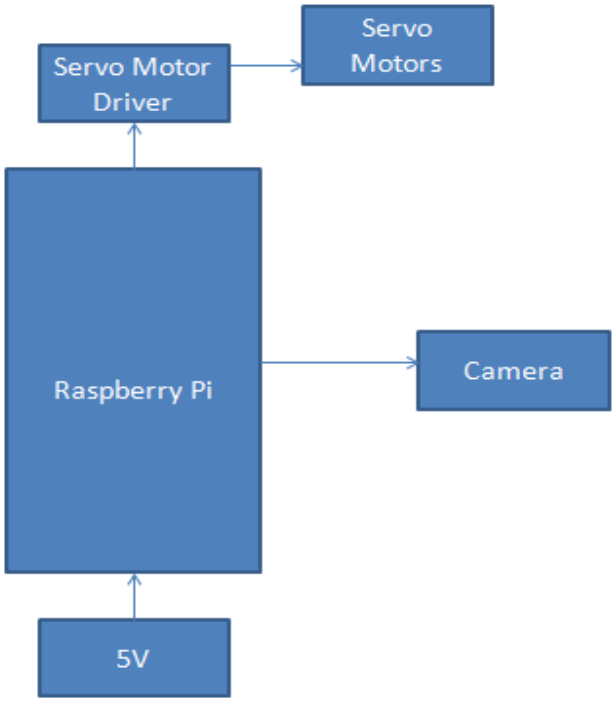

Figure 1: Block diagram of the proposed system

Vision of Project:

Figure 1 shows the block diagram. The AutoPlay Raspberry Chess Board uses computer vision to recognize where the chess pieces are on the board before deciding what move to make. The robot sees through a Raspberry Pi camera module attached with an HDMI cable to a fixture directly above the chessboard. The camera is controlled via Python OpenCV running on the

Raspberry Pi. The raw image is converted to a 480x480px image by warping the perspective so the chessboard squares are equal size and the non-chessboard part of the image is cropped.
In order to understand the state of the game we would have to use image processing to analyze which slot is empty and which is not. And to understand which coin it is we use color classification. Green and orange colors are used and to understand which is the piece we track our pieces from initial point. Figure 2 shows image processing steps for recognizing the piece

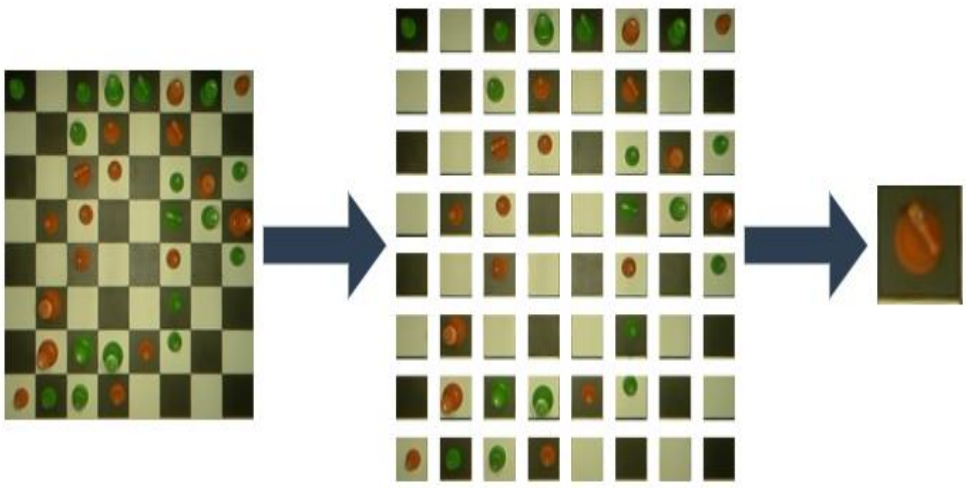

Figure 2: Image Processing steps for recognizing the piece

ARM:

The arm is primarily made out of Actobotics components. It is a Selective Compliance Articulated Robot Arm (SCARA) which means that it can move freely in the XY-axes remaining fixed in the Z-axis. The motion is controlled by the rotation of two servos which are attached to gears at the base of each link of the arm. At the end of the arm is another servo which moves a beam up and down. At the bottom of the beam is an electromagnet that can be dynamically activated to lift the chess pieces. The base of the arm is fixed to the table-top box.

ACTUAL PROTOTYPE:

For the prototype, laser-cut wooden Legos was used. The base that is attached to the table is gear drive pan kit which is engineered by 3D printed parts. A 16.5-inch Lego arm is attached on top of the gear drive pan kit. A rotating gear is attached at the end of this arm along with another servo that rotates this gear. Another 16.5-inch arm is attached on the top of this gear and at the end of this arm is a gear rack kit (also made with 3D printed parts) that controls the z-axis motion of the arm. Figure 3 shows the complete structure of it.

The actual gripper mechanism works by activating an electromagnet at the bottom of a vertically moving beam. Each chess piece has a small metal dowel fitted in a drilled hole on the top.

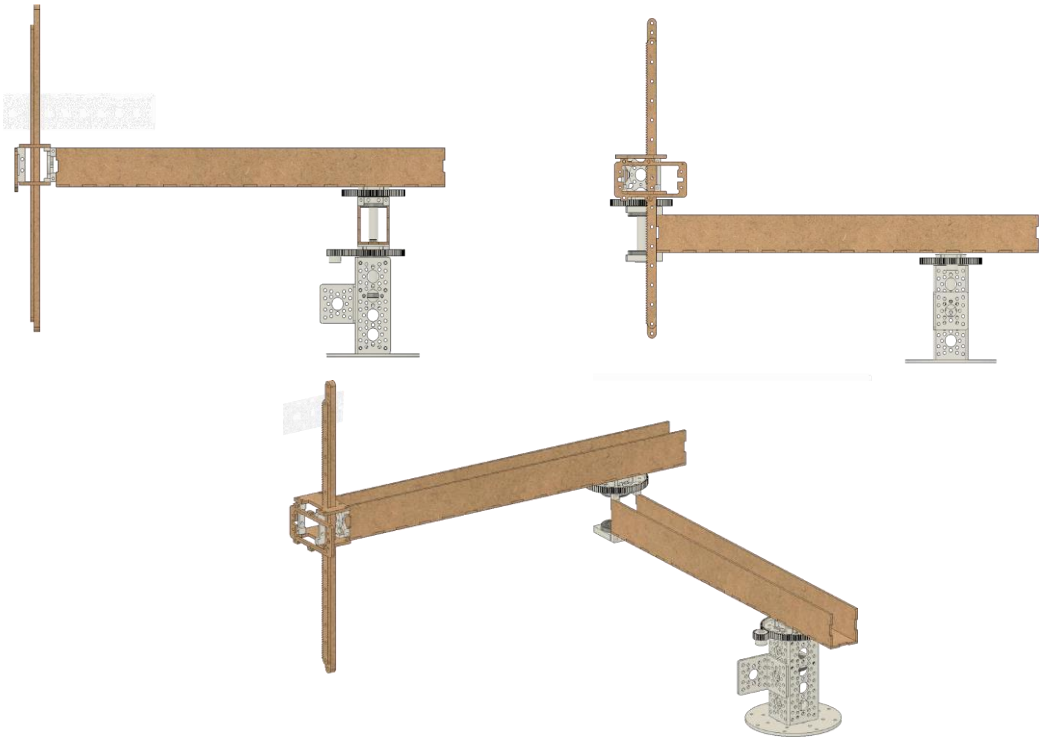

Figure 3: Arm structure

Servos and Control

We have used AX-12 Dynamixel Servos for the core motion of the arm as they're relatively powerful and have easy read/write to registers via serial interface. The servos are directly powered and controlled by an Arbotix-M Robocontroller but the actual commands comes from the Raspberry Pi. The components responsible for controlling the movement of the arms are:

1. Raspberry Pi
2. Arbotix-M Robocontroller
3. FTDI USB to Serial Cable
4. Dynamixel AX-12A Robot Actuator & Included 3 Pin Cable

The microcontroller of Arbotix-M Robocontroller is flashed with the the pypose sketch. Once the pypose sketch is installed on the microcontroller it will act as a pass through so the Raspberry Pi can communicate directly with the servo(s). The Raspberry Pi is connected to the Arbotix-M via the FTDI USB to serial cable.

Chess playing robot (using AI) is responsible for running an action sequence in a loop until it encounters an interrupt signal. Please find the steps mentioned below.

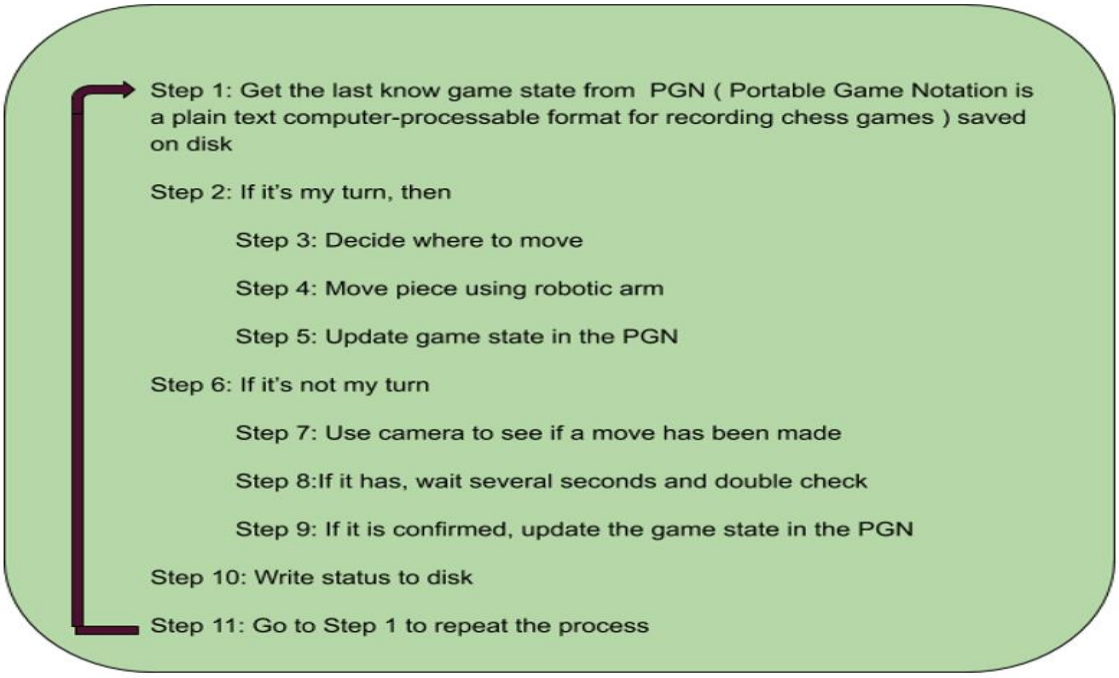

Figure 4 shows the CAD Drawing of Chess Playing Robot (Prototype).

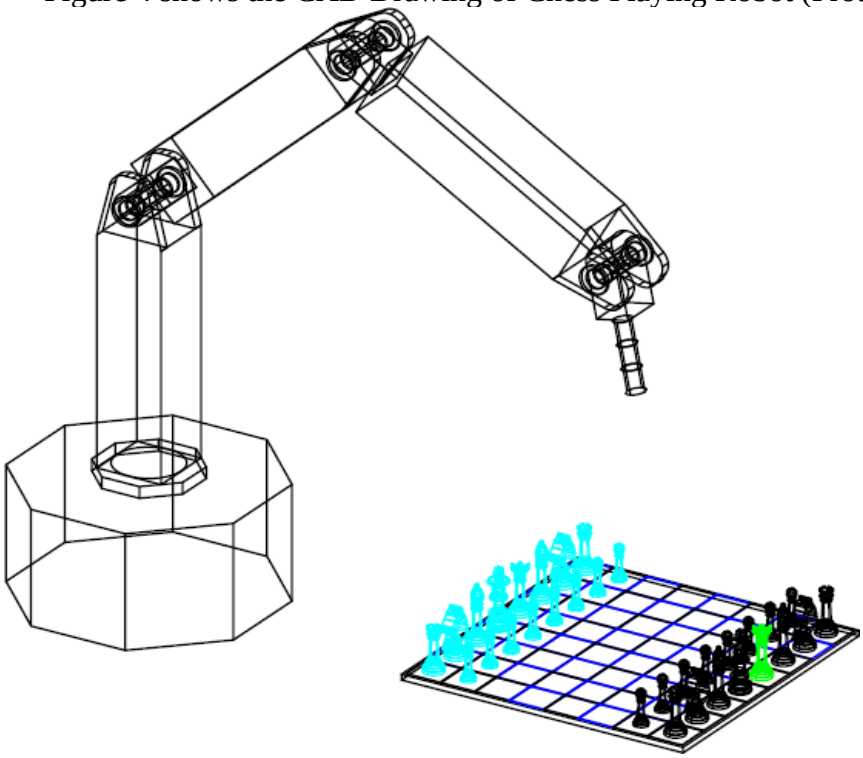

Figure 4: CAD drawing of chess playing Robot (Prototype)

CONCLUSION:

This paper gives an overview of the design and implementation of an autonomous chess playing robot, chess which was built from locally available, simple and low-cost material. The software part is constructed in a separate module so that it can be easily changed or upgraded. In future,

we intend to use a single board computer such as Raspberry Pi inside the mechatronic system to make our proposed robot more user-friendly and robust. This will eliminate the use of a personal computer to run the chess program and make it an independent gaming console. We also intend to include voice recognition system to provide user moves so that disabled persons can also be benefited from our system.

ACKNOWLEDGEMENTS:

Author would like to acknowledge Zaid Kesarani, Gautam Bhattathiri, Raghav Joshi, Siddhant Pandey (4TH Semester B. Tech students, Institute of Advanced Research, Gandhinagar) for the preparation of 3D arm structure.

REFERENCES:

1. Kovacs, G.; Petunin, A.; Ivanko, J.; Yusupova, N. From the First Chess-Automaton to the Mars Pathfinder. Acta Polytech. Hung. 2016, 13, 61–81.

2. Crandall, J.W.; Oudah, M.; Tennom; Ishowo-Oloko, F.; Abdallah, S.; Bonnefon, J.F.; Cebrian, M.; Shariff, A.; Goodrich, M.A.; Rahwan, I. Cooperating with machines. Nat. Commun. 2018, 9, 233. [CrossRef] [PubMed].

3. Kasparov, G.; Friedel, F. Reconstructing Turing's "paper machine". Preprint at https://easychair.org/publications/preprint/WjKW.

4. Van den Herik, H.J. Computer chess: From idea to DeepMind. ICGA J. 2018, 40, 160–176. [CrossRef]

5. Chakraborty, S.; Bhojwani, R. Artificial intelligence and human rights: Are they convergent or parallel to each other? Novum Jus 2018, 12, 13–38. [CrossRef]

6. Castellano, G.; Leite, I.; Paiva, A. Detecting perceived quality of interaction with a robot using contextual features. Auton. Robot. 2017, 41, 1245–1261. [CrossRef]

7. Dehghani, H.; Babamir, S.M. A GA based method for search-space reduction of chess game-tree. Appl. Intell. 2017, 47, 752–768. [CrossRef]

8. Huang, M.-B.; Huang, H.-P. Innovative human-like dual robotic hand mechatronic design and its chess-playing experiment. IEEE Access 2019, 7, 7872–7888. [CrossRef]

9. Lukaˇc, D. Playing chess with the assistance of an industrial robot. In Proceedings of the 3rd International Conference on Control and Robotics Engineering, Nagoya, Japan, 20–23 April 2018; pp. 1–5. [CrossRef]

10. Anh, N.D.; Nhat, L.T.; Van Phan Nhan, T. Design and control automatic chess-playing robot arm. Lect. Notes Electr. Eng. 2016, 371, 485–496. [CrossRef]

11. Wei, Y.-A.; Huang, T.-W.; Chen, H.-T.; Liu, J. Chess recognition from a single depth image. In Proceedings of the IEEE International Conference on Multimedia and Expo, Hong Kong, China, 10–14 July 2017; pp. 931–936. [CrossRef]
12. Larregay, G.; Pinna, F.; Avila, L.; Moran, D. Design and Implementation of a Computer Vision System for an Autonomous Chess-Playing Robot. J. Comput. Sci. Technol. 2018, 18, 1–11. [CrossRef]
13. Xie, Y.; Tang, G.; Hoff, W. Chess Piece Recognition Using Oriented Chamfer Matching with a Comparison to CNN. In Proceedings of the IEEE Winter Conference on Applications of Computer Vision, Lake Tahoe, NV, USA, 12–15 March 2018; pp. 2001–2009. [CrossRef]
14. Czyzewski, M.A.; Laskowski, A.; Wasik, S. Chessboard and chess piece recognition with the support of neural networks. Comput. Vis. Image Underst. 2018, 2, 1–11.
15. Al-Saedi, F.A.T.; Mohammed, A.H. Design and Implementation of Chess-Playing Robotic System. IJCSET 2015, 5, 90–98.
16. Mahmood, N.H.; Long, C.K.M.S.C.K. Smart Electronic Chess Board Using Reed Switch. J. Teknol. 2011, 55, 41–52. [CrossRef]
17. Larregay, G.; Avila, L.; Moran, O. A comparison of classification algorithms for chess pieces detection. In Proceedings of the 17th Workshop on Information Processing and Control, Mar del Plata, Argentina, 20–22 October 2017; pp. 1–5. [CrossRef]
18. Ómarsdóttir, F.Y.; Ólafsson, R.B.; Foley, J.T. The Axiomatic Design of Chessmate: A Chess-playing Robot. Procedia CIRP 2016, 53, 231–236. [CrossRef]
19. Pachtrachai, K.; Vasconcelos, F.; Dwyer, G.; Pawar, V.; Hailes, S.; Stoyanov, D. CHESS-Calibrating the Hand-Eye Matrix with Screw Constraints and Synchronization. IEEE Robot. Autom. Lett. 2018, 3, 2000–2007. [CrossRef]
20. Luqman, H.M.; Zaffar, M. Chess Brain and Autonomous Chess Playing Robotic System. In Proceedings of the International Conference on Autonomous Robot Systems and Competitions, Braganca, Portugal, 4–6 May 2016; pp. 211–216. [CrossRef]
21. Wang, X.; Chen, Q. Vision-based entity Chinese chess playing robot design and realization. In International Conference on Intelligent Robotics and Applications; Springer: Cham, Switzerland, 2015; Volume 9246, pp. 341–351. [CrossRef]
22. Chen, B.; Xiong, C.; Zhang, Q. CCDN: Checkerboard corner detection network for robust camera calibration. In International Conference on Intelligent Robotics and Applications; Springer: Cham, Switzerland, 2018; Volume 10985, pp. 324–334. [CrossRef]
23. Kumar, R.V.Y. Target following Camera System Based on Real Time Recognition and Tracking. Master's Thesis, National Institute of Technology, Rourkela, India, May 2014.

24. Bennett, S.; Lasenby, J. Chess-Quick and robust detection of chess-board features. Comput. Vis. Image Underst. 2014, 118, 197–210. [CrossRef]
25. Matuszek, C.; Mayton, B.; Aimi, R.; Deisenroth, M.P.; Bo, L.; Chu, R.; Kung, M.; Le Grand, L.; Smith, J.R.; Fox, D. Gambit: An autonomous chess-playing robotic system. In Proceedings of the IEEE International Conference on Robotics and Automation, Seattle, WA, USA, 9–13 May 2011; pp. 4291–4297. [CrossRef]
26. Cristian, T.; Carlos,R.; Omar,R. Design and Construction of a Cost-Effective Didactic Robotic Arm for Playing Chess, Using an Artificial Vision System. Electronics 2019, 8, 1154; doi:10.3390/electronics8101154

STUDY ON THE REPERCUSSIONS OF COMMON EFFLUENT TREATMENT PLANT TOWARDS MSMES

Radha Tiwari, Vatsal Chandegara, Himanshu Thakkar

Department of Business Management, Institute of Advanced Research Gandhinagar-382426
*Corresponding Author, E-mail: radha.tiwari@iar.ac.in

Abstract

Water intensive manufacturing enterprises implicates a specific modality of human-nature relations, in which resources are "extracted" from nature to meet the demands of humans and the effluents (wastewater) and wastes produced in this process are ‘dumped’ back into nature (sea, river, lake). For two decades, the common effluent treatment plant has become a silver lining in the cloud for water-intensive units of MSMEs as it comes with benefits of reducing effluent treatment costs, providing better collective treatment, and reducing land cost for small-scale industrial facilities that cannot afford individual treatment plants. CETP is considered a suitable inter- medium between MSMEs and water bodies to mitigate wastewater pollution. This paper strives to explore the pragmatic repercussions of CETP on MSMEs by the study of six CETP in operation at Ahmedabad industrial clusters. The effluents (wastewater drained out from CETP) data is analyzed to find the compliance pattern of CETPs with respect to standard norms and the legal action faced by MSMEs is studied to explore the possible pragmatic repercussions of this technology on MSMEs.

***Keywords*:** common effluent treatment plant, environment, effluent, micro small, medium enterprises

Introduction

India has progressed towards modernization and increased financial liberalization post economic reforms initiated in 1991. Modernizing development flourished the demands of goods across all industrial sectors. Economic reforms and modernizing development supported MSMEs (Micro, Small & Medium Enterprises) growth in India.Modernizing development flourished the demands of goods across all industrial sectors. This ‘modernizing’ implicates a specific modality of human-nature relations, in which resources are extracted from nature to

meet the demands of humans, and the effluents and wastes produced in this process are dumped into the nature. Modernizing development thus extracts what it believes to be ‘good’ from nature and dumps the ‘bad’ it produces back into nature, effectively treating the earth as a giant sewer (Arora *et al*., 2019).

Various industries in MSMEs are water-intensive following extract dump modality by extracting water from water bodies (seas, rivers, lakes) for daily operations and dumping the generated wastewater (effluents) back to the water bodies. To control the exploitation of water bodies from effluents, CPCB (Central Pollution Control Board) put forth standard norms wherein the treated effluents were to be achieved by individual industrial units before dumping it into water bodies. MSMEs struggled to meet these standard norms through their home effluent treatment plant due to high treatment costs. Water bodies created a great loss in ecology by receiving partly treated effluents from the MSMEs cluster for a brief period.

Ahmedabad lies in the western part of India on the banks of the river Sabarmati in north-central Gujarat. Owing to the rich resources and easy availability of water from the Sabarmati River, water intensive industrial units found an economic place for its operations. Ahmedabad was known as the "Manchester of the East" for its textile industry. The textile industry further expanded rapidly during the First World War and benefited from the influence of Mahatma Gandhi's Swadeshi Movement which promoted the purchase of Indian goods (Get Forx Information, 2010).

The textile industry gave rise to dependent goods producing industries ranging from dyestuff and chemicals to industrial solvent MSMEs. Currently, Ahmedabad has over four major industrial clusters namely Naroda, Odhav, Vatva, and Narol on the eastern periphery of the city. These clusters are houses of more than 1500 MSMEs ranging from textiles, dyestuffs, solvents, chemicals, engineering, pharmaceuticals, and petroleum. Majority of the units in these clusters are water-intensive following extract dump modality. CETP (Common Effluent Treatment Plant) seemed to be a silver lining in the cloud for fixing the mismanagement of effluent treatment. CETP comes with the benefits of reducing effluent treatment costs providing, better collective treatment and reducing land cost for small-scale industrial facilities that cannot afford individual treatment plants (Padalkar & Kumar, 2018). CETP are designed to treat effluents for meeting the standards norms for pH, suspended solids (SS), oil and grease, chemical oxygen

demand [1](COD), and biological oxygen demand [2](BOD). In nutshell, CETP shifts the onus of achieving a cleaner environment on its member industrial units who run the CETP. To promote the CETP adaptability, GOI (Government of India) rolled out various subsidies and benefits for industrial clusters. By the end of the year 2019, numerous CETPs were installed and came in operation across various industrial clusters in India. CETP was suited as a dominant pathway for the sustainable development of MSMEs as well as in achieving environmental goals.

Ahmedabad's industrial region houses more than six CETP. This study strives to explore possible repercussions of CETP on MSMEs by studying the compliance pattern followed by the CETP with respect to the standard norms.

COD and BOD are important parameters to find the compliance of effluents drained out from CETP. Pollutant chemical oxygen demand is a measure of water and wastewater quality while biological oxygen demand is a measure of the amount of oxygen that is required by the bacteria to degrade the organic components present in water / waste water (Baboo, 2016). The CETP understudy dumps the treated effluent collectively through Ahmedabad mega pipeline into the Sabarmati River. The treated effluents with higher volume and with pollutants like COD and BOD merge with the river and flow towards the Gulf of Khambhat where the residents of dozens of villages use the river water for irrigation and agriculture practices. (Figure 1)

Table (1) CETP under study

Sr no	Acronym	CETP	Hydraulic Capacity (MLD)	No. of Members (March 2016)	Scale of industry
1	NEPL	Naroda Enviro Projects Ltd	3	255	Medium and small
2	OGEA	Odhav Green Enviro Project	1	2	Medium and small
3	OEPL	Odhav Enviro Project Ltd	1.6	56	
4	GVMMSUV	Gujarat VepariMaha Mandal	1	264	
5	GESCOS	The Green Environment Services	16	673	Medium and small
6	NDES	Narol Dyestuff Enviro Society	0.1	20	Medium and small

[1]COD: Chemical Oxygen Demand is the total measurement of all chemicals (organics & in-organics) in the water / waste water. The chemical oxygen demand is a measure of water and wastewater quality. High level of COD in wastewater indicates higher risk to water bodies.

[2]BOD: Biological oxygen demand is a measure of the amount of oxygen that require for the bacteria to degrade the organic components present in water / waste water.Large quantities of organic matter (microbes and decaying organic waste) in water are a potential risk to aquatic ecosystems and human health. The reduction in the amount of dissolved oxygen as a result of the decomposition of organic matter can endanger aquatic life through asphyxiation and disrupt the ecological balance of the water. Organic matter can also pollute drinking water and bathing water. High levels of BOD can indicate such organic pollution.

Figure (1) CETP location with existing wastewater management infrastructure

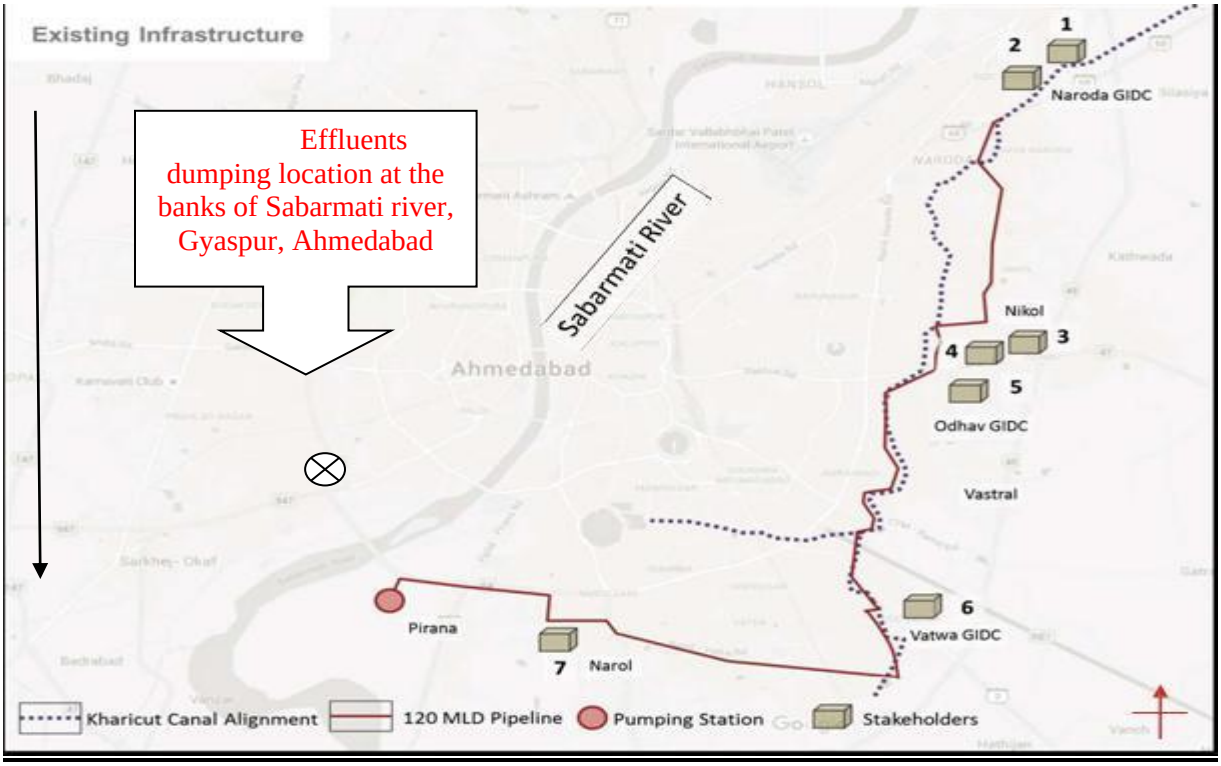

Objective

To explore the repercussions of CETP technology on MSMEs

Research Methodology

Secondary data of pollutants (COD, BOD) were collected from GPCB. The data contained the monthly average value of pollutants in the discharged effluents from CETP. Data comprises of 47 samples spread over a time period of 3 years i.e., from 2016-2019. The statistical tool frequency distribution is used to observe the compliance pattern of CETP with respect to standard norms by categorizing data into above standard norms and below standard norms. Pairing of two samples T-test is used to check whether the standard norms are met by the plants over the time period of study.

Figure (2) Frequency distribution of BOD pollutant

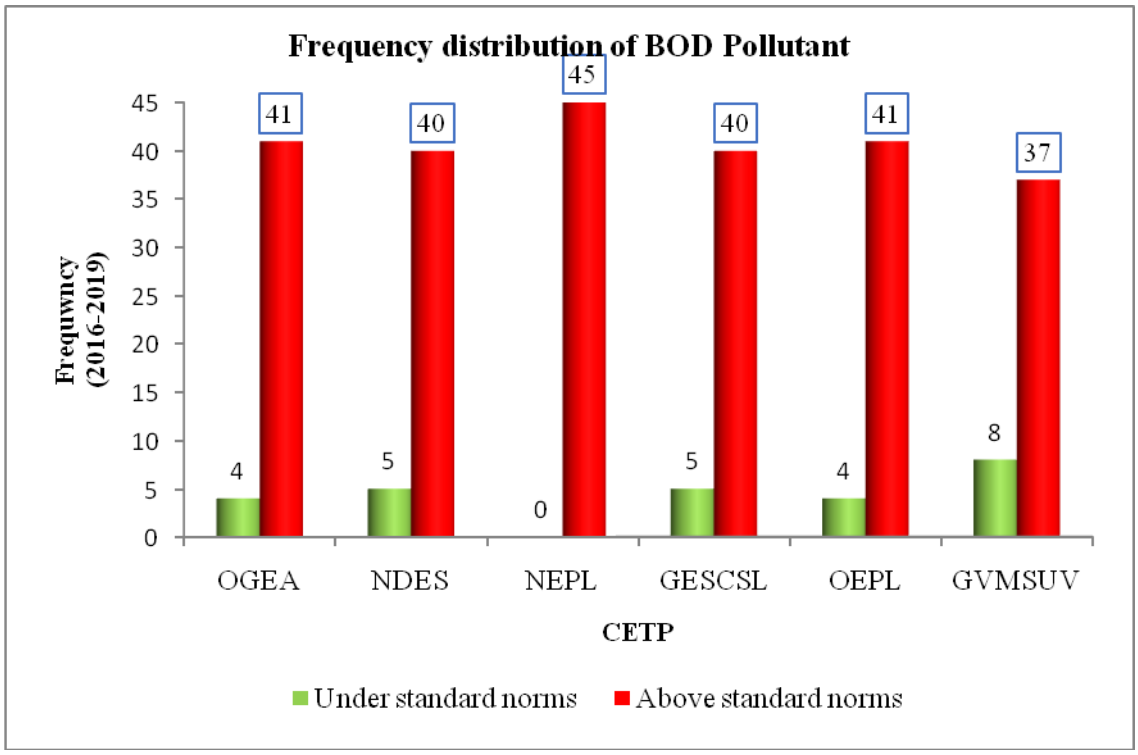

(Source: CETP results, Gujarat Pollution Control Board)

Figure (2) shows the compliance pattern followed by CETP for BOD pollutant in respect to standard norms with the help of frequency distribution. Biochemical oxygen demand (BOD) represents the amount of oxygen that microorganisms consume in the process of destroying organic wastes. The BOD value is expressed in milligram of oxygen consumed per liter (Mg/L). The higher the BOD, the lower is the amount of dissolved oxygen available for marine animals. To maintain oxygen level and to control the water pollution, the Central Pollution Control Board of India has set the BOD standard norms of 30 mg / L. The chart shows the scenario of BOD level. It is found that all CETPs are unable to meet the standard norms at a great extent. NEPL is the most violated CETP. It is unable to meet the standard norms even once in 45 months. The rest of the CETP – OGEA, NDES, GESCL, OEPL, and GVMSUV has followed the standard norms for 4, 5, 5, 4, and 8 months respectively, and violated the standard norms for 41, 40, 40, 41, and 37 months respectively.

Figure (3) Frequency distribution of COD pollutant

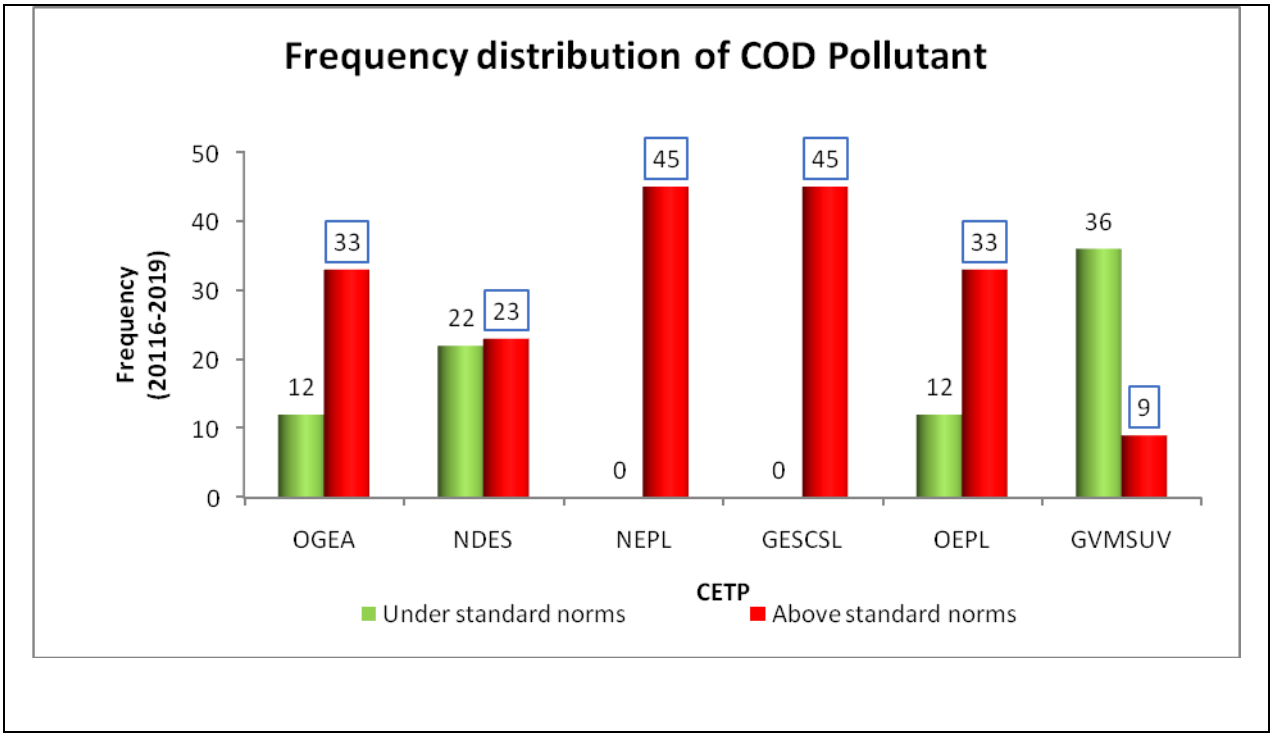

(Source: CETP Results, Gujarat Pollution Control Board)

Figure (3) shows the compliance pattern followed by CETP for COD pollutant with respect to standard norms with the help of frequency distribution. Chemical Oxygen Demand (COD) is a method of estimating oxygen required for the portion of organic matter in water waste that is subjected to oxidation and also the amount of oxygen depleted from organic matter receiving water as a result of bacterial action (Khan & Ali, 2018; Curran, 2006). In simple words, COD is a measure of all chemicals present in water or wastewater. The COD value is expressed in milligram of oxygen consumed per liter (mg/L) with standard norm of 250 mg / L. The chart shows the situation of COD level. It is found that all CETPs are unable to meet the standard norms at a great extent. NEPL and GESCL are the most violated CETP. They are not able to meet the standard norms even once in 45 months. The rest of the CETP – OGEA, NDES, OEPL, and GVMSUV has followed standard norms for 12, 22, 12, and 36 months respectively, and violated the standard norms for 33, 23, 33 and 9 months respectively.

Hypothesis Testing

H_0: There is no significant difference between COD standard and final effluent discharged by CETP.

Except GVMSUV, the significance P value is < 0.05. Hence, Ho was rejected and H1 was accepted. Hence, it is evident that pollutant COD is exceeding standard norms.

Table (2) Result of Paired samples T-test

COD						
CETP	OGEA	NDES	NEPL	GESCOS	OEPL	GVMSUV
T-stat value	3.634	3.071	3.071	7.884	4.602	1.526
P value	0	0.002	0.002	0	0	0.067
H0 (A/R)	R	R	R	R	R	A
A - Hypothesis accepted , R - Hypothesis Rejected						

BOD						
CETP	OGEA	NDES	NEPL	GESCOS	OEPL	GVMSUV
T-stat value	7.918	4.013	7.735	5.601	6.819	3.053
P value	0	0	0	0	0	0.002
H01 (A/R)	R	R	R	R	R	R
A - Hypothesis accepted , R - Hypothesis Rejected						

(Source: Computed by Author)

$H_0$1: There is no significant difference between BOD standard and final effluent discharged by CETP.

The significance P value of all CETPs is < 0.05. Hence, Ho was rejected and H1 was accepted. Therefore, it is evident that pollutant BOD is exceeding standard norms.

Table (2) shows the result of paired two sample t-test for pollutants COD and BOD. Hence pollutants COD and BOD are exceeding standard norms from 2016 to 2019.

According to a rigorous technical analysis by Padalkar & Kumar (2018) in their common effluent treatment plant (CETP), reliability analysis and performance evaluation manifest that major onus for decreased efficiency of CETP to treat the effluent as per the standard norms borne by member industrial units. CETP was found in overloaded conditions most of the time after receiving exceedingly high volumes of effluents and pollutant concentration than the designed capacity from industrial units.

The compliance pattern of individual CETP from 2016 to 2019 demonstrates the stress borne by member industrial units to fulfill the environmental goal of mitigating wastewater pollution while striving to meet the production demand.

Table 3 shows the range of BOD for the Sabarmati River (2007-2019) obtained from statistical analysis of time series data for various stretches (fig 4) of the river spread over Ahmedabad district. Biochemical oxygen demand (BOD) is the amount of dissolved oxygen used by microorganisms in the biological process (Naik, 2019). The health of a river and the efficiency of the water treatment are classified based on BOD. The greater the BOD, the lower is the amount of dissolved oxygen available for marine animals. The greater the BOD, the higher threat water bodies possess to the environment (ForumIAS, 2018).

Stretch no. 4 is the dumping location of effluents from CETP through Ahmedabad mega pipeline. The BOD level at this stretch fluctuates at an unprecedented level from standard norms of 3 mg/L. Further, the direction of the Sabarmati River is downstream towards the Gulf of Khambhat (Fig 1) wherein dozens of villages' residents use the river water for irrigation and agricultural practices. According to an assessment conducted by CPCB on Indian rivers during 2018, the BOD level of 4.0-147 mg/L was found in Sabarmati River, categorizing it in the priority of five rivers and declared it as the third most polluted river in India. (ForumIAS, 2018; Koshy, 2018).

Chronological study done by Mudrakartha & Sheth (2006) titled unclogging the Khari River: Stakeholders Come Together to Halt Pollution shows how the CETP came into action to mitigate water pollution of Khari River by industrial clusters of Ahmedabad and was considered to be the best possible solution for mitigating water pollution. It seems that the same situation is forming its roots for Sabarmati River in the present scenario inspite of having CETP as a knight in shining armor.

Table (3) Sabarmati River stretch with BOD range from 2007-2019

Sr No.	Sabarmati River stretch name	Range
1	Sabarmati River- Hansol Bridge	1.9 to 45
2	Sabarmati River- Railway Bridge	2 to 12
3	Sabarmati River- Vasana-Narol Bridge	40-117
4	Sabarmati River- V.N Bridge	2.2 to 210
5	Sabarmati River- Miroli	38 to 70
6	Sabarmati River- Vautha Village	27 to 49
7	Khari River-Lali	8 to 135

(Source: Annual Reports, Gujarat Pollution Control Board)

Figure (4) Pictorial representation of Sabarmati river stretches

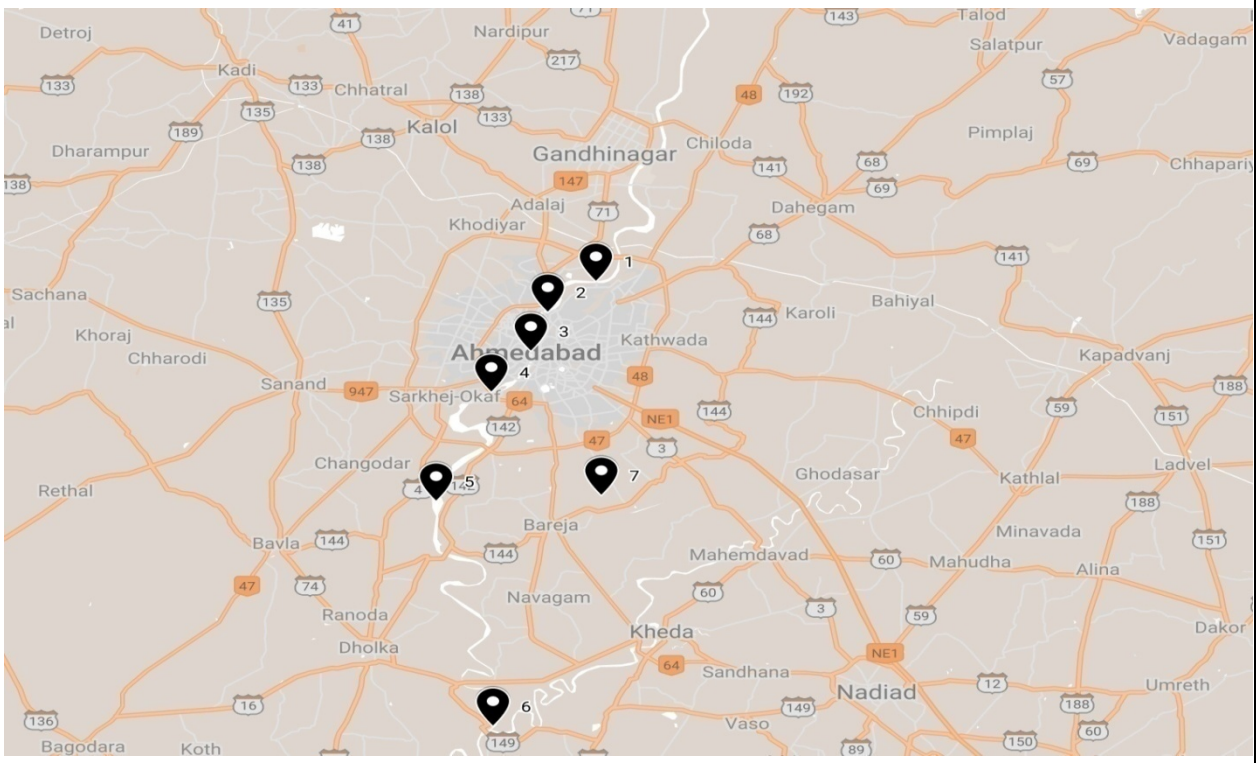

(Source: Google maps)

Table (4) Action taken by the Government against defaulting units under water Act 1974 in Gujarat

	Notice of directions issued under Section 33 A of the water act ,1974 to the defaulting units	Closure directions issued under Section 33 A of the water act ,1974 to the defaulting units
2008	7024	2673
2009	8543	3444
2010	9053	4048
2011	9053	4048
2012	9707	4603
2013	10413	5771
2014	11305	6952
2015	12265	7901
2016	13485	8875
2017	14763	9569
2018	15854	10356
2019	17263	11383

(Source: Yearly Annual Reports of GPCB from 2008-2019)

Table 4 shows the action taken by government against the defaulting units violating the law under water Act, 1974. Under this act, defaulting units failing to meet the standard norms faces stringent actions. The data shows an increase in the actions taken against defaulting unit from 2008-2009 which relates strongly with the study carried out for compliance pattern of CETPs. The action of industrial closure, fines, and class lawsuit has a negative effect on MSMEs in view of meeting production demands while meeting environmental laws.

Under a report submitted to the national green tribunal principal bench by GPCB in 2019, CETP at Narol operated by M/s Narol Textile Infrastructure and Enviro Management was found to be in the red category with non compliance to standard norms during 2017-2019. The CETP was not meeting the norms, causing pollution in the Sabarmati River. In view of the said report, the Tribunal directed recovery of compensation and reduction of pollution load by decreasing capacity of the units contributing to the pollution and to take further remedial steps. Under polluter pays principle, the following formula was adopted for environment compensation from units -

EC = PI x N x R x S x LF

Where,

EC- Environmental Compensation in Rupees

PI- Pollution Index of the Industrial Sector

N- Number of days the violation has taken place

R- Factor of EC in Rupees

S- Factor for the scale of operation of industrial unit

LF- Location Factor

Given this formula, GPCB estimated environment compensation of nearly Rs 3 corers from defaulting units at Ahmedabad industrial clusters for the non-compliance period 2017-2019. The report mentioned taking further stringent actions and limiting industrial unit outputs to reduce the load on CETP, if non-compliance kept on repeating. This came out as a huge financial blow to the MSMEs sector.

With the study of non-compliance pattern of major CETPs on which most of MSMEs relies for wastewater treatment and the comprehensive literature study of legal action faced by MSMEs, we boil down below possible pragmatic repercussions of CETP towards MSMEs:

1. Unwelcomed cost to MSMEs in the form of fines, temporary shutdown, and/or permanent shutdown

2. Unwelcomed effect on the agriculture sector depended on the Sabarmati river which may force high-class lawsuits and action on MSMEs

Conclusion

Common effluent treatment plants have become a dominant pathway for reducing effluent treatment costs, providing better collective treatment, and reducing land cost for MSMEs industrial clusters. The compliance pattern found the violation of standard norms by CETP at a great extent, while the t-test confirms these results for individual plants. Historical analysis of Sabarmati River stretches and the effluent dumping site shows the indication of a major problem to be faced by MSMEs in near future from environment protection laws. Though CETP was brought to control the water pollution, the study found CETP to be a major drawback. MSMEs are facing a major challenge to control water pollution while meeting the production demand for consumers due to a lack of innovation in effluent treatment technology and wastewater management.

References

1. Kovacs, G.; Petunin, A.; Ivanko, J.; Yusupova, N. From the First Chess-Automaton to the Mars Pathfinder. Acta Polytech. Hung. 2016, 13, 61–81.
2. Crandall, J.W.; Oudah, M.; Tennom; Ishowo-Oloko, F.; Abdallah, S.; Bonnefon, J.F.; Cebrian, M.; Shariff, A.; Goodrich, M.A.; Rahwan, I. Cooperating with machines. Nat. Commun. 2018, 9, 233. [CrossRef] [PubMed].
3. Kasparov, G.; Friedel, F. Reconstructing Turing's "paper machine". Preprint at https://easychair.org/publications/preprint/WjKW.
4. Van den Herik, H.J. Computer chess: From idea to DeepMind. ICGA J. 2018, 40, 160–176. [CrossRef]
5. Chakraborty, S.; Bhojwani, R. Artificial intelligence and human rights: Are they convergent or parallel to each other? Novum Jus 2018, 12, 13–38. [CrossRef]
6. Castellano, G.; Leite, I.; Paiva, A. Detecting perceived quality of interaction with a robot using contextual features. Auton. Robot. 2017, 41, 1245–1261. [CrossRef]
7. Dehghani, H.; Babamir, S.M. A GA based method for search-space reduction of chess game-tree. Appl. Intell. 2017, 47, 752–768. [CrossRef]
8. Huang, M.-B.; Huang, H.-P. Innovative human-like dual robotic hand mechatronic design and its chess-playing experiment. IEEE Access 2019, 7, 7872–7888. [CrossRef]

9. Lukaˇc, D. Playing chess with the assistance of an industrial robot. In Proceedings of the 3rd International Conference on Control and Robotics Engineering, Nagoya, Japan, 20–23 April 2018; pp. 1–5. [CrossRef]
10. Anh, N.D.; Nhat, L.T.; Van Phan Nhan, T. Design and control automatic chess-playing robot arm. Lect. Notes Electr. Eng. 2016, 371, 485–496. [CrossRef]
11. Wei, Y.-A.; Huang, T.-W.; Chen, H.-T.; Liu, J. Chess recognition from a single depth image. In Proceedings of the IEEE International Conference on Multimedia and Expo, Hong Kong, China, 10–14 July 2017; pp. 931–936. [CrossRef]
12. Larregay, G.; Pinna, F.; Avila, L.; Moran, D. Design and Implementation of a Computer Vision System for an Autonomous Chess-Playing Robot. J. Comput. Sci. Technol. 2018, 18, 1–11. [CrossRef]
13. Xie, Y.; Tang, G.; Hoff, W. Chess Piece Recognition Using Oriented Chamfer Matching with a Comparison to CNN. In Proceedings of the IEEE Winter Conference on Applications of Computer Vision, Lake Tahoe, NV, USA, 12–15 March 2018; pp. 2001–2009. [CrossRef]
14. Czyzewski, M.A.; Laskowski, A.; Wasik, S. Chessboard and chess piece recognition with the support of neural networks. Comput. Vis. Image Underst. 2018, 2, 1–11.
15. Al-Saedi, F.A.T.; Mohammed, A.H. Design and Implementation of Chess-Playing Robotic System. IJCSET 2015, 5, 90–98.
16. Mahmood, N.H.; Long, C.K.M.S.C.K. Smart Electronic Chess Board Using Reed Switch. J. Teknol. 2011, 55, 41–52. [CrossRef]
17. Larregay, G.; Avila, L.; Moran, O. A comparison of classification algorithms for chess pieces detection. In Proceedings of the 17th Workshop on Information Processing and Control, Mar del Plata, Argentina, 20–22 October 2017; pp. 1–5. [CrossRef]
18. Ómarsdóttir, F.Y.; Ólafsson, R.B.; Foley, J.T. The Axiomatic Design of Chessmate: A Chess-playing Robot. Procedia CIRP 2016, 53, 231–236. [CrossRef]
19. Pachtrachai, K.; Vasconcelos, F.; Dwyer, G.; Pawar, V.; Hailes, S.; Stoyanov, D. CHESS-Calibrating the Hand-Eye Matrix with Screw Constraints and Synchronization. IEEE Robot. Autom. Lett. 2018, 3, 2000–2007. [CrossRef]
20. Luqman, H.M.; Zaffar, M. Chess Brain and Autonomous Chess Playing Robotic System. In Proceedings of the International Conference on Autonomous Robot Systems and Competitions, Braganca, Portugal, 4–6 May 2016; pp. 211–216. [CrossRef]
21. Wang, X.; Chen, Q. Vision-based entity Chinese chess playing robot design and realization. In International Conference on Intelligent Robotics and Applications; Springer: Cham, Switzerland, 2015; Volume 9246, pp. 341–351. [CrossRef]

22. Chen, B.; Xiong, C.; Zhang, Q. CCDN: Checkerboard corner detection network for robust camera calibration. In International Conference on Intelligent Robotics and Applications; Springer: Cham, Switzerland, 2018; Volume 10985, pp. 324–334. [CrossRef]
23. Kumar, R.V.Y. Target following Camera System Based on Real Time Recognition and Tracking. Master's Thesis, National Institute of Technology, Rourkela, India, May 2014.
24. Bennett, S.; Lasenby, J. Chess-Quick and robust detection of chess-board features. Comput. Vis. Image Underst. 2014, 118, 197–210. [CrossRef]
25. Matuszek, C.; Mayton, B.; Aimi, R.; Deisenroth, M.P.; Bo, L.; Chu, R.; Kung, M.; Le Grand, L.; Smith, J.R.; Fox, D. Gambit: An autonomous chess-playing robotic system. In Proceedings of the IEEE International Conference on Robotics and Automation, Seattle, WA, USA, 9–13 May 2011; pp. 4291–4297. [CrossRef]
26. Cristian, T.; Carlos,R.; Omar,R. Design and Construction of a Cost-Effective Didactic Robotic Arm for Playing Chess, Using an Artificial Vision System. Electronics 2019, 8, 1154; doi:10.3390/electronics8101154

A REVIEW ON THE IMPACT OF MOBILE PHONES IN MICRO AND SMALL ENTERPRISES IN DEVELOPING COUNTRIES

Oindrila Banerjee*

Dept. of Commerce, Sammilani Mahavidyalaya (*Affil. University of Calcutta*), BaghaJatin, Kolkata 700094, India

*Corresponding Author, E-mail: oirini@gmail.com

Abstract

The current paper aims to highlight the influence of mobile communication on micro and small enterprises in developing countries. Mobile communication has been found to make great impact on an enterprise's both internal (process related) and external (market related) aspects which are related to porter's value chain and value system models, respectively. Primarily, mobile communication facilitated information flow which led to increased productivity, reduced cost, and expansion of market.

Keywords: Micro and Small, Enterprise, Mobile Phone, Developing

Introduction

Micro and small enterprise (MSE) generally refers to a business characterized by a set of certain parameters, such as less than 50 employees, operated singly or by a few members, low initial capital requirements, limited resources and small area of operation. Only a small fraction of the MSEs has the potential for growth; however, most remain small, struggle to survive, and yield a low return on labor and capital. [1] They suffer from poor infrastructure, unskilled labor and lack of security. [2] In spite of all these limitations, the MSEs play a significant role in the economy of the developing countries. Primarily, the MSEs help lower the poverty level in the developing countries by creating job opportunities, increasing production and thereby resulting in wealth creation. The majority of the MSEs in the developing world are sole proprietorships, and firms with less than 10 employees vastly outnumber the larger enterprises3.

Most of the operations of MSEs are executed via friends, family members and social network. Unlike large firms whose advertisements depend upon marketing agencies, the advertisements of MSEs rely largely on their marketing capabilities through word of mouth and networking.[2] To achieve better individual addressability and access relevant social and economic activities,[4] mobile phones have become an integral part of today's MSEs. Since the first decade of the 21st century, the use of mobile phones has greatly increased among the MSEs. According to Hawkins, 'information' is the key element for productivity, competitiveness, and wealth creation.[5] In the systematic and smooth flow of this information, the Information and Commutation Technology (ICT), of which mobile telephony is a fundamental segment, plays an imperative role. Research has shown that adopting ICT (mobile phones) can generate wealth, power and knowledge over time.[2]

The present article aims to highlight some of the important roles that mobile phones play in MSEs in the developing countries from firms' both internal (process related) and external (market related) standpoints. Different types of MSEs have been explored, viz. agriculture, fisheries, poultry, weaving and carpentry. The immense significance of mobile phones throughout the supply chain has made it a primary tool of business for the MSEs in the developing countries. In parallel, a marked decay in the usage of landline telephones can be observed in comparison with the mobile communication.

Advantages of Mobile over Landline: The Mobility Itself

The main difference between a landline and a mobile phone is the mobility itself. While landlines connect places, mobiles connect people to people, regardless of time, location and situation. Moreover, it is cheaper to build towers than lay cables, prepay accounts have no startup costs and inexpensive/used handsets are readily available. Furthermore, the portability of a mobile phone makes it a personal device which can be used easily for both personal and business functions simultaneously. Therefore, mobile phone has come as a substitute for landline rather than a complement to it and has been largely adopted by the MSEs in the current days.[6] Analyses have shown that mobility can enhance roaming businesses and prompt service.

The Influence of Mobile Phone on MSEs

Although MSEs are of various kinds and operate under different business layouts, the overall role of the mobile phone in the MSEs is common to all and can be broadly

categorized into two types– i) mobile influences the internal process of an enterprise, which relates to Porter's value chain model [7] (an attribute of firm), e.g. increase operational ability, ii) mobile influences network of relationships external to the enterprise to gain competitive advantages, related to Porter's value system [7] (an attribute of a market).

FIRMS' INTERNAL ASPECT

Mobile Phone Enhances Operational Ability

Mobile phone enhances operational ability of a firm. For example, Kerala fishermen use mobiles to coordinate the timing and location to drop nets and search for fish.[8] Similarly, Jagun et al. described how weavers call customers during mid-process to revise plans for the garments they are creating. [9] In their study on carpentry in Lima, Peru, Cáceres et al. mentioned that for contracting new workers (mainly during peak periods), the cellular phone enables quick search of people, and thereby, helps the microentrepreneur ensure that orders can be met. With respect to clients, the mobile phone facilitates making any changes during the production process and helps avoid wastage costs from a returned or defective product.[10] In a study of a poultry farm in Ghana, Folitse et al. found that the business relied largely on mobile communication with fellow-farmers and veterinary doctors, and 94% information exchanged was on nutrition, feeding and drug administration.[11]

FIRMS' EXTERNAL ASPECT

Mobile Phone Compensates Non-Agglomeration

Agglomeration refers to sharing of common location by MSEs which allows increased association among themselves. Such cluster offers a variety of advantages, such as increased flow of information, and reduced transport, communication and transaction costs.[12] In general, for MSEs, agglomeration facilitates– 1) value-addition, via possibilities of joint investments and increased product sell, and 2) product and process improvement.[10,12] Interestingly, mostly in Latin America (say Peru), such agglomeration is not common and the MSEs over there are deprived of the benefits of agglomeration. However, a case study by Cáceres et al. of the carpentry sector at Vila El Salvador, Lima, Peru revealed that the use of mobile phones can alleviate many short-comings of non- agglomeration. [10] The positive impacts of mobile communication can be experienced in vertical relationships (producer-customer or producer-input provider), but not in the horizontal

relationships among the microentrepreneurs. The authors found that the benefits of mobile phones are most prominent in marketing and client relations. For initial ordering of furniture, queries, finding the status of the order, and finally confirming the delivery date when the order is ready, the mobile phones have the maximum usage. This removes uncertainty, saves a lot of time and transportation cost. Mobile phones were also found to be useful in obtaining new clients from the recommendations of the old ones.

Mobile Phone Reduces Information Asymmetry

The best possible allocation of resources for their maximal usage is significantly controlled by two primary factors, viz. price and market signals. Price transmits the information required to make effective decisions on both production and consumption.[13] Otherwise, large parts of a market remain ignorant of crucial market information, which may sometimes even lead to collapse of the market. McMillan[14] says: "Information is the lifeblood of markets. A market works badly if information does not flow through it. Rarely does information flow absolutely freely, but well-functioning markets have various mechanisms to aid its movement." The problem in developing countries is that the markets function poorly, and according to McMillan, this is because of poor internal flow of information.[14] One characteristic feature of these markets is the deviation from the economic principle that prices of homogeneous goods sold at different locations should be equal, the net of transportation costs.[13] According to Stigler, "Price dispersion is a manifestation, and indeed, is the measure of ignorance in the market".[15] Mobile phones, by virtue of their role as carriers and conduits of information, ought to reduce the information asymmetries in markets, thereby making the undeveloped markets more efficient.

A case study on the fishermen of Kerala by Abraham et al. revealed that mobile telephony does rectify market asymmetries and facilitate free flow of information through the market.[8] Fresh fish being a highly perishable commodity requires the shortest possible supply chain with as little involvement of intermediaries as possible. For such rapid business, ready access and smooth flow of information across the market is absolutely necessary. The authors found that after the introduction of mobile phones there was a reduction in price dispersion and intra-day price fluctuation. The merchants, owners and agents make majority of their business-related calls outside their local areas to monitor prices at distant markets which indicates a greater market integration. By communicating information on large shoals of fish, wastage of time and resources in searching fish could be greatly diminished. A significant reduction in risk and

uncertainty in such a volatile commodity via mobile use was also admitted by the fishermen. One of the best uses of the mobile phone for the fishermen was that they can call the landing centers to find where the highest prices for their catch are and then subsequently land there. The fishermen feel safer and more secured, as claimed by 70% of the surveyed.

Mobile Phone Aids Competitive Advantage Gaining

To be in a competitive advantageous position, the value system needs to be run most efficiently. Some important segments of the value system that are mediated by mobile phones are considered below.

***Increased Market Efficiency and Sales*–** Jensen in his study on the Keralan fishermen observed that before mobile phones came into usage, almost all the sales used to be conducted via beach auctions.[16] Later, fishermen with mobiles, started carrying contact numbers of hundreds of potential buyers in their handsets. While still in the sea, they call several buyers in different markets before deciding where to sell their catch. Fishermen, who previously were limited to the buyers at a single port, could scan multiple markets almost simultaneously, selecting the best price and best place to sell their catch. Mobile phones can thus reduce search costs and transportation costs, and thereby, increase market efficiency and sales.

***Expansion of Market Size*–** Mobile phones play crucial roles within network of relationships and inter-dependencies external to an enterprise, such as suppliers, transporters, wholesalers, retailers and customers. [17] Using mobile phones, the MSEs can exchange distant information both within their network or can further expand their network domain by establishing new contacts with potential buyers or sellers who were previously out of reach. This causes expansion of market size by bringing a larger number of buyers and sellers into the marketplace. [16] Akin to the above-mentioned Keralan fishermen who can call buyers in several markets, Aker observed that even grain traders can search over a greater number of markets using mobile phones and can sell in more markets.[18]

***After-Sales and Customer Service*–** Molony described how Tanzanian exporters of carved wood use their mobiles to obtain feedback between and after sales, which in turn led to gain faith of the customers and enhance the quality of their product and service. [19] Mobile phone has made the task of keeping in contact with customers and clients more

convenient and has allowed a prompter service. Such interaction turns out to be an advantage because it builds trust between the MSEs and customers.

Conclusions

The current paper provided a brief review of mobile phone usage by MSEs in developing countries from both internal and external perspectives of an enterprise. The primary use of mobile phone was found to facilitate and enhance the flow of information, which in turn leads to enhanced operational ability, market expansion, and increased sales. Therefore, for the MSEs, mobile makes the business more productive and less costly. However, no evidence has been found to-date whether mobile communication has enabled any new business startups. Finally, the present paper, apart from giving a brief overview, also raises a new question that how mobile banking and mobile wallets influence the MSEs. This will be an interesting topic to explore in the future.

References

1.La Porta, R., and Shleifer, A. (2008). The Unofficial Economy and Economic Development. Brookings Papers on Economic Activity. 2008:275-363.
2.Litondo, K., and Ntale, J. (2013). Determinants of Mobile Phone Usage for E-Commerce among Micro and Small Enterprises in the Informal Sector of Kenya. International Journal of Applied Science and Technology. 3:16-23.
3.Mead, D.C., Leidholm, C. (1998). The dynamics of micro and small enterprises in developing countries. World Development, 26:61–74.
4.Castells M., Ferna´ndez-Arde`vol M., Qiu J.L., Sey A. (2007). Mobile Communication and Society: A Global Perspective (Information Revolution and Global Politics). MIT Press: Cambridge, MA.
5.Hawkins, R.J. (2002), Forward: The Global Information Technology Report 2001-2002 (World Economic Forum). Oxford University Press: pp 38–44, http:// www.caribbeanelections.com/eDocs/development_reports/gitr_2001_2002.pdf
6.Hamilton, J. (2003), Are main lines and mobile phones substitutes or complements? Evidence from Africa. Telecommunications Policy, 27: 109–133.
7.Porter, M.E. (1985). Competitive advantage: Creating and Sustaining Superior Performance. Free Press: New York.
8.Abraham, R. (2007). Mobile phones and economic development: Evidence from the fishing industry in India. Information Technologies and International Development, 4:5– 17.
9.Jagun, A., Heeks, R., Whalley, J. (2008). The Impact of Mobile Telephony on Developing Country Micro-Enterprise: A Nigerian Case Study. Information Technologies and International Development 4:47–65.
10. Cáceres, R., Agüero, A., Cavero, M., and Huaroto, C. (2012). The Impacts of the Use of Mobile Telephone Technology on the Productivity of Micro- and Small Enterprises: An

Exploratory Study into the Carpentry and Cabinet-Making Sector in Villa El Salvador. Information Technologies & International Development. 8 (Special Bilingual Issue):77- 94.
11. Folitse, B., Manteaw, S., Dzandu, L., Obeng-Koranteng, G., and Bekoe, S. (2018). The Determinants of Mobile-Phone Usage Among Small-Scale Poultry Farmers in Ghana. Information Development. 35:564-574.
13. Visser, E. (1999). A comparison of clustered and dispersed firms in the small-scale clothing industry of Lima. World Development, 27: 1553–1570.
14. Eggleston, K., Jensen, R., Zeckhauser, R. (2002). Information and communication technologies, markets and economic development. Discussion Paper 0203, Department of Economics, Tufts University.
15.McMillan, J. (2002) Reinventing the Bazaar: A Natural History of Markets, 1 st Ed. W. W. Norton & Co. Publisher: New York.
16. Stigler, G. (1961). The Economics of Information. Journal of Political Economy, 69:213-225.
17. Jensen, R. (2007). The Digital Provide: Information (Technology), Market Performance, and Welfare in the South Indian Fisheries Sector. Quarterly Journal of Economics, 122: 879–924.
18. Donner, J., Escobari, M. (2010). A Review of Evidence on Mobile Use by Micro and Small Enterprises in Developing Countries. Journal of International Development. 22:641-658.
19. Aker, J. C. (2008). Does Digital Divide or Provide? The Impact of Cell Phones on Grain Markets in Niger. Working Paper No. 177. Durham, NC: Bureau for Research and Economic Analysis of Development. Retrieved 27 April 2020 from http:// ibread.org/bread/system/files/bread_wpapers/177.pdf
20 Molony, T. (2006). 'I don't trust the phone; it always lies': Trust and Information and Communication Technologies and Tanzanian Micro- and Small Enterprises. Information Technologies and International Development 3: 67–83

NATURAL SCIENCES

A multi-disciplinary research journal

Volume 1; Issue 1(2020)

The Journal of Natural Sciences
Institute of Advanced Research
Koba Institutional Area
Gandhinagar – 382 426
India